CARDIAC CALCIUM HANDLING IN THE MOUSE MODEL OF DUCHENNE MUSCULAR DYSTROPHY

Peter James Woolf Bsc (Hons)

Submitted for the completion of the degree of

Doctor of Philosophy

at the

Department of Biological and Physical Sciences

Faculty of Sciences

October 2003

ABSTRACT

The dystrophinopathies are a group of disorders characterised by cellular absence of the membrane stabilising protein, dystrophin. Duchenne muscular dystrophy is the most severe disorder clinically. The deficiency of dystrophin, in the muscular dystrophy X-linked (*mdx*) mouse causes an elevation in intracellular calcium in cardiac myocytes. Potential mechanisms contributing to increased calcium include enhanced influx, sarcoplasmic reticular calcium release and\or reduced sequestration or sarcolemmal efflux. This dissertation examined the potential mechanisms that may contribute to an intracellular calcium overload in a murine model of muscular dystrophy. The general cardiomyopathy of the *mdx* myocardium was evident, with the left atria from *mdx* consistently producing less force than control atria. This was associated with delayed relaxation. The role of the L-type calcium channels mediating influx was initially investigated. Dihydropyridines had a lower potency in contracting left atria corresponding to a reduced dihydropyridine receptor affinity in radioligand binding studies of *mdx* ventricular homogenates ($P<0.05$). This was associated with increased ventricular dihydropyridine receptor protein and mRNA levels ($P<0.05$). The function of the sarcoplasmic reticulum in terms of release and also sequestration of calcium via the sarco-endoplasmic reticulum ATPase were investigated. A lower force of contraction was evident in *mdx* left atria in response to a range of stimulation frequencies ($P<0.05$) and concentrations of extracellular calcium ($P<0.05$). However, in the presence of 1 nM Ryanodine to block sarcoplasmic reticular calcium release, increased stimulation frequency caused similar forces to those obtained in control mice suggesting enhanced calcium influx via L-type calcium channels in *mdx*. Rapid cooling contractures showed a reduced contracture in *mdx* compared to control in response to cooling. This suggests some dysfunction in SR storage, which may be associated with the delayed relaxation time. Concentration-response curves to inhibitors of the sarco-endoplasmic reticulum showed no difference in function of the enzyme responsible for calcium uptake into the sarcoplasmic reticulum. Although sarco-endoplasmic reticulum ATPase mRNA was upregulated, no functional benefit was evident. This study indicates that a deficiency of dystrophin leads to upregulation of L-type calcium channels that contribute to increased calcium influx, with no functional change in sarcoplasmic reticular sequestration. Upregulation of the influx pathway is a potential mechanism for the calcium overload observed in *mdx* cardiac muscle.

CERTIFICATION OF DISSERTATION

This thesis is my own work, except where otherwise acknowledged, and the work is original and has not been previously submitted for any other award at any other University or Institution of tertiary education.

_____ _____

Signature of Candidate Date

ENDORSEMENT

_____ _____

Signature of Principal Supervisor Date

_____ _____

Signature of Associate Supervisor Date

ACKNOWLEDGEMENTS

I must initially acknowledge that the concentration response curve data for Bay K 8644 and Nifedipine was performed by Dr. Lucy Sai Lu. The data for Figure 4.1, 4.2, 4.3 and 4.4 were supplied by Dr. Lu but analysed and presented by the candidate. I have presented this data in my thesis for completeness.

To my supervisor Andrew, without your continual guidance, support and enthusiasm I would not be where I am today. I sincerely and respectfully offer you my heartfelt gratitude for your major role in helping me grow as a scientist and a person. You have been a true mentor in every sense of the word.

To Janice, without your love and tenacity I would not have accomplished many of the things that I have today. I owe much of this work to you for encouraging me to become the person that I am today.

To my families I thank you for your patience and care throughout some trying times. Without your love I would not have had the favourable outcome that I have today.

To Sean Holroyd and Mike Watson thank you for the many hours you have spent with me in the lab, thank you for the guidance and direction that you both offered during my studies. Also to Lindsay Brown for access to the molecular laboratory required to conduct the RT-PCR studies.

To my lab colleagues Lucy Sai Lu, Anthony Leicht, Kate Roper, Richard Ryan, Connie Murray, Lisa Conlan, Christel van Erp, Nicki Laws and Ronita Sharma I thank you for the stimulation of thoughts and the technical support and friendly atmosphere that you provided me with for the many hours in the lab. To Andrew Fenning, Julian de Looze and the rest of the Brown lab thank you for your assistance. Also thanks to David Adams, David Saint, Peter Molenaar, Lea Delbridge and their labs for exchange of ideas.

To the technical staff at USQ, in particular Graham Holmes, Pat McConnell, Kath Watson and Adele Jones, thank you for helping with my many and varied enquiries. To Sammy Quattromani I thank you for keeping all the computers running (most of the time!) To the departmental secretary Debbie White thank you for dealing with my many enquiries. To Ruth Hilton at the Research and Higher Degrees office I thank you for your common sense support, belief and patience throughout my studies. To Oliver Kinder many thanks for providing materials for weird, whacky and wonderful applications.

To my friends and colleagues in the postgrad room at USQ, and throughout my travels as a doctoral student, thank you for sharing the thoughts and problems that we are all faced with undertaking a doctoral degree. Finally, to my friends around the world I thank you for your care and support and for being able to successfully distract me from my work whenever it was required! Cheers!

GLOSSARY OF ABBREVIATIONS

BMD	Becker Muscular Dystrophy
BTZ	Benzothiazepine
C57	C57Bl10ScSn
$[Ca^{2+}]_i$	Intracellular Calcium Concentration
Ca^{2+}/Ca/Ca^{++}	Calcium
$CaCl_2$	Calcium Chloride
CICR	Calcium-induced calcium release
CPA	Cyclopiazonic Acid
CRC	Concentration-response Curve
DHPR	Dihydropyridine receptor
DMD	Duchenne Muscular Dystrophy
DMSO	Dimethyl Sulfoxide
DTZ	Diltiazem
EC_{50}	Effective Concentration that produces 50% of the maximum response
FOC	Force of Contraction
g	Gram
Hz	Hertz
K^+	Potassium
LA	Left Atria
M	Molar
MB	Megabases
Mdx	Muscular dystrophic X-linked
mg	Milligram
min	Minute (s)

mL	Millilitre
mM	Millimolar
mN	MilliNewton
mRNA	Messenger RNA
Na^+	Sodium
NCE	Mitochondrial Sodium/Calcium exchanger
NCX	Sarcolemmal Sodium/Calcium exchanger
NFD	Nifedipine
NSB	Non-specific binding
O_2	Oxygen
pD_2	-log EC_{50}
PLB	Phospholamban
RCC	Rapid Cooling Contracture
RLB	Radioligand Binding
RNA	Ribonucleic Acid
RT-PCR	Reverse-transcriptase – polymerase chain reaction
RyR	Ryanodine Receptor
SD	Standard Deviation
SEM	Standard Error of the Mean
SERCA	Sarco-endoplasmic reticulum Ca^{2+}-ATP-ase
SR	Sarcoplasmic Reticulum
TPSS	Tyrodes Physiological Salt Solution
μM	Micromolar
VRL	Verapamil
vs	Versus

CONTENTS

LIST OF TABLES

LIST OF FIGURES

LIST OF PUBLICATIONS

Full publications arising from this thesis include:

1. **Peter J. Woolf**, Sai Lu, Sean M. Holroyd, Lindsay Brown and Andrew J. Hoey (2003) Calcium influx and sequestration in dystrophin-deficient cardiac muscle. *Submitted to Journal of Molecular and Cellular Cardiology.*

Abstracts arising from this thesis include:

1. **Peter J. Woolf**, Sai Lu and Andrew J. Hoey (2002) Regulation of calcium influx in dystrophic cardiac muscle. *Proceedings of the Australian Health and Medical Congress, Melbourne, Australia.*

2. **Peter J. Woolf**, Sai Lu and Andrew J. Hoey (2002) Regulation of calcium influx in cardiomyocytes from mice with Duchenne Muscular Dystrophy. *Proceedings of the Australian Society for Medical Research, Brisbane, Australia.* – Runner up for Queensland Premier's Award for Medical Research (Pre-Doctoral Category).

3. **Peter J. Woolf**, Sai Lu, Richard B. Ryan & Andrew J. Hoey (2001) Characteristics of the dihydropyridine receptor in cardiac muscle. *Proceedings of the Australasian Society of Clinical and Experimental Pharmacologists and Toxicologists, Dunedin, New Zealand.*

4. Andrew J. Hoey, Sai Lu, **Peter J. Woolf**, Richard B. Ryan (2001) Cardiac dysfunction in mice with Duchenne muscular dystrophy. *Proceedings of the Queensland Health and Medical Research Scientific Meeting, Brisbane, Australia.*

5. **Peter J. Woolf**, Sai Lu, Richard B. Ryan & Andrew J. Hoey (2001) Changes in cardiac dihydropyridine calcium channel receptors from dystrophin deficient mice. *Proceedings of the International Society for Heart Research, Brisbane, Australia.*

6. Andrew J. Hoey, **Peter J. Woolf**, Sai Lu & Richard B. Ryan (2001) Cardiac dysfunction in the mouse model of Duchenne muscular dystrophy. *Proceedings of the International Society for Heart Research, Brisbane, Australia.*

7. **Peter J. Woolf**, Sai Lu & Andrew J. Hoey (2000) The electrophysiological and contractile effects of calcium channel antagonists on the left atria of muscular dystrophy (*mdx*) mice. *Proceedings of the Australasian Society of Clinical and Experimental Pharmacologists and Toxicologists, Newcastle, Australia.*

CHAPTER 1 - INTRODUCTION

1.1 Dystrophinopathies

Duchenne Muscular Dystrophy (DMD) and its allelic variant Becker Muscular Dystrophy (BMD) are genetic neuromuscular disorders caused by a mutation on the X chromosome (Xp21), a gene that encodes for the protein dystrophin. A complete loss of dystrophin leads to the most severe form of the muscular dystrophies, DMD, while a partial loss of dystrophin (the protein is either truncated or expressed partially) leads to the less severe BMD. Similarly, X-linked cardiomyopathy is due to a mutation at the same chromosomal site. Together these conditions are known as dystrophinopathies, since the dystrophin gene is affected in all the disorders. Several animal models have been identified with X-linked dystrophinopathies, including the *mdx* (Muscular dystrophy X-linked) mouse and GRMD (Golden retriever muscular dystrophy) dog. To date, the exact roles of dystrophin are not completely defined, but it is understood to be involved in cell membrane structural organisation, control of calcium regulation and signal transduction.

The absence of dystrophin in muscle leads to impaired sarcolemmal integrity, along with alterations in signal transduction that lead to a loss of intracellular calcium homeostasis. Such a disruption in intracellular calcium homeostasis, leading to intracellular calcium overload, is a significant feature of dystrophin-deficiency. Increased intracellular calcium levels have been measured in at-risk foetuses, premature infants with DMD, in whom necrosis was absent (Bertorini *et al*., 1984; Emery & Burt, 1980), DMD affected individuals (Bertorini *et al*., 1982; Bodensteiner & Engel, 1978) and animal models of DMD (Mallouk *et al.*, 2000). This calcium

overload is one of the earliest pathological manifestations and is generally accepted as a contributing factor to the pathogenesis of dystrophinopathies (Wrogemann & Pena, 1976). This calcium overload has been implicated in activation of calcium-dependent proteolytic enzymes. Proteolysis leads to cellular necrosis, subsequent fatty infiltration and fibrosis. These processes of fatty infiltration and fibrosis contribute to a hypertrophy of cardiac and skeletal muscle without any functional advantage, and eventually loss of tissue function.

The clinical features of DMD due to the absence of dystrophin, manifest progressively. The major clinical features of DMD include a slowed development of motor skills, a loss of ambulation from 10-15 years of age, and progressive skeletal, cardiac and smooth muscle deterioration. Death usually occurs in the early twenties due to cardiac or respiratory failure. The partial expression of dystrophin as in BMD, results in a spectrum of both skeletal and cardiac muscle involvement, ranging from Duchenne-like symptoms and prognosis to near normal skeletal and cardiac muscle function, with some BMD patients being ambulatory into their eighties. In contrast, patients with X-linked dilated cardiomyopathy do not usually develop skeletal muscle myopathy, with selective impairment of the myocardium progressing to dilated cardiomyopathy.

1.2 The History of Duchenne Muscular Dystrophy

Edward Meryon was the first to describe DMD in 1851. Meryon described eight affected boys in three families and detailed family trees of affected individuals,

tracing the condition in cousins to three sisters. Meryon observed muscle fibres microscopically, reporting diffuse sarcomeres and breakdown of the sarcolemma.

Meryon concluded that the disease was familial and not a disease of the affected nervous system, but his work became overshadowed by that of Duchenne (Emery, 1993; Hoffman, 2001).

DMD was named after the after French neurologist Duchenne de Boulogne who wrote extensively about the disease in the mid 1800s. His studies built up a picture of the condition affecting muscle tissue directly, rather than as a secondary (neurogenic) effect of a disturbance of the nervous system. Duchenne correctly identified DMD as not involving the spinal cord. Duchenne correctly defined the disease as being progressive in terms of loss of mobility. He observed that the lower limbs were affected initially followed by the upper limbs. Duchenne used a needle-harpoon technique to take muscle biopsies from patients with Duchenne muscular dystrophy over many years. Studying the biopsies, Duchenne observed an increase in interstitial connective tissue in affected muscles with the production of fibrous and adipose tissues in the latter stages of the disease. Duchenne observed that the onset of the disease was in childhood, affected boys more often than girls, and could affect several members of the one family. Duchenne's name remains eponymous with DMD, for his early work in identifying the pathogenesis of the disease (Emery, 1993). Extensive research into Duchenne muscular dystrophy has since been undertaken (Table 1.1) which is improving the longevity and quality of life of sufferers considerably.

Table 1.1 Landmarks in the History of Duchenne Muscular Dystrophy

Nineteenth century	DMD recognised as a specific clinical disorder
1959-60	Elevated serum creatine kinase levels reported in patients and female carriers (Ebashi *et al.*, 1959; Okinaka *et al.*, 1959).
1978-82	DMD mapped to Xp21 by X/A translocations (Verellen *et al.*, 1978) and DNA markers (Murray *et al.*, 1982).
Early 1980s	DMD shown to be allelic (Kingston *et al.*, 1983). Prenatal diagnosis of DMD developed (Wassner *et al.*, 1982).
1985	Gene-specific probes (Kunkel *et al.*, 1985).
1987-88	cDNA cloned and sequenced (Koenig *et al.*, 1987). Protein product (dystrophin) identified (Hoffman *et al.*, 1987). Dystrophin localisation and functional studies began (Sugita *et al.*, 1988).
1989-90	Myoblast transfer experiments in mice (Partridge *et al.*, 1989) and humans (Karpati, 1990) commenced.
1990-91	Direct gene transfer (Wolff *et al.*, 1990) attempted.
1995	Adhalin has a role in DMD (Mendell *et al.*, 1995).
1996-97	Recombinant vectors deliver therapeutic genes (Petrof *et al.*, 1996). Cloning of the DMD gene (Davies, 1997).
1997	Stem cells identified as potential therapeutics (Smith & Schofield, 1997).
1998	Sarcoglycans (Urtasun *et al.*, 1998) and dystroglycans (McDearmon *et al.*, 1998) play a role in DMD.
1999	Antisense oligonucleotides improve expression of dystrophin (Wilton *et al.*, 1999)

Table adapted from Emery (1993).

Alterations in calcium handling are not uncommon in cardiac diseases. Given the aetiology of DMD, it could be expected that calcium handling will be significantly altered in dystrophic hearts.

1.3 Calcium Handling in Cardiac Tissues

Calcium handling in cardiac tissues is considerably different to that in skeletal muscle. In the myocardium, calcium influx occurs via voltage gated L-type calcium channels while T-type calcium channels provide only a minor contribution in cardiomyocytes. Influx via the L-type calcium channel triggers calcium-induced-calcium-release (CICR), a mechanism whereby inflowing calcium flows across the T-tubule membrane and binds to ryanodine receptors on the SR membrane, causing them to open, thus resulting in release of calcium from the sarcoplasmic reticulum (SR). Calcium binds to troponin causing the actin and myosin filaments to interact allowing development of contractile force. Calcium is then actively sequestered back into the SR by the sarco-endoplasmic reticulum ATPase (SERCA). The sarcolemmal sodium/calcium exchanger (NCX) also assists in returning calcium to resting intracellular levels by extruding calcium out of the cytoplasm into the extracellular fluid. Mitochondrial calcium plays a minor role in the myocardium.

As an intracellular calcium overload is observed in dystrophin deficient muscle, dysfunction of any of the calcium handling mechanisms described above may be implicated in the loss of calcium homeostasis. There is currently a paucity of knowledge regarding calcium regulation in dystrophin-deficient myocardial tissues, with the only available information being drawn from studies on dystrophic skeletal muscles and a very small number of studies using dystrophic cardiac tissues.

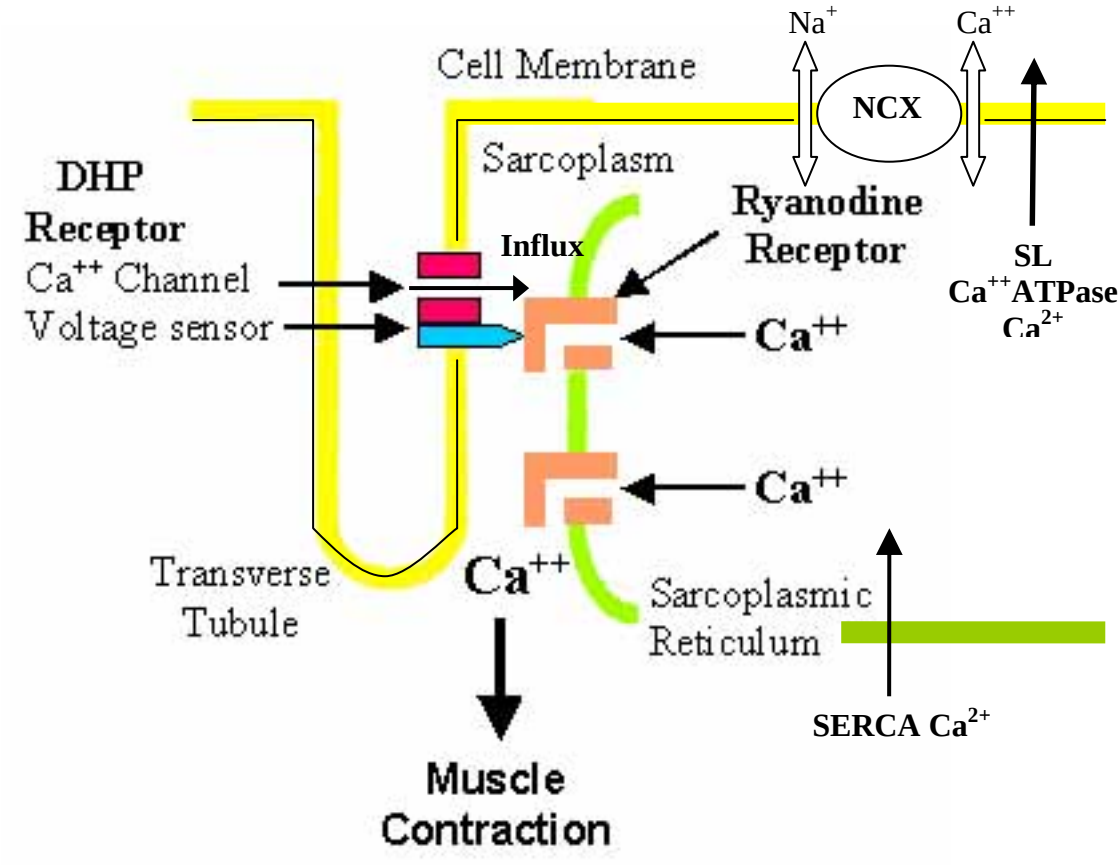

Figure 1.1 Calcium handling pathways in cardiomyocytes. Calcium flows in from the extracellular space through L-type calcium channels where the dihydropyridine receptors (DHP) act as voltage sensors. The influx of calcium triggers calcium-induced calcium release from the sarcoplasmic reticulum via the Ryanodine sensitive receptors. This released calcium and the calcium influxed via the L-type calcium channels binds to the cardiac troponin to produce contraction of the muscle. Calcium is then sequestered back to the SR by sarco-endoplasmic reticulum calcium ATP-ase (SERCA). Calcium efflux occurs simultaneously via the Na^+/Ca^{2+} exchanger (NCX) and the sarcolemmal Ca^{2+}-ATPase (SL Ca^{++}-ATPase).

1.4 Requirements for Further Study of Cardiac Dysfunction in Dystrophinopathies

The improved management of the skeletal, and hence respiratory aspects of DMD, has caused cardiac pathophysiology to become an increasingly important determinant of the sufferers' functional capacity and life span (Eagle *et al.*, 2002). Therefore research into cardiac implications in dystrophinopathies and particularly DMD, is becoming increasingly important, but as yet, is in its infancy.

The therapeutic regimes currently used to treat cardiomyopathy rely on modifying neurohumoral activation and positive inotropes that increase intracellular calcium levels. Calcium channel blockers are also well established in the treatment of certain cardiovascular disorders including hyperplasia and arrhythmias. However, intracellular calcium overload is a prominent pathological feature of dystrophic muscle cells and is likely to have a pathogenic role in cardiac tissue necrosis in DMD. It would therefore appear that, theoretically, the application of conventional medications, such as positive inotropic drugs that enhance intracellular calcium levels, could be deleterious. Yet this does not appear to have been taken into account when treating DMD/BMD-associated cardiac manifestations, as no studies have questioned the suitability of the positive inotropic drugs for treatment of DMD-induced congestive heart failure (CHF). Furthermore, it remains unknown whether there are DMD-induced specific changes in the responsiveness of dystrophic hearts to agents that modulate intracellular calcium.

There is evidence that treatment with calcium channel blockers could reduce necrosis in dystrophic skeletal muscle (Duarte *et al.*, 1992; Hotchkiss *et al.*, 1995; Yoshida *et al.*, 1997) although the outcomes of clinical trials and experiments in a sarcoglycan deficient cardiomyopathy (Cohn *et al.*, 2001) are inconclusive. In cardiomyocytes, the majority of the cardiac dystrophin has been found to be associated with the diadic junction region of the transverse tubule (T tubules) membrane system, which is also the area where the dihydropyridine receptor (DHPR) component of the L-type calcium channels is located (Bers, 1991). Therefore, dystrophin has been suggested as having a role in anchoring or modulating the activity of the cardiac DHPR. As

dystrophin is deficient in DMD/BMD, it is feasible that alterations of L-type calcium channels may contribute to the increase in intracellular calcium levels in DMD. However, no study has been conducted to examine the function of the cardiac L-type calcium channels in any model of DMD. Thus, the affinity and function of the cardiac L-type calcium channels need to be investigated.

The sarcoplasmic reticulum as the major storage site of calcium in the cardiomyocytes may be implicated in dysfunctional calcium handling. Similarly, mechanisms of sequestration such as SERCA and the intraluminal SR calcium binding proteins, and the release of calcium from the SR are potential contributors to the intracellular calcium overload. SERCA has been implicated in cardiomyopathies where a delayed relaxation has been observed. A delayed relaxation has been observed in dystrophin-deficient myocardium (Sapp *et al.*, 1996) but as yet the mechanisms remain to be elucidated. The calcium binding proteins have been shown to be downregulated in dystrophic skeletal muscle (Culligan *et al.*, 2002) causing a calcium leak from the SR. Whether the calcium binding proteins play a role in the cardiomyopathy observed in dystrophinopathies remains to be determined.

Futile calcium cycling such as SR leak calcium cycling leads to physiological consequences such as altered metabolism in dystophin-deficient skeletal muscle (Even *et al.*, 1994; Braun *et al.*, 2001). It is unknown whether dystrophin-deficiency related alterations in calcium handling lead to altered oxygen usage in myocardium.

1.5 Aims and Objectives

The broad objectives of this research were to characterize myocardial calcium handling in a murine model of dystrophin-deficiency. More specifically, the objectives were:

1. To examine the electrophysiological characteristics of dystrophic myocardium in response to three major classes of L-type calcium channel antagonists and concurrently ascertain their effect on force of contraction;
2. To determine the density and function of the dihydropyridine receptor on the L-type calcium channel.
3. To examine SERCA function and regulation in dystrophic myocardium.

1.6 Contributions

Preliminary experiments in our laboratory demonstrated impaired calcium regulation in cardiac muscle in young and old *mdx* from both sexes (Lu & Hoey, 2000a & 2000b). Similarly, an altered relaxation time was observed in left atria from *mdx* in our laboratory (Lu and Hoey, 2000a & 2000b) and in another study (Sapp *et al.*, 1996). Experiments in the current study examined the function of the cardiac L-type calcium channels by utilizing three classes of calcium channel antagonists. Experimental results provided clear evidence of a reduced affinity of sarcolemmal L-type calcium channels from atria of *mdx* mice to dihydropyridine compounds. Further studies examined the affinity and density of the DHPR, along with its mRNA levels. These studies showed a reduction in the affinity of the DHPR for [^{3}H]-PN 200-110, along with an increase in receptor density in *mdx* ventricles, and a two-fold increase in mRNA for the DHPR in both atria and ventricles of *mdx*. These data suggest that

dystrophin-deficiency results in a conformational change in the DHPR, and upregulation of the receptor. It remains unknown, however, whether this upregulation is primarily a consequence of dystrophin deficiency or is secondary to the intracellular calcium overload. Studies that examined sequestration function revealed no change in the function of SERCA, even though SERCA mRNA was upregulated. The upregulation of the SERCA mRNA may be a consequence of intracellular calcium overload, but due to post-transcriptional mechanisms is not observed as a functional change.

1.7 Significance

The observed persistent abnormal calcium handling in both atria and ventricles of *mdx* may lend further support to the hypothesis that the *mdx* is a useful model for the study of dystrophin-deficiency-related cardiac disease. The finding that L-type calcium channels are upregulated could provide a further insight into the mechanisms underlying dysfunction of the calcium regulation in dystrophic hearts, and may offer alternative treatment options for delaying the onset of CHF in DMD.

CHAPTER 2 – LITERATURE REVIEW

2.1 Prognosis and Development of Dystrophinopathies

Duchenne muscular dystrophy is caused by a mutation on the short arm of the X chromosome, at the Xp21 allele. Since the gene is X-linked, transmission of DMD is maternal, although approximately one third of DMD cases arise as spontaneous (*de novo*) mutations. Studies have shown the incidence of DMD ranges from approximately 1 in 3950 live male births in the United States (Boland *et al.*, 1996) and in the 1980's at 1 in 5400 live male births in Australia (Cowan *et al.*, 1980). The most common incidence quoted is 1 in 3500 live male births (Emery, 1991). Spontaneous mutations occur frequently at an incidence of about 1 in 12000 births due to the large size of the dystrophin gene (2.4 MB), and as high as 62% of cases may have no previous familial history (Alcantara *et al.*, 1999). The rare X-linked dilated cardiomyopathy also occurs due to a mutation in the dystrophin gene at the Xp21 allele. Although both DMD and BMD have been recognised for more than 100 years, the aetiology was not completely understood until the identification of the primary biochemical defect in 1987 (Hoffman *et al.*, 1987). Table 2.1 presents a comparison of Duchenne and Becker muscular dystrophies and X-linked cardiomyopathies along with cardiac manifestations of these diseases.

In DMD, the protein product of the dystrophin gene, also known as dystrophin, is absent from all muscle types – striated skeletal and cardiac, and smooth (Boland *et al.*, 1996; Serio *et al.*, 2001), as well as some neuronal cell types (Lidov *et al.*, 1990; Anderson *et al.*, 2002). Loss of dystrophin has several pathophysiological

consequences, and there are many independent mutations that lead to dystrophin-deficiency in humans, dogs, cats and mice (Hoffman & Dressman, 2001). Long before

Table 2.1: Etiology of Duchenne and Becker Muscular Dystrophy and X-linked dilated cardiomyopathy

Type	*Incidence*	*Protein defect*	*Non-cardiac clinical features*	*Heart block*	**Cardiac Arrhythmias*	*Cardiomyopathy*
Duchenne	1 in 3500 live male births	Dystrophin	Onset of severe muscle weakness, proximal-girdle distribution at 2 to 5 y in a male; loss of ambulation by 11y; calf pseudohypertrophy; mild cognitive impairment; Serum CK 10 to 100 times normal; death in twenties	+	+	+ + +
Becker	10 times less frequent than DMD[a]	Dystrophin	Onset of mid-moderate muscle weakness, proximal-girdle distribution from childhood-adulthood in male; ambulation beyond 16; calf pseudohypertrophy; Serum CK 10 to 100 times normal; normal to reduced lifespan	+	+	+ + +
X-linked dilated cardiomyopathy	Very rare	Cardiac dystrophin only	No skeletal muscle weakness but some cramping, exertional myalgias, myoglobinuria, calf pseudohypertrophy; mild myopathic changes may be present in muscle biopsy; Serum CK 1 to 100 times normal	-	+	+ + +

Each of these dystrophies is X-linked, with the defect localised to Xp21. [a] – De La Porte *et al.*, 1999 * Clinical significance based on prevalence and severity; +, mild, + +, moderate, + + +, severe, CK – creatine kinase. Adapted from Cox and Kunkel, 1997.

the visible onset of the disease, high serum creatine kinase (SCK) levels (Hoffman *et al.*, 1987) and high intracellular calcium in muscle cells are present in affected

individuals. A study using electron microscopy revealed that the first ultrastructural change was dilation of the sarcoplasmic reticulum (SR) with subsequent alterations in myofibrils and mitochondria, concurrent with rupture of the sarcolemma in the skeletal muscles from DMD patients (Watkins & Cullen, 1987). Histologically, DMD is characterized by a progressive myopathy resulting in myofibre death, reactive fibrosis, fatty infiltration of muscle tissue, and ultimately, complete loss of muscle function.

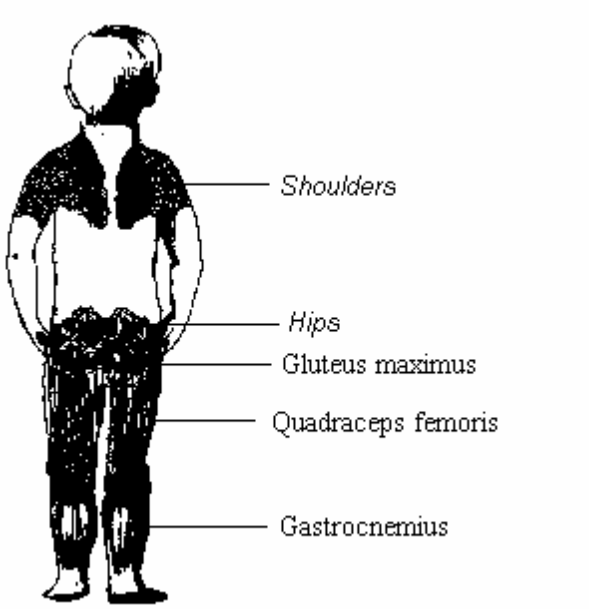

Figure 2.1 Muscle groups affected by DMD (Figure adapted from McCance & Huether, 1990 pg 1376).

Proximal muscle groups (See Figure 2.1 for muscle groups affected in DMD), which tend to contain some of the large myofibres, bear more weight and so are affected first in DMD. Compared with concentric types of exercise, eccentric exercise (lengthening contractions), where the myofibrils contract but the myofibre is extending, probably generate the most shear force on the membrane and cause the most damage to the compromised dystrophin-deficient fibres (Hoffman & Dressman, 2001). The lack of

dystrophin seems to be associated with a lack of intracellular calcium homeostasis. In skeletal muscle, sarcolemmal tears are thought to be responsible for the initial excessive influx of calcium, with leak channels eventually manifesting in the primary sarcolemmal tears. The first manifestations of the loss of dystrophin in smooth and cardiac muscle is as yet unknown, although a similar mechanical stabilisation role for dystrophin in the myocardium has been shown recently (Hainsey *et al.*, 2003).

One of the first outward clinical signs of DMD is a delayed achievement of motor milestones, usually evident by 18 to 20 months of age and apparent in most cases before the age of 5 years. Symptoms include difficulty with walking and stair climbing, weak reflexes, a waddling gait and toe walking. Pseudo-hypertrophy (enlargement) of the gastrocnemius muscle is the most obvious and consistent feature in the early stages of DMD, caused by muscle fibre hypertrophy and an excess of adipose and connective tissue (Murphy *et al.*, 1986). Permanent muscle contractures occur in the legs and heels due to shortening of muscle fibres and fibrosis of the connective tissue, causing an inability to use those muscles. Gower's sign (from a prone position, the child ‘climbs' the lower extremities to stand upright) is also a common feature. Muscle involvement is always progressive, bilateral and symmetrical (Fig 2.1). Without intervention, 95% of boys with DMD are wheelchair bound by the age of 12 years. Once wheelchair bound, scoliosis and joint contractures tend to develop rapidly. Extreme muscle weakness and subsequent postural changes cause abnormal bone development, which causes skeletal deformities of the chest and other areas. Involvement of the intercostal muscles, diaphragm and cardiac muscle contributes to deterioration of respiratory and cardiac function respectively (Emery, 1993). Death usually occurs before reaching 20 years of age, often from respiratory

failure (Newsom-Davis, 1980), while at least 30-40% of mortality can be attributed to cardiac failure (Radda, 1999). Intellectual impairment occurs in approximately 19% of boys with DMD, evidently from a loss of the smaller neuronal dystrophin in that subset of boys, and impairment does not worsen as the disorder progresses (Hinton *et al.*, 2000).

2.2 Dystrophin and the Dystrophin-Associated Glycoprotein Complex

The dystrophin gene is the largest known gene at 2.4 MB consisting of 79 exons. It encodes the rod-shaped cytoskeletal protein dystrophin (Koenig *et al.*, 1988) that has a molecular weight of 427kD, comprising 3600 amino acids, making it one of the largest known proteins. Dystrophin is composed of four domains: an amino-terminal actin-binding domain; a central rod domain that contains spectrin-like repeats; a cysteine-rich domain suggestive of calcium-binding motifs; and a unique carboxy-terminal domain that penetrates the plasma membrane and interacts with dystrophin-associated glycoproteins. Dystrophin lies along the inner surface of the plasma membrane in skeletal, cardiac and smooth muscle cells, and acts as a link between the actin cytoskeleton, the plasmalemma, and the surrounding basal lamina (Fig 2.2). In DMD, the complete absence of dystrophin leads to disruption of the transmembrane complex and a loss in the integrity of the plasmalemma (Cox & Kunkel, 1997) causing fibre necrosis (Ervasti & Campbell, 1993). The underlying mechanisms that

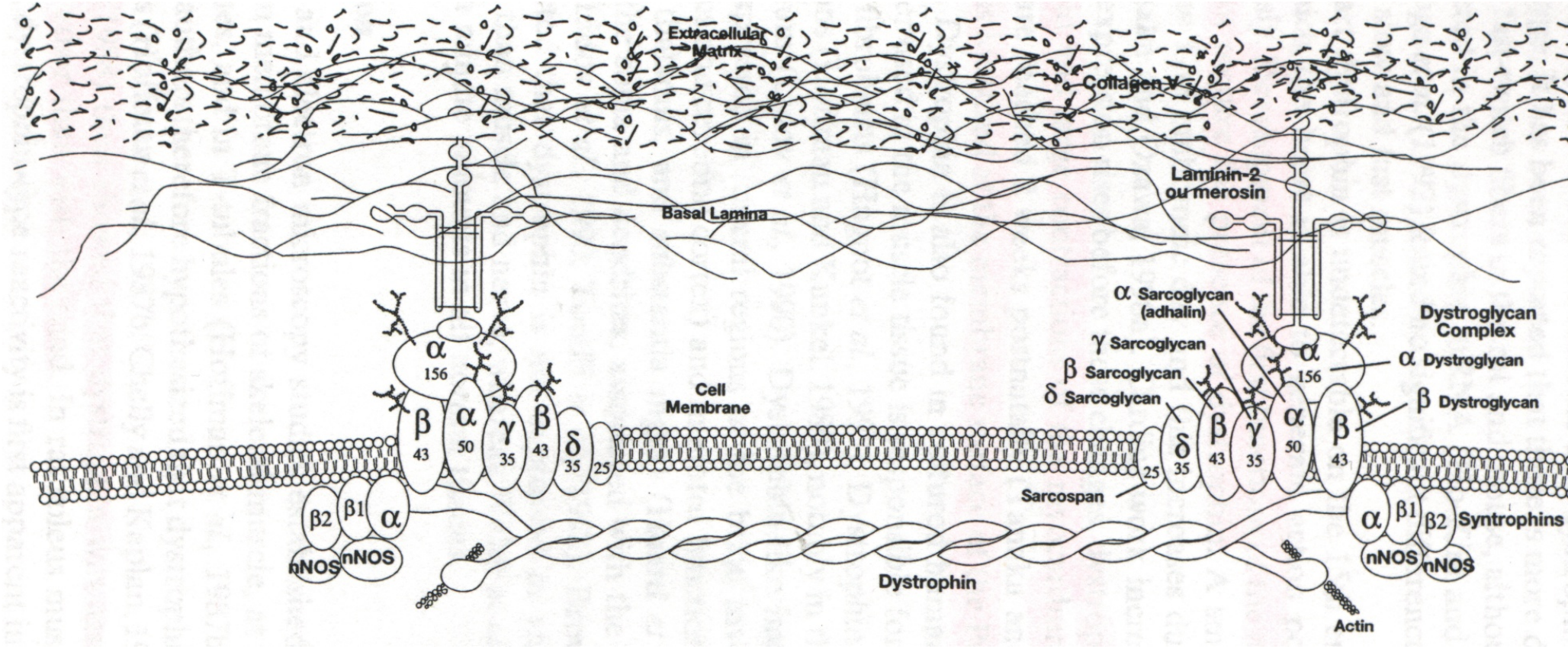

Figure 2.2: Schematic model of the dystrophin-glycoprotein complex as a transsarcolemmal link between the subsarcolemmal cytoskeleton and the extracellular matrix (From De La Porte *et al.*, 1999).

lead to fibre necrosis are not well understood and seem to be specific for each muscle type.

There are several proteins associated with dystrophin that together form the dystrophin-associated glycoprotein complex (DAGPC). The DAGPC aids dystrophin in its ability to stabilize the plasma membrane against mechanical stress (Ervasti & Campbell, 1993) although alternate functions (eg, the organization of membrane proteins, signal transduction and calcium regulation) have been proposed (Ahn & Kunkel, 1993). Two actin-binding proteins, dystrophin and α-actinin, are known to link membrane-associated elements to the cytoskeleton. Dystrophin and its associated proteins have also been implicated in playing a role in receptor and/or channel localization (Sadeghi *et al.*, 2002). Dystrophin has further been postulated to bind the contractile filaments to the internal membrane system, thereby ensuring a link between the membranes that release calcium and the contractile proteins that are activated by this calcium (Slater, 1987; Hoffman *et al.*, 1987; Tay *et al.*, 1989).

Several of these associated proteins have now been shown to underlie the pathogenesis of other types of muscular dystrophy. The DAGPC in striated muscle includes the α-, (156 kDa) and β-dystroglycan (43 kDa) and the α-, (adhalin, 50 kDa) β-, (43 kDa) γ-, (35 kDa) and δ-sarcoglycan (35 kDa) along with sarcospan (25 kDa; Crosbie *et al.*, 1997) (De La Porte *et al.*, 1999; Hainsey *et al.*, 2003). The syntrophin complex consists of α-syntrophin (59 kDa), β_1-syntrophin (59 kDa) and β_2-syntrophin

(59 kDa) and links sodium channels of the membrane to the actin cytoskeleton (Fig 2.3; De La Porte *et al.,* 1999; Brown, 1997).

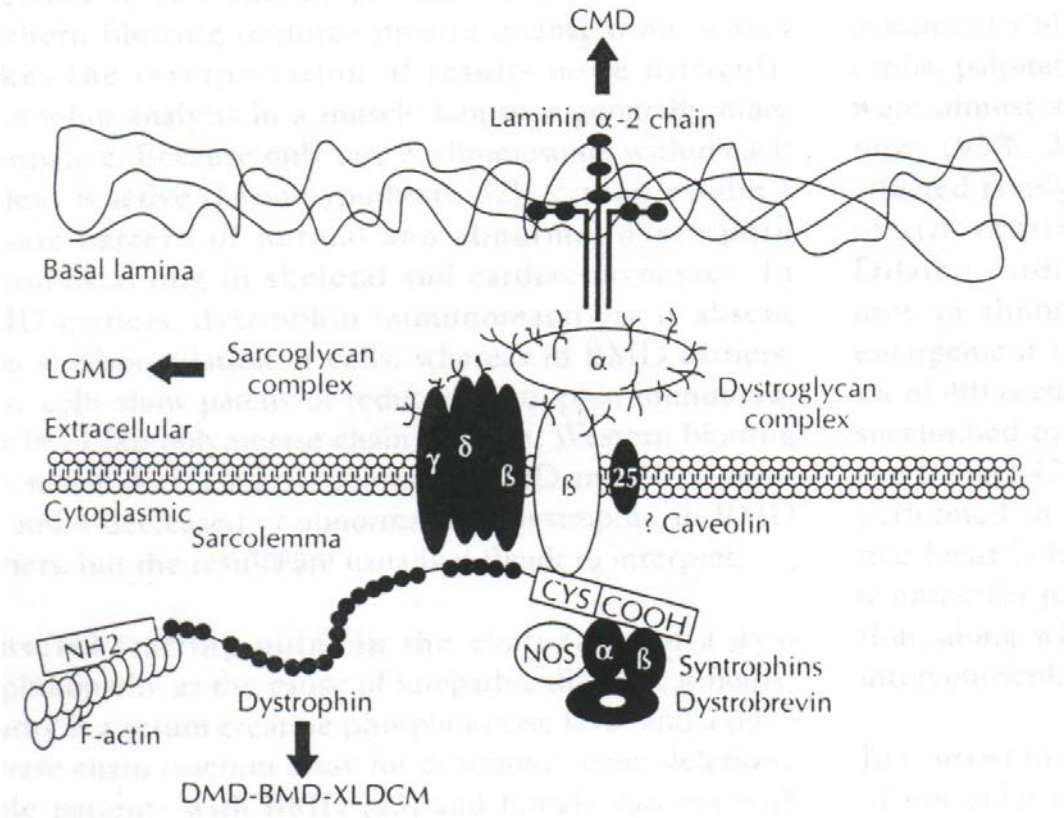

Figure 2.3: The dystrophin-glycoprotein complex and muscular dystrophies that arise due to primary defects in different members of the complex (From Cox & Kunkel, 1997) LGMD = Limb Girdle Muscular Dystrophy, XLDCM = X-linked dilated cardiomyopathy, CMD = Congenital Muscular Dystrophy. An arrow indicates the disease state that arises from a dysfunction in that section of the dystrophin-glycoprotein complex.

Dystrophin, the syntrophin complex, α-dystroglycan, and a muscle form of dystrobrevin (78 kDa) are peripheral membrane proteins, whereas the sarcoglycan complex and β-dystroglycan are integral membrane proteins. The sarcoglycans are a group of single-transmembrane proteins that form a subcomplex within the DAGPC. Mutations within the genes encoding α, β, γ, and δ sarcoglycans have been shown to possibly cause four to six known types of autosomal recessive Limb Girdle Muscular Dystrophies (LGMD; Fig. 2.3), while mutation of the γ-sarcoglycan is the basis

underlying the cardiomyopathy observed in the cardiomyopathic hamster (Sakamoto *et al.,* 1997). The sarcoglycanopathies are characterized by relatively well-preserved dystrophin immunostaining, but a marked deficiency of the entire sarcoglycan subcomplex. The α-2 chain of laminin, formerly called merosin, is an extracellular matrix protein that directly binds to the DAGPC via the α-dystroglycan, a process that has been shown to be calcium dependent (McDearmon *et al.*, 1998). A primary defect in the laminin α-2 chain underlies a form of congenital muscular dystrophy associated with leukodystrophy-like lesions in the brain that are detectable by MRI (magnetic resonance imaging) (Cox & Kunkel, 1997; Brown, 1997). The DAGPC has been shown to bind to F-actin for stabilisation (Rybakova & Ervasti, 1997) and is drastically reduced in patients with DMD. Loss of the DAGPC, even when truncated dystrophin is present, leads to severe muscular dystrophy (Matsamura *et al.*, 1993).

2.3 Cardiac Dysfunction in Dystrophinopathies

2.3.1 Cardiac Manifestations

Although the overt clinical symptom in DMD/BMD is skeletal muscle wasting, both conditions are frequently associated with myocardial impairment (Boland *et al.*, 1996; Hunsaker *et al.,* 1982; Melacini *et al.,* 1996), manifesting predominantly as cardiomyopathy and congestive heart failure (CHF) (Cox & Kunkel, 1997). Primary cardiac involvement in the muscular dystrophies should not be surprising given that cardiac and skeletal muscles are both striated. The most common cause of death in BMD patients is heart failure (Finsterer & Stollberger, 2003). Even carriers who are heterozygous for a loss of dystrophin show cardiac dysfunction due to dystrophin-deficiency. Because X-chromosome inactivation is sporadic (arbitrary) in the

myocardium, there is a patchwork of dystrophin positive and dystrophin negative cardiomyocytes. Therefore, cardiac disease in adult female carriers of the X-linked dystrophinopathies is often observed due to the structural abnormality in some of the cells (Melacini *et al.*, 1998; Davies *et al.*, 2001; Nolan *et al.*, 2003). The incidence of cardiac abnormalities associated with this partial loss of cardiac dystrophin is quite high. In a study of cardiac abnormalities in 129 carriers of DMD/BMD only 38% showed completely normal cardiac parameters (Hoogerwaard *et al.*, 1999). Therefore most carriers present with some degree of cardiac abnormality due to the sporadic loss of dystrophin in the myocardium.

Cardiac dysfunction in DMD has been shown to be early in onset and progressive in its nature throughout life (Backman & Nylander, 1992). During the progression of DMD the incidence of cardiomyopathy becomes increasingly prevalent such that more than 90% of patients eventually manifest significant cardiac defects (Megeney *et al.*, 1999). Dilated cardiomyopathy is a feature of DMD and BMD (Gnecchi-Ruscone *et al.*, 1999; Bia *et al.*, 1999) and cardiac dysfunction is a more frequent cause of death in patients with BMD than patients with DMD (Melacini *et al.*, 1993; Vrints *et al.*, 1983), although progression of myocardial damage is not identical in the two myopathies (Saito *et al.*, 1996). The incidence of arrhythmia has been shown to be higher in boys with DMD and significant decreases in heart rate variability are observed more often than the normal population, along with almost all DMD patients presenting with some degree of ECG abnormalities (Ishikawa *et al.*, 1999). Persistent tachycardia is usually an early manifestation of cardiomyopathy seen in almost all DMD patients over 10 years of age (Gardner-Medwin, 1980), and it has been shown that ventricular arrhythmias correlate with the degree of myocardial dysfunction

(Ishikawa *et al.*, 1999). Congestive heart failure ultimately manifests, with cardiac failure being a leading cause of mortality (30-50% of DMD patients die from cardiac failure; Ishikawa *et al.*, 1999), along with respiratory failure. Figure 2.4 shows the clinical cardiac manifestations of DMD and BMD progressing with age.

It has been speculated that cardiomyopathy may be secondary to skeletal myopathy (Megeney *et al.*, 1999), although this remains controversial with subsequent studies suggesting that cardiomyopathy is completely independent of skeletal muscle degeneration (Zhu *et al.*, 2002). The cardiomyopathy in X-linked cardiomyopathy arises without any skeletal muscle involvement showing that an X-linked loss of dystrophin can directly cause cardiomyopathy. Although cardiac degeneration is progressive, there appears to be little correlation between its severity and skeletal muscle involvement, physical condition, vital capacity, respiratory status (Ishikawa *et al.*, 1999) or dystrophin absence in the vasculature (Hainsey *et al.*, 2003).

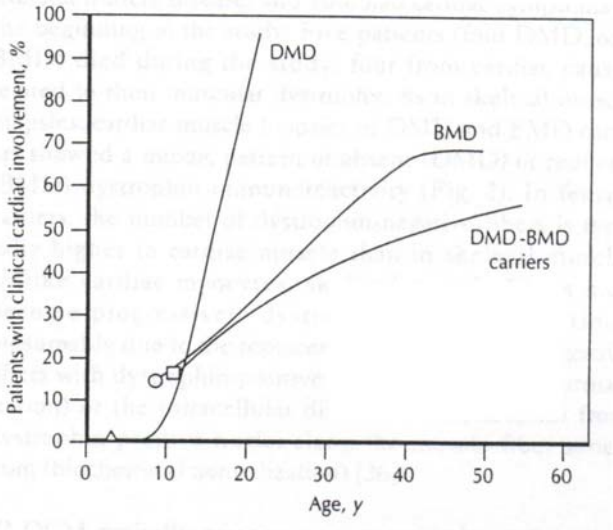

Figure 2.4: Prevalence of clinical cardiac involvement in DMD, BMD and carriers according to age. Clinical involvement is defined as arrhythmia, cardiomyopathy, and regional wall abnormalities as determined by ECG, echocardiography or both (Cox & Kunkel, 1997).

2.3.2 The Role of Cardiac Dystrophin

If cardiomyopathy is taken in its widest possible context to include both primary and secondary lesions of the myocardium, then this term is appropriate in dystrophin-deficiency and recognises that muscular dystrophy is a generalised myopathy (Hunter, 1980). The role of dystrophin in cardiac development has been studied previously. In the rat heart dystrophin is undetectable on the 15th embryonic day, the stage at which the heart is able to generate action potentials and beat spontaneously. Development of the first functions of the myocardium therefore does not require the presence of dystrophin (De La Porte *et al.,* 1999). A small quantity is detected on the 17th embryonic day, a stage where cardiac work increases, and expression of dystrophin increases during the perinatal period. Because its expression rises before cardiac work begins, dystrophin may be necessary for rapid and large contractions of the myocardium. Adult levels of dystrophin are reached 2 weeks postnatally (Tanaka & Ozawa, 1990).

Cardiac dystrophin is normally localised at the membrane surface of the Purkinje cells (Bies *et al.,* 1992). At the ultrastructural level, the dystrophin-deficient heart exhibits disordered abnormalities of the Z bands, SR dilation, and changes of the nuclei (Wakai *et al.,* 1988), along with an increase in the number and a change in the structure of mitochondria (Sapp *et al.,* 1996). It has been shown recently that dystrophin plays a mechanical role in cardiomyocytes similar to its role in skeletal muscle by linking the submembranous actin cytoskeleton to the extracellular matrix through its direct interaction with the DAGPC (Hainsey *et al.,* 2003). Earlier, Cziner

and Levin (1993) proposed that dystrophin was required to physically reinforce the sarcolemma against axial stress, and this postulation has since been supported by Saito *et al.,* (1996). Dystrophin abnormality has also been observed in cardiac myocytes acutely injured by exposure to isoprenaline (Miyazato *et al.,* 1997), showing dystrophin abnormality can occur in the absence of an X-chromosomal gene defect. Therefore it appears that dystrophin abnormality may occur due to mechanical strain resulting from high force contractions.

The function of α-actinin is to anchor parallel filaments of F-actin throughout the cytoskeleton in all tissue types, as well as to anchor antiparallel actin filaments in muscle tissue, forming the Z line in skeletal and cardiac muscle and the cytoplasmic-dense bodies in smooth muscle. An early abnormality in dystrophin-deficient mice is the scattered focal streaming of Z lines (Torres & Duchen, 1987). Several types of ion channels may also associate with α-actinin (Sadeghi *et al.,* 2002). Within adult mouse cardiac tissue, the L-type calcium channel was found to colocalise with dystrophin at both the Z and M lines, whereas α-actinin was found to colocalise with the channel only over regions of the Z line. Together, these data suggest a regulatory role for the actin binding proteins α-actinin and dystrophin, acting on the calcium channel by either direct or indirect interactions (Sadeghi *et al.,* 2002). Approximately 40% of dystrophin is tightly bound to the contractile apparatus (Braun *et al.,* 2001). The loss of that particular dystrophin fraction appears to be causative in the development of cardiac insufficiency. Another group has identified that cardiac dystrophin is distributed between two distinct pools, a soluble cytoplasmic pool and a membrane bound pool (Peri *et al.,* 1994) however they do not speculate on the roles of these

pools. The authors speculate that the distinct properties of cardiac dystyrophin suggest unique roles for the protein in cardiac versus skeletal muscle (Peri *et al.,* 1994).

A highly significant correlation between dystrophin and other calcium regulating proteins has been recognised (Gurusinghe *et al.,* 1991). In particular, a major portion of the dystrophin sequence has been found to contain repeating units of approximately 100 amino acid residues. These repeating units were found to exhibit significant homology to troponin I (Gurusinghe *et al.,* 1991). Troponin I binds to the calcium binding proteins calmodulin and troponin C. The regions of highest homology were characterised by patterns of high localisation of charged amino acids and thus could represent a possible calmodulin or troponin C surface accessible binding site (Gurusinghe *et al.,* 1991). The expression of cardiac troponin has been found to be unchanged in both patients with DMD and *mdx* mice (Hammerer-Lercher *et al.,* 2001). Subcellular localisation studies have indicated that dystrophin is associated with the diadic junction, providing further support that dystrophin could be involved in controlling intracellular calcium homeostasis (Hoffman *et al.,* 1987).

2.4 Animal Models of Dystrophinopathies and Related Conditions

There are a number of animal models that have been identified to examine the progressive pathophysiology of Duchenne muscular dystrophy and experimental therapeutics for the disease. The *mdx* (muscular dystrophy X-linked) mouse has become the most popular animal model due to its relative inexpensiveness, its short gestation period and small size. Cats and mice show a more benign disease than

humans, with muscular hypertrophy as one of the more obvious symptoms (Hoffman & Dressman, 2001). The golden retriever or GRMD dog (Kornegay *et al.,* 1988) is probably the best model of DMD in terms of its similarity to the pathophysiology observed in the human male (Cooper *et al.,* 1988). However this model is quite expensive, has considerable variability in its phenotype and controversy surrounds the use of dogs for medical research. Various other species of animals with muscle weakness exist and have been studied, including the hamster, cat (Ytterberg, 1991), chicken (Dawson, 1966), sheep (Paulson *et al.,* 1966), mink (Hegreberg *et al.*, 1974), duck (Rigdon, 1964), cow (Poukka, 1966), and even a zebra fish (Bolanos-Jimenez *et al.,* 2001), but none of these have been shown to be strictly comparable to human muscular dystrophy.

2.4.1 The GRMD Dog

The GRMD dog was first described by Kornegay *et al.,* in 1988. Creatine kinase levels are elevated from the first week of life onwards, but symptoms usually manifest at approximately 8 weeks when muscular weakness develops and then worsens progressively over subsequent months. As in humans, muscular weakness is paralleled by a progressive loss of muscle tissue and development of fibrosis. Dystrophin-deficiency affects the entire musculature and in particular there is a reduction in respiratory capacity. As in DMD, the muscle necrosis is inadequately compensated by regeneration and the resulting loss of muscle mass is accompanied by fibrous and fatty infiltration and diffuse calcification of the muscles, matched by rapid development of clinical muscle weakness and contractures during the first few months of life (Partridge, 1991). Cardiomyopathy is a significant feature of dystrophin-deficiency in the GRMD dog (Moise *et al.*, 1991) and death usually occurs around

one year of age (Valentine *et al.*, 1992; De La Porte *et al.*, 1999).

2.4.2 The *mdx* Mouse

The *mdx* is a naturally occurring mutation that was found in a colony of C57BL10 ScSn mice (Bulfield *et al.*, 1984); hence these mice (C57) have become the control for *mdx*. The *mdx* mouse mutation is a premature stop codon at exon 23 of the dystrophin gene and hence it resembles the genetic defect of boys with DMD quite closely. Muscle fibres in old *mdx* show variation in size with many atrophied and split (Pastoret & Sebille, 1995). Progressive and degenerative changes observed in *mdx* resemble DMD closely and imply that there are basic pathological similarities between the murine and human diseases (Pasoret & Sebille, 1995; Lefaucher *et al.*, 1995). The female *mdx* in breeding colonies are homozygous, so that inbred strains of the *mdx* continually exhibit the Xp21 mutation and subsequent dystrophin-deficiency. Bulfield *et al.,* (1984) initially reported the *mdx* mouse mutation and provided evidence for dilation of the SR as an early change in affected myofibrils, a change similar to those observed in boys with DMD. They also observed the development of electron-dense bodies in the mitochondria and disruption of the plasmalemma and basal lamina, which again mimics the pathophysiology observed in boys with DMD. The pathology of skeletal muscle in *mdx* shows necrosis, regeneration and the persistence of central nuclei (Torres & Duchen, 1987). However, after marked necrosis from 21 days of age (McGeachie *et al.*, 1993) the *mdx* shows skeletal muscle recovery from approximately 40 days of age due to the upregulation of a dystrophin-related protein, utrophin, which effectively prolongs the life span of these mice and decreases skeletal muscle atrophy. Utrophin is a close homologue of dystrophin (69% across 3500 amino acids) (Keep *et al.*, 1999), so there is speculation that upregulation

of utrophin may be able to functionally compensate for the lack of dystrophin (Fisher *et al.*, 2001). Utrophin upregulation thus far has not been shown to be able to prevent life-threatening myocardial dysfunction (Fanin *et al.,* 1999) although further studies are warranted as this study examined one DMD and one BMD case only. Utrophin shares sequence similarity with dystrophin but instead is localised to neuromuscular and myotendinous junctions in mature skeletal muscle and to intercalated discs and microvasculature smooth muscle in the heart (Sewry *et al.,* 2001). Due to changes such as these, there is consideration of the similarity of the pathogenesis of dystrophy in *mdx* compared to DMD, with some authors suggesting that *mdx* is not an appropriate model to study skeletal muscle myopathy (Rouger *et al.*, 2002).

Mice deficient in dystrophin have significant tachycardia, decreased heart rate variability, and altered autonomic heart rate modulation in comparison to wild-type control mice, findings consistent with clinical observations of autonomic dysfunction in DMD (Gnecchi-Ruscone *et al.,* 1999; Chu *et al.,* 2002). *Mdx* mice display abnormal electrocardiograms (ECGs) (Bia *et al.,* 1999), decreased atrioventricular conduction time and impaired baroreceptor reflex control in conscious animals that is consistent with observations in DMD patients (Chu *et al.,* 2002). Conduction abnormalities in *mdx* are associated with morphological changes, including multifocal areas of fibrosis, vacuolization and fatty infiltration throughout the entire conduction system (Bia *et al.,* 1999). *Mdx* heart also develops hypertrophy that does not contribute to greater contractile force by 6 months of age (Bia *et al.,* 1999).

At 12-14 weeks of age the pathophysiology of the *mdx* myocardium is evident by altered contractile function (Sapp *et al.*, 1996). Cardiomyocytes from 8-10 week old

mdx mice have been reported to have a reduced threshold for the development of sarcolemmal injury under mechanical stress (Danialou *et al.,* 2001). *Mdx* myocardium exhibit myocardial lesions, characterised by necrosis, macrophage infiltration and inflammation along with a diminished number of functional myocardial fibres which are replaced with connective tissue (Bia *et al.,* 1999). The *mdx* mouse therefore shows significant similarity in cardiac dysfunction to that observed in boys with DMD. The *mdx* mouse is therefore an appropriate model to study dystrophin-deficient cardiomyopathy.

2.4.3 Other Animal Models of Muscular Dystrophy

2.4.3.1 Feline X-linked muscular dystrophy

Dystrophin deficiency has also been described in the feline X-linked muscular dystrophy (FXMD) cat. It is characterised by muscle hypertrophy and resembles DMD in displaying accumulation of calcium, but differs in showing no fatty infiltration with only moderate fibrosis, no loss of muscle fibres, and no progressive muscle weakness (De La Porte *et al.,* 1999). This model is rarely used in the research of dystrophinopathies.

2.4.3.2 Dystrophic Syrian Hamster

The dystrophic Syrian hamster is known to have δ-sarcoglycan deficiency, thus, it is recognised as a good model for clarification of the pathogenesis of sarcoglycanopathy. In Syrian hamsters, the muscle lesions closely resemble those of the *mdx*, and the hamsters also have increased resting intracellular calcium levels (Camacho *et al.,* 1988). Although signs of skeletal muscle dysfunction are mild,

cardiac muscle is preferentially involved, leading to fatal cardiac insufficiency around one year of age (Nonaka, 1998).

2.4.3.3 The Cardiomyopathic Hamster

The cardiomyopathic hamster has a γ-sarcoglycan deficiency that leads to a dysfunctional DAGPC and subsequent cardiomyopathy. More heart research has been dedicated to this model of cardiomyopathy than the *mdx* mouse, so this model may lend some insight into the cardiac dysfunction observed due to a loss of the DAGPC. The lack of membrane proteins in the cardiomyopathic hamster is directly related to increased sarcolemmal permeability and subsequent cell rupture (Ikeda *et al.,* 2000).

An altered calcium homeostasis leading to an intracellular calcium overload plays a primary role in the development of necrosis in the cardiomyopathic hamster (Palmieri *et al.,* 1981). Initially calcium influx was implicated as a major contributor to the cardiac dysfunction. Kuo *et al.,* (2002) observed increased DHPRs in radioligand binding, although Howlett & Gordon (1987) observed no increase in the density of the DHPRs. Another major calcium transporter, SERCA, was also expressed in normal levels in the cardiomyopathic hamster heart (Kuo *et al.,* 2002), while recently an abnormal activation and high levels of the mitochondrial sodium/calcium exchanger were reported (Kuo *et al.,* 2002). The effects of increased cytosolic calcium have been associated with a loss of matrix calcium, resulting in impaired oxidative phosphorylation and thus a loss of mitochondrial metabolism, which may be a contributor to altered metabolism (Kuo *et al.,* 2002). The elevation in calcium also induces opening of mitochondrial permeability pores that in turn lead to caspase activation and cell death (Kuo *et al.,* 2002). In conclusion, it would appear that a loss

of γ-sarcoglycan alone may lead to a loss of calcium homeostasis in the myocardium that may be similar to the pathogenesis in *mdx*.

2.5 Current Research and Therapeutic Strategies

Experimental therapeutics of the muscular dystrophies has made impressive advances on several fronts. Muscle gene delivery has been successful in rodent models, correction of the dystrophin gene mutation has been reported in dog, and several reports of progress on myogenic stem cell characterisation are highlighting cell transplantation as a possible therapeutic approach. Bone marrow transplantation has been shown to regenerate cardiomyocyte dystrophin (Bittner *et al.*, 1999). The consequences of primary dystrophin-deficiency are being continually advanced and drugs targeting specific biochemical pathways are being tested in several animal models. Drug discoveries are continually being implemented in human clinical trials (Hoffman & Dressman, 2001). Physical management has long been an approach used to increase longevity in human males with Duchenne muscular dystrophy (Dubowitz & Heckmatt, 1980) and survival is now significantly prolonged with the use of physical medical interventions, therefore the prevention of cardiac complications takes on ever-increasing importance (Ishikawa *et al.*, 1995).

2.5.1 Myoblast Transfer

With rapid advances in the molecular genetics of DMD, myoblast transfer (cell transplantation) and gene therapy have both been proposed as potential treatments. Myoblasts are muscle precursor cells capable of migrating to the site of muscle

damage, fusing with other myoblasts and thus regenerating the muscle. The aim of myoblast transfer is to incorporate donor myoblasts (containing dystrophin) into dystrophin-deficient tissue. Initial experiments in *mdx* mice were promising, but efficient transfer of myoblasts into human muscles has not yet been successful. The major problem is a reduced replicating ability after the age of 2 years (Miller & Hoffman, 1994). Also, as with any other transplantation, the injected material is often rejected by the recipient. The final difficulty is that such an approach would also not influence the brain for the approximately 19% of boys with intellectual impairment.

2.5.2 Gene Therapy

Successful gene therapy will require the efficient delivery of a dystrophin expression vector to the muscles of the body (Chamberlain, 2002). The process of gene therapy has been thwarted by the enormous size (2.4MB) and complexity of the dystrophin gene. Therefore the generation of mini-genes that can express therapeutic levels of functional protein may alleviate part of the problem. This has involved isolating the dystrophin gene from DNA and identifying the gene promoter, a sequence of DNA that ensures that the gene is 'turned on' in the appropriate tissue. The promoter and associated gene are then cloned, a process whereby a microorganism such as a virus is induced to synthesize millions of copies (hence viral vector). An appropriate delivery vector must also be identified, an organism that does not produce an immunological or toxic response (Chamberlain, 2002). Results from animal experiments have shown that direct injection of the cloned mini-dystrophin gene itself is not efficient, with only a low level of expression (Miller & Hoffman, 1994). The rod structure, and its length have been shown to be crucial determinants for the function of micro-dystrophin (Sakamoto *et al.,* 2002). The muscle isoform of dystrophin is encoded on a

14Kb mRNA, and cDNA produced has prevented dystrophy in *mdx* muscles (Cox *et al.,* 1993). New adenovirus-based gene delivery systems are being developed, along with retroviruses, adeno-associated viruses and plasmids (Chamberlain, 2002). However, delivery of the gene to muscle continues to be problematic for the following reasons. Firstly, in order to obtain the maximum therapeutic effect, a large proportion of myofibres must be formed, yet with muscle as such a large target tissue (30% of the body mass), with a unique cellular structure, it is difficult to successfully infiltrate the target adequately. Secondly, there is an aggressive immune attack against infected cells. Thirdly, adenovirus can only infect neonatal muscle and has not been successful at inducing gene expression in more mature tissues (Hoffman *et al.*, 1997).

Even when solutions for systemic delivery and efficiency are found, transgenic gene therapy will still suffer from the major shortcoming of being *preventive* rather than *curative* of existing damage, because it is unlikely to reverse the physiological and anatomical lesions at all sites, or be effective at any stage of the disorder. Furthermore, neural defects and secondary complications (such as joint contracture and scoliosis) will not be rectified (Kakulas, 1997). Recently Yue *et al.,* (2003) used adeno-associated virus-mediated microdystrophin gene therapy in the *mdx* mouse heart with successful restoration of the dystrophin-glycoprotein complex achieved when tested 10 months after the procedure. This procedure was also able to improve the sarcolemma integrity in the *mdx* heart. These procedures hold promise for future therapeutic value, although their implementation in boys with DMD is still in the distant future.

2.5.3 Exon Skipping

Mann *et al.,* (2001) reported an antisense-induced exon skipping mechanism that was able to produce functional dystrophin in the *mdx.* These antisense oligonucleotides modify processing of the dystrophin at the pre-mRNA level, so that exons are skipped and a shorter version of dystrophin is produced in the muscle. The group have since refined their technique by identifying sensitive regions of the gene to induce skipping, and by reducing the size of the antisense oligonucleotide. This has produced increased function of the skeletal muscle of *mdx* (Lu *et al*., 2003) and demonstrated increasing feasibility of an antisense-oligonucleotide based therapy for the treatment of DMD (Mann *et al.,* 2002).

2.5.4 Utrophin Upregulation

An alternative approach may lie in the identification of proteins similar in tissue distribution and function to dystrophin. Upregulation of utrophin has shown beneficial effects in animal models (Deconinck *et al.,* 1997; Gillis & Deconinck, 1998; Rafael *et al.,* 1998). It has been hoped that the administration of pharmacological agents to stimulate transcription and thus increase the specific expression of utrophin may compensate for the loss of dystrophin and assist in overcoming the dystrophin deficiency. However, research has indicated that upregulation of utrophin in dystrophin-deficient cardiomyocytes is unable to prevent the development of life-threatening myocardial dysfunction in humans (Fanin *et al.,* 1999).

Although these therapies hold tremendous promise and are the future for treating dystrophin-deficient conditions, understanding the pathogenesis of the disease is still of vital importance. Also, these therapies are still many years from human therapeutic

use, so drug therapy to increase life quality and quantity are important. Gene therapies will probably not completely correct the loss of dystrophin, with most therapies improving prognosis to BMD-like pathology, with partial expression of dystrophin. Therefore drug therapy will likely continue to be required to treat dystrophin-deficient conditions.

2.5.5 Drug therapy

DMD is a progressive disease, with patients largely symptom free before five years of age. Although the complete correction of the biochemical defect is the clear goal in therapeutics for DMD, it should be equally viable to slow or ideally halt disease progression with the use of drug therapy aimed at correcting a well-defined pathogenesis of the disease with further research.

2.5.5.1 Glucocorticoids

The pharmacological agents that have shown the greatest success in slowing the progression of DMD are the corticosteroids such as prednisone and deflazacort (Dubrovsky *et al.*, 1998). The exact mechanism of their beneficial effects remains unknown, although it has been reported that prednisone stimulates myogenesis in human and rat muscle cells and increases the expression of dystrophin-associated proteins (Vandebrouck *et al.*, 1999). Deflazacort has been shown to promote myogenic repair and stimulate fibre growth in *mdx* skeletal muscle (Anderson *et al.*, 1996), as well as decreasing myocardial lesions and preventing cardiomyopathy in *mdx* (Skrabek & Anderson, 2001). Part of the beneficial effect of the glucocorticoids in DMD patients could be attributed to a reduction in calcium influx (Reilly *et al.*, 1996) and in the size of calcium pools in dystrophic muscle fibres (De La Porte *et al.*,

1999), hence reducing calcium-induced tissue injury. The antiinflammatory effects of the corticosteroids are also of benefit since chronic inflammation has been shown to be associated with dystrophin-deficient skeletal muscle (Porter *et al.,* 2002). Clinical trials of glucocorticoids have documented benefits in palliation of DMD (Burrow *et al.,* 1991). Kissel *et al.,* (1991) suggest that glucocorticoids improve strength in DMD through primarily immunologic mechanisms involving T lymphocytes. In contrast to normal muscle where glucocorticoids promote muscle proteolysis, Rifai *et al.,* (1995) alternatively proposed that improved strength of dystrophic muscle was mediated by inhibition of muscle proteolysis rather than stimulating muscle protein synthesis. Glucocorticoids may enhance muscle strength and function for up to two years (Khan, 1993) and are at present the only valid muscle-sustaining treatment, though some patients experience side effects such as Cushingoid symptoms and are advised to discontinue treatment.

2.5.5.2 β-Adrenergic Agents

It was initially speculated that muscular dystrophy was due to a defect in sympathetic innervation of skeletal muscle (Dubowitz & Heckmatt, 1980), so sympathomimetics were some of the first treatments aimed at rectifying the pathogenesis of muscular dystrophy. The β-adrenergic agonists have recently been nominated to potentially improve skeletal muscle strength in dystrophinopathies, although it appears that such a strategy could have deleterious effects by increasing the mechanical workload on the heart and the risk of further myocardial injury (Danialou *et al.,* 2001). Conversely, the use of pharmacological interventions that reduce cardiac workload, such as β-blockers could be beneficial in not only treating established cardiomyopathy, but also

preventing the onset of cardiomyopathy in these patients if instituted sufficiently early in life.

2.5.6 Summary of Current and Future Therapeutics

Although gene therapy and stem cells show promise and hope for the future abolition of Duchenne muscular dystrophy, at least in its current prognosis, these experimental therapeutics remain somewhat distant clinically. The glucocorticoids currently provide the best therapeutic strategy, but their exact mechanism of action remains unknown, and side effects may be too severe for the continuation of treatment for some DMD patients. Therefore, other strategies to inhibit the progression of this disease are still required.

The presence of a high concentration of calcium is considered a major pathological contributor to muscle necrosis in dystrophic skeletal muscle. The role of calcium is of utmost importance in the myocardium. Calcium is involved in the electrical signalling of the pacemaker and it is the ion that is released from the sarcoplasmic reticulum to bind to the contractile proteins of the myocardium to produce the contraction of the cardiac muscle. Calcium is also a very important contributor to arrythmogenesis, an affliction that occurs frequently in the cardiomyopathy associated with DMD. Intracellular calcium has been shown to be elevated in dystrophic myocardium, although the mechanisms responsible remain to be elucidated. To better understand the mechanisms contributing to this intracellular calcium overload and therefore the potential to direct therapies towards this, there remains a need for further research on the regulation of calcium in the myocardium.

2.6 Cardiac Calcium Cycling

Calcium ions are second messengers in signalling pathways in a variety of cell types. Calcium regulates muscle contraction, the electrical signals which determine the cardiac rhythm; and cell growth pathways in the heart (Marks, 2001). In cardiac excitation-contraction coupling at the cellular level action potentials pass over the surface membrane and activate voltage sensitive calcium channels that open rapidly, allowing extracellular calcium to flow into the cytoplasm (Lamb, 2000). The calcium enters the cell and binds to and opens specialised calcium release channels (type 2 ryanodine receptors; RyR) in the nearby sarcoplasmic reticulum (SR) membrane. The calcium flows out of the SR and activates other RyR release channels, thereby reinforcing calcium release. This phenomenon is known as calcium induced calcium release (CICR) (Fabiato & Fabiato, 1975). SR calcium release is controlled by the L-type calcium current because independent, elementary events of SR calcium release are "recruited" by calcium flowing through single L-type channels, and not by the average concentration of calcium within the cell (Wier & Balke, 1999). The rapid rise in cytoplasmic calcium concentration activates the contractile apparatus, which produces force, before the calcium is subsequently taken up into the SR by the sarco-endoplasmic reticulum calcium ATPase (SERCA). Calcium is also removed from the cytoplasm by the sodium/calcium exchanger (NCX) and the membrane bound sarcolemmal Ca^{2+}-ATPase. Both these processes remove calcium from the intracellular space to the extracellular space.

With little known about calcium handling in dystrophin-deficient cardiomyocytes, each mechanism that involves the movement of calcium is a potential source that may

contribute to the intracellular overload. Each of these mechanisms will be discussed further in the following sections.

2.6.1 The Action Potential

The cardiac action potential is characterised by the movement of three predominating ions; sodium, calcium and potassium. The upstroke of the action potential (Fig 2.5) is due to sodium influx and is known as the depolarising current and is followed by calcium influx, responsible for the plateau phase of the action potential in human myocardium. However its contribution to a plateau in murine myocardium is rather insignificant. Finally the repolarising current or inward rectifier is due to the efflux of potassium ions. The only study to observe the ventricular cardiac action potential in a model of DMD was Pacioretty *et al.,* (1994) who studied the Xmd (GRMD) dog cardiac action potential. Pacioretty *et al.,* (1994) observed a reduction in the transient outward current, which should produce delayed repolarisation of the action potential, however it must be acknowledged that the canine cardiac action potential is quite different from the murine cardiac action potential. Pacioretty *et al.,* (1992) published an abstract on the Xmd and *mdx* action potential characteristics obtained from isolated myocytes. The *mdx* ventricular action potential duration was unchanged in animals less than 6 months of age, while the action potential duration is significantly shorter in older animals. The abstract does not elucidate on actual ages or methods of cell isolation or recordings. The abstract did however speculate that the transient outward current may be increased, and the inward calcium current decreased in DMD, without providing any evidence to support the speculations. The cellular cytoskeleton contributes to the regulation of both voltage- and ligand-gated ion channels, and L-type calcium channels in cardiac and smooth muscle have been reported as being

regulated by actin filament organization (Sasaki *et al.*, 1987). This is important in dystrophin-deficiency, as actin filament organisation may be disrupted.

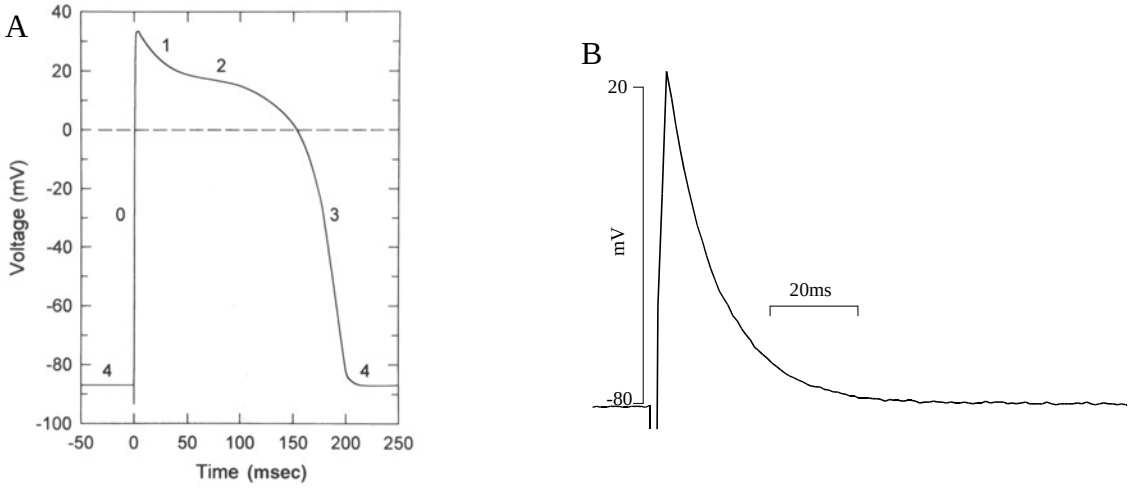

Figure 2.5 A comparison of human and murine action potentials. A A human ventricular cardiac action potential. 4) Resting membrane potential is set by a large K^+ permeability due to a combination of the leak K^+ channel and a voltage-gated K^+ channel (called the inward rectifier K^+ channel) that is open at rest 0) The rising phase of the action potential is due to the cardiac voltage-gated Na^+ channel. 1-2) As the voltage-gated Na^+ channels produce the rising phase and then start to inactivate two channels will now be opening, the delayed rectifier K^+ channel and the L-type Ca^{2+} channel. This plateau is a balance between the open Ca^{2+} channels and the open K^+ channels. 3) Finally the L-type Ca^{2+} channels inactive and the voltage-gated K^+ channels will now dominate and the membrane potential will repolarise to resting membrane potential. Then the voltage-gated K^+ channels will close, the voltage-gated Na^+ channels will switch from the inactive to the closed state and the membrane is set back at 4) ready to fire again. B A representative murine atrial action potential from a C57 mouse in the absence of drug for comparison. The dominant ion channels are still represented, although the contribution of the L-type calcium channel to the plateau phase is negligible.

2.6.1.1 L-type Calcium Channels

The mechanism mediating the majority of calcium influx in adult mammalian myocardium is the specific voltage-sensitive L-type channel which is often called the dihydropyridine receptor after the specific, high affinity blocking agent (Schramm *et al.*, 1983). T-type or fast current via the T-type calcium channels is negligible in most ventricular cardiomyocytes (Bers, 2002), although it is somewhat more important in

skeletal muscle. The L-type Ca^{2+} channel is the most sophisticated of all surface membrane channels consisting of a functional main unit (α_1) containing four domains, each with six spans, a voltage sensor and a pore loop. It contains at least three other subunits and a number of phosphorylation sites at the C-terminal (Fig 2.6).

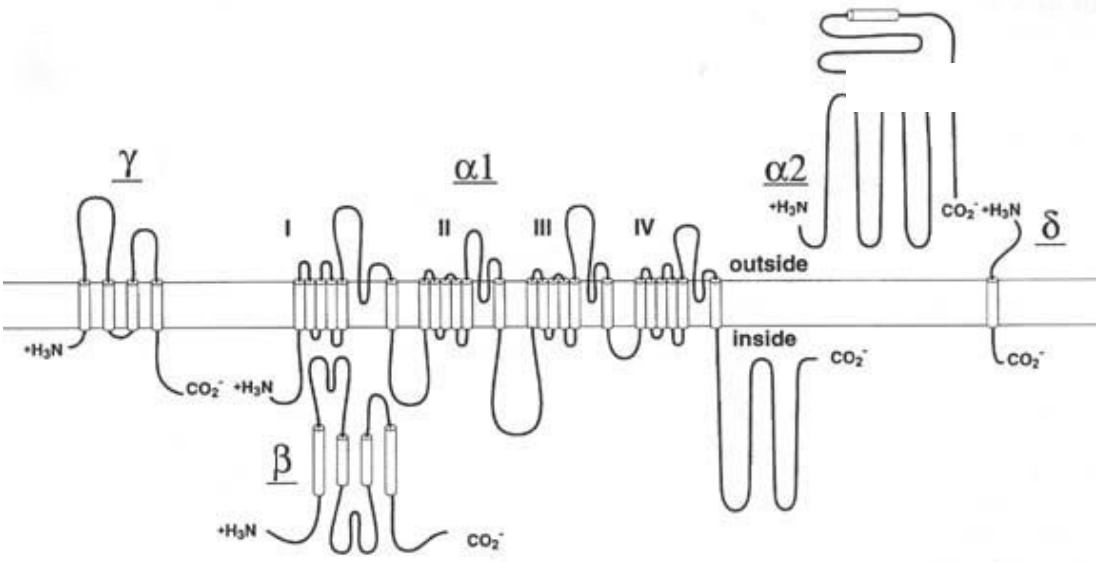

Figure 2.6 The subunits of the L-type calcium channel. The structure consists of four subunits each with six transmembrane spans and a pore loop. From http://medweb.bham.ac.uk/research/calcium/SupportFiles/subunit3.htm

Thus it is a voltage – and at the same time receptor-operated channel. Drugs may bind to the L-type calcium channel and induce increased opening of the channel. L-type calcium channels are located primarily at the sarcolemmal SR junctions where the RyR exist. Opening of the channel is usually voltage activated, with depolarisations to -40mV causing opening of the L-type calcium channels. Channel inactivation can be mediated by voltage or chemical mechanisms. Normally repolarisation of the myocytes initiates inactivation so prolongation of the APD (ie delayed repolarisation) will delay inactivation, therefore the channels remain open for a longer period of time. During excitation-contraction coupling, SR calcium release also contributes to inactivation of the current through the L-type calcium channels by a negative

feedback mechanism. The total calcium influx through the L-type calcium channel is reduced by about 50% when SR calcium release occurs (Bers, 2002). Thus SR calcium release and the L-type current can create local negative feedbacks on calcium influx (Bers, 2002). When there is high calcium influx or release, further influx of calcium is turned off (Bers, 2002). Increased calcium influx through L-type calcium channels can in turn produce an increase in SR calcium content that may induce arrhythmia (Tweedie *et al.,* 2000).

Because of their central role in excitation-contraction coupling, L-type calcium channels are a key target of the therapeutic class of drugs known as L-type calcium channel blockers used to regulate chronotropic and inotropic actions. L-type calcium channel blockers, a group of organic substances that bind to specific sites at the calcium channels, are now well established in the treatment of angina pectoris, arterial hypertension and supraventricular arrhythmias. They are not only important therapeutics, but are also valuable tools for the study of the function of L-type calcium channels. Based on their pharmacological profile they can be divided into three classes: (1) dihydropyridines (eg. nifedipine), (2) phenylalkylamines (eg. verapamil) and (3) benzothiazepines (eg. diltiazem). Pharmacological observations suggested that the three antagonists bind to three separate receptor sites on the α_1-subunit of L-type calcium channels that are allosterically linked (Hockerman *et al.,* 1997; Nakayama & Kuniyasu, 1996). The three classes differ in their pharmacological profile and safety, with differences in their tissue selectivity. Although all these compounds exhibit negative inotropic effects, they exhibit different chronotropic effects due to different influences on neuro-hormonal activity (Hjemdahl & Wallen, 1997; Noll *et al.,* 1998).

2.6.1.1.1 Dihydropyridines

The L-type calcium channel represents the major entry pathway of extracellular calcium. The DHPR agonist and antagonist molecules interact with distinct sites on the α_1-subunit of the L-type calcium channel (Tang *et al.*, 1993). Nifedipine is a commonly used representative of dihydropyridines (Table 2.2). It selectively inhibits the transmembrane influx of calcium ions into cardiac muscle and vascular smooth muscle. As a consequence, nifedipine dilates major coronary arteries and arterioles in normal and ischaemic regions, inhibits coronary artery spasm, reduces myocardial oxygen requirements and decreases peripheral vascular resistance.

Dihydropyridine binding is voltage dependent, and this may explain the higher selectivity of this class of drugs for vascular smooth muscle, as it is more depolarised and can undergo a more sustained depolarisation than cardiac muscle (Bers & Perez-Reyes, 1999). Vascularly selective dihydropyridines usually elicit increases in heart rate *in vivo* by a vasodilatation-triggered, baroreceptor-mediated reflex increase in sympathetic tone, renin release and elevated plasma catecholamines, resulting in indirect cardiostimulation (Hjemdahl & Wallen, 1997; Scholz *et al.*, 1997). The radiolabelled [^{3}H]-PN 200-110 acts similarly to nifedipine by blocking the dihydropyridine site to block the L-type calcium channel, but is used for ligand-receptor binding studies.

2.6.1.1.2 Phenylalkylamines

Verapamil, a representative of phenylalkylamines binds at an internal site on the α_1-component of the L-type calcium channel (Table 2.2). Its binding is facilitated by the repetitive depolarisation of cardiac tissue, a phenomenon described as use-

dependence. The distinction between voltage- and use-dependence may explain why this drug is not as highly selective as nifedipine (its activity increases with a maintained level of depolarisation), instead being equipotent for both the myocardium and the vasculature (Ferrari *et al.,* 1994). The mechanism of the anti-anginal and antiarrhythmic effects of verapamil is related to its specific cellular action of selectively inhibiting transmembrane influx of calcium in cardiac muscle and in cells of the sinoatrial (SA) and atrioventricular (AV) nodes. Verapamil is also a potent smooth muscle relaxant. Its vasodilatory and myocardial contractility depressant properties are largely independent of autonomic influences and this is evident by normal plasma noradrenaline measurements after verapamil administration.

2.6.1.1.3 Benzothiazepines

Diltiazem, a benzothiazepine is also a calcium ion influx inhibitor (Table 2.2). Like verapamil, diltiazem is prominently frequency-dependent. This largely contributes to its anti-arrhythmic and cardiac depressant action (Triggle, 1999). It also decreases sinoatrial and atrioventricular conduction in isolated tissues and has a negative inotropic effect in isolated myocardial preparations. It is used for the treatment of hypertension and angina as it dilates epicardial and subendocardial arteries.

Furthermore, an inhibitory effect on the mitochondrial Na^{+}/Ca^{2+} exchange (NCE) has been claimed for diltiazem that is unique among calcium channel antagonists (Vaghy *et al.,* 1982; Schwartz, 1992). This effect may, in turn, decrease oxidative phosphorylation and the production of high-energy phosphates (Cox & Matlib, 1993).

2.6.2 The Sarcoplasmic Reticulum

2.6.2.1 SR Calcium Release

Calcium is released from the intracellular store by release channels located in the junctional part of the reticulum adjacent to the T-tubules. They have a tetrameric structure with huge cytoplasmic domains, which include associated intraluminal calcium binding proteins such as calsequestrin. It is now called the Ryanodine receptor (RyR) after the experimentally used channel blocking alkaloid. During each contraction cycle the SR is loaded partly by calcium ions entering the cell but mainly by calcium ions that have just been released from the actomyosin interaction. Reduced SR function is described in various forms of cardiac hypertrophy and heart failure (Meyer *et al.,* 2001).

Dysfunction in a small number of SR Ca^{2+} release channels has been shown to profoundly affect cardiac function (Meyer *et al.,* 2001). The cardiac ryanodine calcium release channel is stimulated to release calcium by calcium influx via the L-type calcium channels. In cardiac muscle, calcium release from the SR is stimulated by caffeine (mM range), by ryanodine (nM range) and by calcium (μM range), and inhibited by higher concentrations of ryanodine (μM range) and ruthenium red (Marks, 2001; Ehrlich *et al.,* 1994). Caffeine has a dual action on calcium flow, by inhibiting SERCA and inducing opening of the ryanodine receptor (Ritter *et al.,* 2000). Caffeine also has an effect of increasing myofilament sensitivity to calcium (Wendt & Stephenson, 1983).

Ryanodine has been shown not to interfere with SR sequestration (Bers & Bridge, 1989). Dantrolene acts to inhibit calcium release via the Ryanodine receptors on the

SR (Table 2.2). Dantrolene is used clinically in the treatment of malignant hyperthermia (Bertorini *et al.,* 1991). In malignant hyperthermia, like DMD, there is a defective influx and efflux of calcium from the SR. Dantrolene has undergone clinical trials in DMD patients over a two-year period with a reduction in serum creatine kinase observed (Bertorini *et al.,* 1991). The authors also observed a trend towards a "lessening of muscle deterioration" (Bertorini *et al.,* 1991) during the dantrolene trial. Therefore drugs that decrease intracellular calcium levels may be of therapeutic value in DMD, although more extensive trials need to elucidate mechanisms of action and effectiveness in reducing the intracellular calcium overload associated with dystrophin-deficiency.

2.6.2.2 SR Calcium Sequestration

Cytosolic calcium removal is essential for relaxation of the myocardium. The onset of relaxation is synchronised with repolarisation. This feature is important physiologically because frequency-dependent shortening of the action potential abbreviates not only the refractory period but also the contraction-relaxation cycle and in turn causes a relative prolongation of ventricular filling time. In rats and mice, which have a high level of activity of SERCA and a relatively high $[Na^+]_i$, NCX is responsible for approximately 10% of relaxation (Barry, 2000). Contributions of each of the calcium removal pathways in rodent heart are as follows: 92% of calcium sequestration and/or extrusion by the SERCA, 7-10% by the NCX and approximately 1% by the slow systems (sarcolemmal Ca^{2+}-ATPase and the mitochondrial calcium uniporter) (Bers, 2002). SERCA therefore plays the major role in relaxation of the myocardium and is regulated by an associated inhibitory protein, phospholamban

Table 2.2 Pharmacological agents that affect calcium handling in cardiac myocytes.

	Calcium influx modulators		***SR calcium flux modulators***
1. L-type calcium channel modulators	***Stimulators***	***Blockers***	
a) Dihydropyridines	Bay K 8644	Nifedipene	
b) Phenylalkylamines		Verapamil	
c) Benzothiazepines		Diltiazem	
2. SR calcium pump inhibitors			Caffeine, Cyclopiazonic Acid
3. RyR stimulators, SR calcium channel release promoter			Ryanodine, Caffeine
4. SR calcium channel release inhibitor			Dantrolene

(PLB). Decreases in the levels of PLB or increases in its phosphorylation status result in an increase in the apparent calcium affinity of SERCA, and augment cardiac contractile parameters (Sato *et al.*, 2001). The ratio of PLB/SERCA has been accepted as a major determinant of lusitropy (Mirit *et al.*, 2000). SERCA regulation is of vital importance, as overexpression of SERCA and a higher accumulation of SR calcium have been linked with an acceleration of spontaneous cell death caused by protease-induced apoptosis (Culligan & Ohlendieck, 2002). Alternatively, an underexpression or dysfunction of SERCA will lead to an accumulation of cytosolic calcium, a dysfunctional SR and a lengthened relaxation time. Relaxation time has also been determined to be impaired at higher stimulation frequencies, and when intracellular calcium is elevated (Maier *et al.*, 1998).

Specific inhibitors of calcium removal mechanisms are important pharmacological tools that may help to elucidate functional differences between normal and

dystrophin-deficient cardiac tissues. Cyclopiazonic acid (CPA) is able to inhibit SERCA from functioning so that uptake of calcium to the SR is abolished. Thapsigargan is a selective inhibitor of SERCA in cardiac muscle. Concentrations higher than 50μM of thapsigargin and CPA are required in multicellular preparations of rat and rabbit heart to induce significant inhibition of SERCA (Baudet *et al.*, 1993; Pery-Man *et al.*, 1993). Both thapsigargin (Nario & Satoh, 1996) and CPA (Pery-Man *et al.*, 1993) have been shown to decrease force of contraction, decrease time to peak force, attenuate the force-frequency relationship and significantly delay relaxation time (Kocic *et al.*, 1998).

2.6.3 Regulation of Responsiveness to Calcium in the Heart

Cardiac calcium cycling involves movement of calcium ions from the extracellular space through L-type calcium channels to the cytosol. This movement of calcium ions initiates calcium-induced calcium release (CICR). CICR initiates a massive outflow of calcium from the intracellular store, the sarcoplasmic reticulum (SR). All calcium ions in the cytosol are able to bind to the contractile proteins to produce shortening of the myocardial fibres. Finally removal of calcium to produce relaxation involves extrusion of ions to the extracellular space by the sodium-calcium exchanger (NCX) and sequestration of calcium back into the SR by the sarco-endoplasmic reticulum ATPase (SERCA).

Three features of cardiac calcium handling are unique. First, the voltage sensitivity of the RyR is dwarfed by the sensitivity to calcium ions entering the cell through the membrane channels. Therefore CICR becomes the major influence in SR calcium release. Second, the amount of calcium release and hence the force of contraction

depends on autonomic heart rate variability and variations in the availability of reticular calcium that account for the force-frequency relationship of the myocardium. Third, an increased sarcomere length increases the sensitivity of troponin C to calcium, partly accounting for the Starling principle (Metzger *et al.*, 1989). There are also differential interactions of calmodulin with the RyR channels that may contribute to differences in the calcium dependence of SR calcium release in cardiac muscle (Fruen *et al.*, 2000).

Importantly in the pathophysiology of high intracellular calcium and in normal conditions, high intracellular calcium favours calcium efflux, whereas positive membrane potentials and high intracellular sodium favour the NCX operating in reverse mode. The NCX has a reversal potential that depends on the electrochemical gradients for both calcium and sodium. At rest, this reversal potential is around -40mV (Niggli, 1999). A depolarisation of the cell membrane beyond the reversal potential is expected to activate calcium influx via the NCX, for example, early during the action potential, immediately before the intracellular calcium concentration starts to rise. Later during the action potential, the elevation of intracellular calcium shifts the reversal potential of the NCX to more positive potentials and the NCX starts to remove calcium from the cytosol (Niggli, 1999).

2.7 Potential Sites of Dysfunctional Calcium Handling in Dystrophic Hearts

Calcium homeostasis in cardiomyocytes is maintained via precise control of intracellular calcium concentrations in a range from ~ 100nM during diastole to a

peak of ~ 1000nM in systole (Marks, 2001). In failing myocardium, cardiac force may be insufficient due to modification of the calcium sensitivity of the myofilaments, and/or a deterioration of the calcium signals due to dysfunction in one of the calcium handling proteins (Niggli, 1999). Studies on failing hearts have found resting intracellular calcium to be slightly elevated whereas calcium transients were reduced in amplitude and exhibited a slower decay (Niggli, 1999). For efficient excitation-contraction coupling and relaxation, the cycling of intracellular calcium must be rigidly linked to sarcolemmal depolarisation during the action potential (Bers, 2002). Thus, a longer opening of L-type calcium channels or an increase in their density, or SR calcium overload would therefore produce a greater intracellular calcium concentration which should theoretically produce action potential duration prolongation (APD). Sustained depolarisation of the cardiomyocyte plasma membrane decreases the rate of extrusion of calcium by the NCX. In general, less calcium is extruded by the NCX at more positive potentials. This voltage-dependence of the NCX is such that a prolonged APD leads to higher intracellular calcium levels and decreased calcium extrusion (Marks, 2001). Therefore a dysfunction in one mechanism of calcium handling may alter other processes involved in calcium regulation causing a cascade effect.

It is not clear yet whether alterations of cardiac calcium signalling are pathogenic to a particular disease or an adaptive consequence of deteriorated cardiac function (Niggli, 1999). It appears probable that calcium channel abnormalities play a role in the potential for arrhythmias in DMD (Sadeghi *et al.,* 2002). SR calcium overload has also been proposed as a contributing factor to the development of aberrant calcium fluxes due to calcium influx via the L-type calcium channel. Thus both the L-type

calcium channel and the RyR have been implicated in the dysregulation of calcium signalling that may contribute to cardiac arrhythmias (Marks, 2001). In other studies of cardiac dysfunction, changes were observed in the expression of calcium handling proteins and/or their mRNA and often these changes were paralleled by alterations of transport function. In yet other studies, changes of calcium signalling appeared to result from a functional modification of a particular transporter and not from a change in the amount of expressed protein (Niggli, 1999). Therefore both protein and mRNA expression and function should be investigated concurrently to correctly ascertain the basis for dysfunctional calcium handling.

Given that a calcium overload of all muscle types seems to be associated with myopathy in dystrophin-deficiency, there is a requirement for further study to disseminate potential mechanisms of the calcium overload.

2.7.1 The L-type Calcium Channel

The DHPR are a point of contention in research into dystrophin-deficiency and other myopathies associated with a loss of the DAGPC. Studies have shown either no change or an increase in DHPR, dependent on the model of dystrophin-deficiency used and the age of the experimental animals. Two studies have evaluated the L-type calcium channel in *mdx*. Alloatti *et al.,* (1995) studied currents from the L-type calcium channel and Sadeghi *et al.,* (2002) determined interaction of the *mdx* cardiac L-type calcium channel with actinin and dystrophin-binding proteins. Neither study showed conclusive evidence for changes in L-type calcium channels in *mdx.* Sadeghi *et al.,* (2002) showed that inactivation was delayed in the cardiac L-type calcium channel in *mdx* neonatal cardiomyocytes. How this related to activity of adult *mdx*

myocytes that exhibit myopathy is unclear. Influx mechanisms as the main source for calcium entry into the cell remain a potential cause for intracellular calcium overload in dystrophin-deficient conditions.

In cardiac myocytes from *mdx* mice, inactivation of the L-type calcium channel was reduced by a positive shift in the voltage dependence of activation, a likely allosteric change in channel conformation that made it more sensitive to stimulation by the β-adrenergic agonist *l*-isoproterenol and the dihydropyridine agonist *l*-Bay K 8644 (Sadeghi *et al.,* 2002).

Verapamil has been reported to reduce heart lesion in dogs and dystrophic hamsters (Reimer *et al.*, 1977; Wrogemann & Pena, 1976; Jasmin *et al.*, 1979), inhibit the protein degradation in *mdx* myotubes (Kamper & Rodemann, 1992), and also inhibit calcium-induced efflux of CK (Anand & Emery, 1982) and it thus may be useful in treatment of DMD-associated cardiovascular disorders.

2.7.2 SR Mechanisms

Uptake mechanisms such as SERCA have been shown to be altered in conditions where an abnormality of calcium handing is already present. This along with a delayed relaxation time exhibited in *mdx* tissues previously (Alloatti *et al.,* 1995) suggests that there may be a role in the cardiac dysfunction for SERCA. A recent report indicated a downregulation of SERCA in *mdx* heart in 5 month old mice (Rohman *et al.,* 2003). It is unclear whether SERCA is altered at 12-14 weeks in *mdx* myocardium, and whether potential alterations contribute to cardiomyopathy observed in dystrophin-deficiency. Sapp *et al.,* (1996) observed decreased force in *mdx* left

atria compared to control, especially at long test intervals. The authors suggest that there may be a leaky SR or dysfunctional SERCA. Since relaxation time has also been shown to be delayed in both *mdx* atria (Sapp *et al.,* 1996) and DMD ventricles, there is a possibility that dystrophin-deficiency leads to a dysfunctional SERCA.

2.7.2.1 The Ryanodine Calcium Release Channel

The ryanodine receptor as the release channel for calcium from the SR remains a candidate for dysfunctional calcium handling. Two reports have described cardiac ryanodine receptors in dystrophic cardiac tissue. Both studies observed a downregultion of the ryanodine receptor as measured by binding sites for ^{3}H-ryanodine in cardiomyopathic hamsters (Lachnit *et al.,* 1994) and decreased levels of ryanodine receptor mRNA in *mdx* (Rohman *et al.,* 2003). Rohman *et al.,* (2003) used 5 month old *mdx* mice for their study, it is unknown whether levels of the ryanodine receptor are altered at 12-14 weeks when the cardiomyopathy is first observed, or when the changes observed in their study are manifested.

2.7.3 Calcium Leak

The possibility of an SR calcium leak cannot be discounted in *mdx* cardiomyocytes. Studies have shown that SR calcium stores in ryanodine-treated animals can be depleted during prolonged rest periods (Meyer *et al.,* 2001). The leak-induced reduction in SR calcium load was associated with a prolongation of relaxation and a slower rate of contraction. Cardiac hypertrophy was also evident in the study, and atrial natriuretic factor mRNA was increased while SERCA mRNA was decreased (Meyer *et al.,* 2001). In dystrophin-deficient conditions a delayed relaxation of the myocardium has been observed, but rate of contraction is usually normal. Since

Meyer *et. al.* (2001) showed that an SR leak can lead to contractile dysfunction and altered SERCA it is important to determine whether such a SR leak develops in dystrophic hearts.

2.7.4 Calcium Binding and Associated Proteins

Several calcium-related signalling molecules, such as calcineurin, calmodulin (CaM)-kinase, and calcium-dependent protein kinase C (PKC) have been suggested to play key roles in myocardial hypertrophic responses (Sato *et al.*, 2001). Calcium regulatory proteins such as calcineurin have been shown to be involved in the hypertrophic response that precedes heart failure (Marks, 2001). The RyR is a macromolecular signalling complex in which signalling proteins, including kinases, phosphatases and adaptor or anchoring proteins, are bound to specific binding domains on the cytoplasmic portion of the channel (Marx *et al.*, 2000). The RyR is phosphorylated by PKA, PKC, PKG and CamKII (Witcher *et al.*, 1992; Takasago *et al.*, 1989; Hohenegger & Suko, 1993; Hain *et al.*, 1995). Defective regulation of the RyR in heart failure is associated with PKA hyperphosphorylation resulting in increased sensitivity to calcium-dependent activation (Marks, 2001). PKA phosphorylation affects at least three important targets that regulate cardiac excitation-contraction coupling: the L-type channel, phospholamban which regulates SERCA activity and the RyR. In failing hearts, PKA mediated phosphorylation of RyR is over-stimulated and pathological consequences could include depletion of SR calcium stores required for EC coupling as well as aberrant release of SR calcium during diastole which may serve as triggers for fatal cardiac arrhythmias (Marx *et al.*, 2000). Calcineurin and p38 mitogen-activated protein kinase (MAPK) are up-regulated in the hearts of *mdx* mice (Nakamura *et al.*, 2002). Phosphorylated p38 MAPK, phosphorylated extracellular

signal-regulated kinase 1/2 and calcineurin are up-regulated in exercised *mdx* hearts compared to exercised C57 or non-exercised *mdx* hearts. These data suggest that physical exercise accelerates the dystrophic process through activation of intracellular signalling molecules in dystrophin-deficient hearts (Nakamura *et al.,* 2002). The SR calcium load and subsequent release are regulated by calsequestrin, a luminal SR protein, with high capacity and low affinity for calcium (Sato *et al.,* 2001). Transgenic mice overexpressing calsequestrin show disturbed calcium handling associated with cardiac hypertrophy (Meyer *et al.*, 2001).

Skeletal muscle studies in *mdx* have shown that the calcium binding proteins are altered, and not in as great an abundance as in normal skeletal muscle (Culligan *et al.*, 2002). There is a possible role for dysfunctional SR calcium binding in the cardiomyopathy associated with dystrophin-deficiency.

2.7.5 Calcium Efflux

Finally, efflux of calcium may be affected in dystrophin-deficient myocardium, since the primary cause of the cardiomyopathy is a loss of structural integrity of the sarcolemma. The NCX may be reduced, dysfunctional, or contributing to the calcium overload by operating in reverse mode.

2.8 Insights From Skeletal Muscle

Dystrophin-deficient skeletal muscle has been studied extensively. The major findings in regard to calcium regulation in *mdx* may offer some insight into the dysfunction in cardiac muscle. Dystrophin-deficient skeletal muscles undergo a characteristic pattern

of myocyte necrosis and regeneration (Cullen & Mastaglia 1980; Torres & Duchen, 1987). Structurally, the T-tubules from *mdx* mice have been examined using electron microscopy and shown to be abnormal (Lucas-Heron *et al.,* 1987), and *mdx* myotubes have a depressed SR and/or SERCA function (Bakker *et al.,* 1993). *Mdx* skeletal muscles produce less force than control, and this force decrement was not simply due to fibre necrosis (Coulton *et al.,* 1988). Skeletal muscle myotubes (Bakker *et al.,* 1993) and fibres (Turner *et al.,* 1991; Ruegg & Gillis, 1999; Mallouk *et al.,* 2000) have been shown to have a higher resting intracellular calcium than control, although some reports have provided evidence against dystrophin-deficiency leading to an intracellular calcium overload (Head, 1993; Pressmar *et al.,* 1994; Gillis, 1996; Collet *et al.,* 1999). Reports have shown that reducing extracellular calcium can improve longevity of *mdx* myofibres (De Backer *et al.,* 2002). *Mdx* skeletal muscles are less able to regulate intracellular calcium levels in the region near the sarcolemma (Turner *et al.,* 1991). This elevation of intracellular free calcium is thought to stimulate the breakdown of muscle proteins by activating cellular proteases (Haws & Lansman 1991; Ruegg & Gillis, 1999).

Mechanosensitive calcium channels (leak calcium channels) are more active in *mdx* skeletal muscles compared to control (Turner 1991; Franco & Laansman 1990; Fong *et al.,* 1990), although other reports suggest that leak calcium channels are not responsibly for the entirety of the elevated intracellular calcium (Pressmar *et al.,* 1994). Haws and Lansman (1991) examined mechano-sensitive Ca^{2+} channel activity in *mdx* skeletal muscle fibres using cell-attached membrane patches at different stages of postnatal development. They revealed very high levels of activity in *mdx* patches, and observed that channel density decreased in normal fibres, whereas it remained

relatively constant in *mdx* fibres, as if channels are down-regulated in normal, but not *mdx* fibres during postnatal development (Haws & Lansman, 1991). They suggest that an early step in the dystrophic process in skeletal muscle may be an alteration of the mechanisms that regulate the expression of functional channels.

Calcium leakage in dystrophic muscle may also be produced by unusual physical interactions between acetylcholine receptors and the dystrophic cytoskeleton during processes associated with localisation and stabilisation of acetylcholine receptors (Carlson & Officer, 1996; Xu & Salpeter, 1997). It is possible that dystrophin is required for anchorage of other membrane-associated channels. Dystrophin deficient skeletal muscle membranes succumb to exercise-induced membrane ruptures more frequently than those of normal fibres (Stevens & Faulkner, 2000). However Dupont-Versteegden *et al.*, (1994) observed a training effect in soleus from *mdx*, a finding that suggested that exercise is not deleterious to *mdx* skeletal muscle. A study that allowed voluntary exercise in *mdx* showed that the dystrophin-deficient mice lacked endurance compared to control mice (Hara *et al.*, 2002). Overall, the weight of data suggests that dystrophin-deficient muscles are less able to continue exercise, and that sarcolemma tears originate from exercise-induced contractions. Ruptures of the skeletal muscle allow for the insertion of calcium leak channels into the sarcolemma during the natural processes of cell membrane resealing. Ion leak channels give rise to localised calcium elevations, contributing to a cycle of enhanced protease activity and leak channel activation (Culligan & Ohlendieck 2002). Recently the leak channels have been suggested to be store-operated transient receptor potential channels (Vandebrouck *et al.*, 2002).

Finally, Dangain & Neering, (1993) suggested that the developmental changes in myofilament sensitivity affect the contractile activity of dystrophic skeletal muscle, rather than an alteration in the calcium handling of the muscle. This postulation is in question, as Divet & Huchet-Cadiou (2002) found no difference between the calcium sensitivity of the contractile apparatus in *mdx* compared to control, even though the *mdx* maximum calcium-induced tension was significantly smaller.

2.8.1 Calcium Influx in Dystrophin-Deficient Skeletal Muscle

Although dystrophic skeletal muscle shows a two to three-fold increase in calcium influx, according to Ruegg and Gillis (1999) the voltage sensitive calcium channels play no role in the intracellular calcium overload. However, both the density of DHPR and the current density were shown to be higher in a DMD cell line than normal cells by Caviedes *et al.,* (1994) although this finding has not been replicated. Therefore current reports in skeletal muscle are contradictory. The cardiac isoform of the DHPR mRNA was upregulated in skeletal muscle from transgenic mice following acute injury (Pereon *et al.,* 1997) but an increase in protein of the DHPR in skeletal muscle has not been shown. The authors attributed this to proteolysis, although it is difficult to determine what mechanism is responsible. Insertion of a cDNA plasmid containing dystrophin has been shown to correct the defect in calcium homeostasis in *mdx* skeletal muscles (McCarter *et al.,* 1997).

2.8.2 Sequestration Mechanisms in Dystrophin-Deficient Skeletal Muscle

Lucas-Heron *et al.,* (1987) observed a decrease in SERCA levels in skeletal muscle of *mdx* compared to C57, and this has since been supported by Divet & Huchet-Cadiou (2002) who observed significantly slower SR calcium uptake following exposure to caffeine. Lucas-Heron *et al.,* (1987) also observed a decreased level of cardiac SERCA when compared to the skeletal muscle of the same species, but no differences in SERCA between dystrophin-deficient and normal mice. SR calcium quantity has been shown to be equivalent between *mdx* and normal mice (Divet & Huchet-Cadiou, 2002). A longer decay time of the calcium transient has been observed *mdx* adult fibres (Gordon & Stein, 1985) and is due to either defective regulation of energy metabolism or by functionally altered SR calcium pumps (Tutdibi *et al.,* 1999). Alternatively, Turner *et al.,* (1991) suggest that calcium sequestration mechanisms are not altered in dystrophin-deficient muscle but are slowed by the higher resting calcium. It is probable that the calcium sequestering mechanisms in *mdx* are continually coping with a calcium overload (Tutdibi *et al.,* 1999). Loss of calsequestrin-like proteins has also been observed (Culligan *et al.,* 2002). Skeletal muscle of *mdx* has also shown decreased oxidative phosphorylation probably as a result of calcium overload of the muscle fibres (Kuznetsov *et al.*, 1998).

2.8.3 Activation of Calcium-Dependent Proteolytic Enzymes

The marked elevation of calcium in dystrophic muscle may contribute to activation of calcium-dependent proteases such as skeletal muscle specific calpains (Culligan & Ohlendieck 2002). Alderton and Steinhardt (2000) suggest that “calcium influx

through calcium leak channels is responsible for the elevated levels of calcium-dependent proteolysis in dystrophic myotubes". Several authors have found an increase in the activity of calpains (Spencer *et al.,* 1995; Nagy & Samaha, 1986) that have been implicated in the proteolysis of calcium leak channels, constitutively activating these channels (Culligan & Ohlendieck 2002). Conversely, protease inhibitors have been shown to reduce calcium-induced protein degradation in *mdx,* suggesting that an increase in intracellular calcium mediates this process (Turner *et al.,* 1993).

2.9 Requirements for Further Studies

The current study aimed to determine whether the reported changes in intracellular calcium concentration were due to defective calcium handling mechanisms in the cardiac muscle of the mouse model of Duchenne muscular dystrophy. The study initially examined the function of the L-type calcium channel by measuring the potency and affinity of drugs that bind to the α_1-subunit of the L-type calcium channel of *mdx* myocardium. The action potential characteristics of *mdx* were then examined, and contractile and repolarisation characteristics in response to drugs that act at the L-type calcium channel.

The density and affinity of the DHPR was then measured, to confirm functional changes observed in the L-type calcium channel. The mRNA for the DHPR was also measured to determine whether regulation factors were altered.

The force-frequency relationship was determined in *mdx* myocardium to ascertain whether the ryanodine receptor or SR mechanisms were altered. The force-frequency relationship was also determined in the presence of ryanodine, dantrolene and caffeine. Rapid cooling contractures measured SR content and active mechanisms involved in sequestering calcium. The response of *mdx* myocardium to an inhibitor of SERCA was measured to determine whether sequestration mechanisms were altered in dystrophic myocardium. The mRNA of SERCA was also measured to determine whether regulation of SERCA was altered in response to dysfunctional calcium handling.

CHAPTER 3 – MATERIALS AND METHODS

3.1 Ethical Considerations

All animal experimentation conformed to NHMRC Animal Ethics guidelines and was approved by the University of Southern Queensland (USQ) Animal Ethics committee before the commencement of any experimentation.

3.2 Experimental Animals

Male C57BL/10ScSn (C57) mice and mutant C57BL/10ScSn *mdx* (*mdx*) mice were used. Mice were used in the age range of 12-14 weeks, and were age matched for all comparisons. Where possible, experiments alternated the use of *mdx* and C57 to avoid systematic bias in data acquisition. *Mdx* mice were obtained either from the USQ breeding colony or from the Animal Resource Centre, Nedlands, Western Australia. Since the two colonies were initiated from the same breeding stock, genetic variation was minimal. All C57 mice were purchased from the Animal Resource Centre. Animals were fed standard mouse chow with water *ad libitum* and housed at 21-24°C under a 12 hour light-dark cycle (6am-6pm).

3.3 Apparatus Calibration and Protocol Optimisation

Throughout all experimentation any apparatus that required calibration was calibrated prior to the commencement of the experimentation. For tissue bath experiments where force transducers were utilised, the transducers were calibrated with 1, 2 and 10mN weights to ensure accuracy. Before experimentation in the radioligand binding studies, the beta radiation-counter and pipettes used were calibrated. Tissue baths were cleaned thoroughly with concentrated nitric acid prior to the commencement of a

new protocol, and cleaned after every experiment utilising contaminant drugs. Nitric acid residues were thoroughly washed out with water purified by reverse osmosis (Ro water). Tissue and perfusion baths were also washed and scrubbed daily with Ro water.

Where a protocol had not been undertaken previously in our laboratory, extensive literature searches were undertaken initially, then the protocol was developed and optimised with and without preliminary use of animals as required.

3.4 Dissection of Cardiac Tissues

After being weighed, mice were anaesthetised by CO_2 inhalation and then euthanased by exsanguination (except where otherwise indicated). The heart was removed and the left and right atria were rapidly dissected free while beating in cold (4°C) pre-carbogenated (95% O_2:5% CO_2) Tyrode physiological salt solution (TPSS) (mM: NaCl 136.9, KCl 5.4, $MgCl_2.H_2O$ 1.0, $NaH_2PO_4.2H_2O$ 0.4, $NaHCO_3$ 22.6, $CaCl_2.2H_2O$ 1.8, glucose 5.5, ascorbic acid 0.3, Na_2EDTA 0.05).

The ventricular chambers were then separated if required, and either prepared for homogenisation, placed in RNA*later*™ or blotted and weighed if not used further. Ventricular tissue was either frozen at –70°C and later used for the radioligand binding protocol, or placed in RNA*later*™ and stored at –20°C for RT-PCR. Atrial tissues, when dissected free, were either immediately utilised for the functional studies (ie the tissue bath studies, microelectrode studies, the oxygen consumption experiments), or placed in RNA*later*™ and stored at –20°C for subsequent RT-PCR experiments.

3.4.1 Papillary Muscles

Attempts were made to use *mdx* papillary muscles in functional protocols, but their higher incidence of contracture or arrhythmias relative to atrial preparations prevented their continued use. These difficulties are presumably due to elevated intracellular calcium exacerbated by cutting injury occurring during dissection. Calcium chelators and butanedione monoxime (BDM) were also trialled in the dissection medium to reduce calcium-induced tissue injury, but *mdx* papillary muscles, which contracted initially, became non-functional before experimentation could be completed. In contrast, our laboratory found that C57 papillary muscles worked quite reliably and consistently, providing further evidence that the inherent calcium overload in *mdx* may be the causative factor. No reports using multicellular isolated *mdx* ventricular preparations have been published thus far. In contrast, several publications have reported significant findings using *mdx* atrial preparations (Lu & Hoey 2000a & b, Sapp *et al.*, 1996).

3.5 Tissue Bath Experiments

Tissue baths (25mL double jacketed) were used for several studies, including the concentration-response curves to Bay K 8644 and nifedipine, the force-frequency studies, and the experiments utilising rapid cooling contractures. Initially the same protocol was used for each of these procedures as follows. A stainless steel hook was placed in one end of each atrium to connect the atrium to the tissue holder made from a length of stainless steel (right atria) or plastic with electrode leads attached (left atria). A silk thread was tied to the other end of the atrium to connect it to a force transducer (FT-102, CB Sciences, Milford, MA, USA) to measure force of

contraction. Atria were subsequently suspended in warm (35±1°C), carbogenated TPSS in tissue baths. Data were recorded via a PowerLab system (AD Instruments) using Chart 3.5.6. Left atria were field stimulated by placing the atria between two platinum electrodes on the tissue holder (AMPI Master 8 stimulator; 1 Hz, 5 ms duration, 20% above threshold) and maintained under optimal preload, the length of tissue which produces the maximal contractile force. Tissues were allowed 45 min to equilibrate with repetitive washes by draining and refilling the bath; before the advent of the relevant test protocol. At the completion of all experiments, the atria were removed, blotted and weighed.

3.5.1 Concentration Response Curves for L-type Calcium Channel Drugs

Concentration-response curves were obtained by cumulative addition of the test compounds. Concentration-response curves were generated to calcium chloride to determine the maximum force of contraction attainable by the tissue. The tissues were then washed repetitively over 30 min to return the contractility to normal. Subsequently a concentration-response curve to the DHP antagonist nifedipine or agonist Bay K 8644 was generated. Similarly concentration-response curves were generated to diltiazem and verapamil.

As DHP drugs are sensitive to light with wavelengths below 450nm, all handling and experiments with Bay K 8644 and nifedipine were carried out under protection from light. In order to avoid indirect receptor-mediated effects of endogenous noradrenaline possibly released by Bay K 8644, tissues were incubated with the β-adrenoceptor blocker (±)-propranolol and α-adrenoceptor blocker prazosin for 30 min before the

concentration-response curve to Bay K 8644 was generated. After experiments with Bay K 8644, the tissue baths were cleaned with nitric acid to eliminate contamination of glassware and then flushed repeatedly with distilled water.

3.5.2 Rapid Cooling Contracture Experiments

3.5.2.1 Preliminary Studies

Preliminary studies for the rapid cooling protocol evaluated the response of the left atria to rapidly exchanging warm TPSS with ice-cold calcium-free TPSS. The solution was exchanged by draining the warm TPSS and replacing TPSS at 0°C with a syringe. Each rapid change elicited a contracture as expected. Temperature was monitored continuously through the preliminary studies to determine the time-course of the rapid cooling effect, that the temperature reached 0°C in the tissue bath, and the time-course of the return of the TPSS in the tissue bath to 35°C. The preliminary studies also evaluated the capability of the myocardium to return to normal force after each rapid cooling contracture (RCC) and evaluated the responsiveness of the tissue to subsequent exposure to cyclopiazonic acid.

3.5.2.2 Comparison of *mdx* and C57 left atria

The left atria were suspended in a 5mL tissue bath maintained at 35±0.5°C and fresh TPSS was exchanged every 10 min while the tissue equilibrated. The atria were field stimulated (5-10V, 0.5ms duration, 1Hz). RCCs were undertaken by cessation of stimulation, rapidly exchanging warm TPSS with ice-cold calcium-free TPSS (as per TPSS without calcium). The tissue was then rewarmed to 35˚C over a 3 min period by replacing with warm TPSS. After 3 min, this procedure was repeated a second and third time with each RCC labelled as RCC1, RCC2 and RCC3 respectively. The

tissue was rewarmed after RCC3 and stimulated to contract for a period of 2 min during which the twitch force returned to normal. This entire protocol was then repeated 2 more times. The RCC1 for the 1st, 2nd and 3rd replicate was averaged, and similarly with RCC2 and RCC3 to give an average for each RCC (see Fig. 3.1). After completion of the third replicate, the tissue was allowed to equilibrate again until force of contraction returned to values measured prior to the RCC protocol. A concentration response curve (0.5 - 40mM) to the SERCA-specific inhibitor cyclopiazonic acid (CPA) was then undertaken.

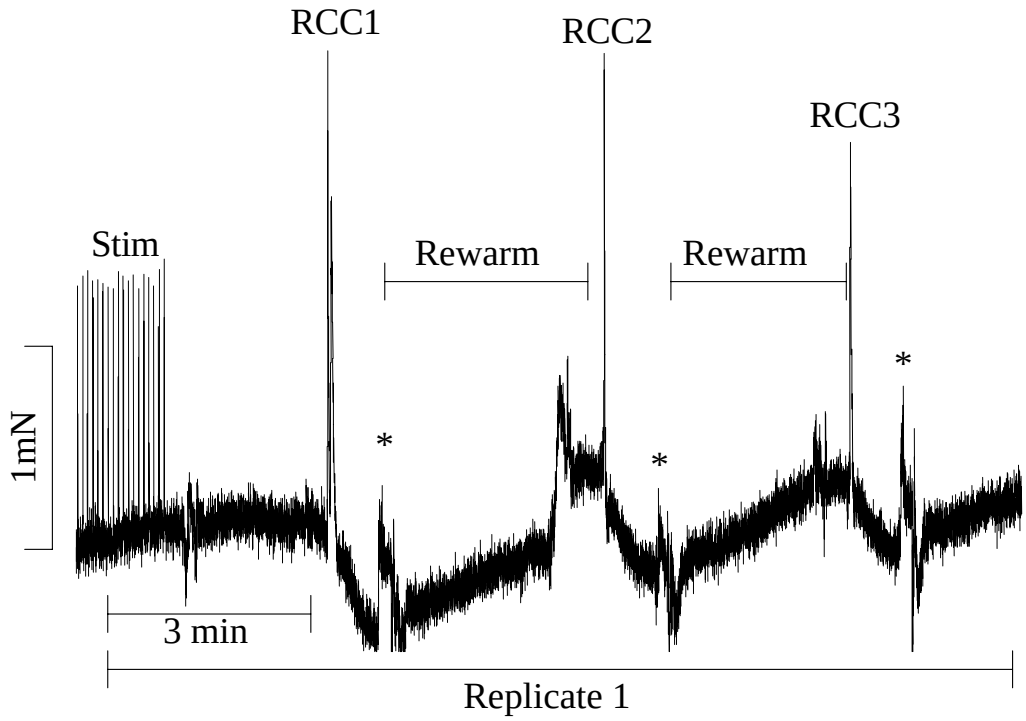

Figure 3.1: Rapid Cooling Contracture Protocol. Three rapid cooling contractures were elicited (RCC1, RCC2 & RCC3) per replicate. Between each RCC the atria was rewarmed over 3min. A wash is indicated by *.

3.5.3 Force-Frequency Experiments

The tissues were maintained under physiological conditions in 25mL water-jacketed tissue baths (35±0.5°C) at optimum preload, and allowed 30 min to equilibrate with

washes every 10 min. In preliminary control experiments, after the equilibration period a force-frequency curve was elicited (5 min at each of 0.05, 0.2, 1, 2 and 5 Hz with 1Hz between each change to restore force to control values; see Figure 3.2 for an example). This was repeated a second and third time to determine the extent of decay of force without the effects of any drug. Having confirmed no difference between the first, second and third force-frequency curves, subsequent experiments were conducted with the second and third curves being generated in the presence of increasing concentrations of the drug of interest (no more than two concentrations per tissue). The tissues were removed from the tissue baths, blotted and weighed.

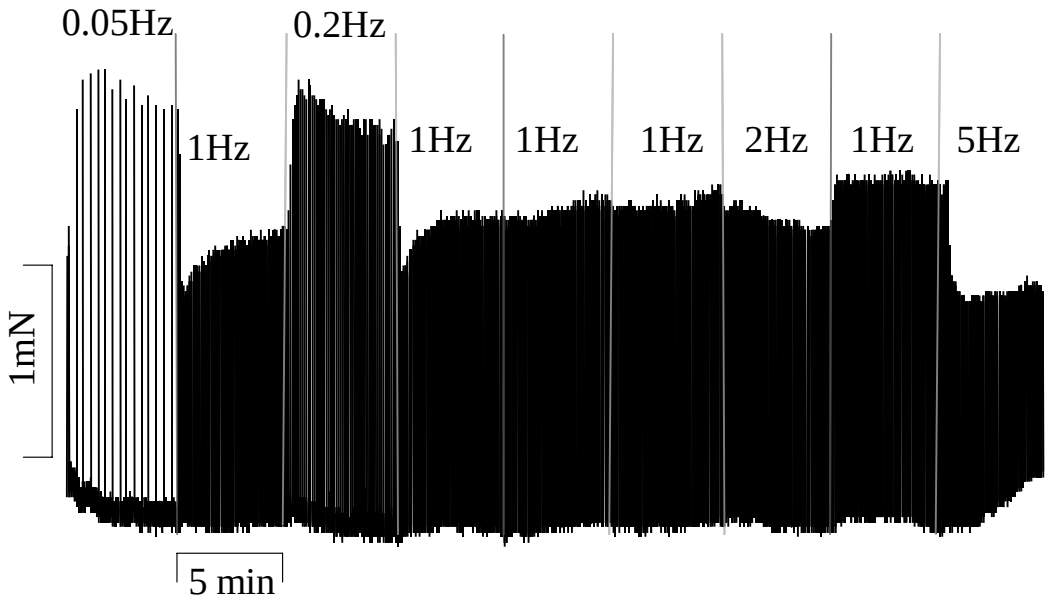

Figure 3.2 A typical force-frequency chart in the absence of drug. Each frequency was tested for 5min, with the tissue being stimulated at 1Hz in between the test frequencies until force returned to basal.

3.6 Microelectrode and Contractility Experiments

Left atria were dissected as described above in section 3.4. Tissues were placed in warm, carbogenated TPSS (35±1ºC) in a 1 mL chamber perfused at 3 mL/min, field stimulated (Grass SD9 isolated stimulator; 1 Hz, 0.5 ms duration, 20% above threshold) and allowed to equilibrate for 45 min. Force of contraction was recorded by a modified AE-801 SensoNor element. Tissues were impaled concurrently with a 3 M KCl filled microelectrode (resistance 2.5-20 MΩ) to record electrophysiological activity using a World Precision Instruments Cyto 721. All data was acquired at 1000Hz and analysed via a PowerLab system (AD Instruments) using Chart 3.5.6.

The tissues were initially exposed to the IC_{50} concentration of a calcium channel antagonist (as determined in the tissue bath studies) until the equilibrium response was attained and then exposed to the concentration of antagonist required to produce the maximum effect. The time interval for drug additions for all three calcium antagonists tested was 30 min and was sufficient to obtain an equilibrium response. As nifedipine and verapamil are sensitive to light, all handling and experiments with these agents were carried out under protection from light.

3.7 Radioligand Binding Experiments

3.7.1 Assay Development

Since this assay had not been used previously in our laboratory, several preliminary experiments were undertaken to optimize the protocol. Initially the incubation temperature was tested at 20°C and 35°C. Secondly, the optimal amount of incubation time was determined by removing incubation tubes at 0, 5, 15, 30, 60, 90, 120 and

150 min. Third, nifedipine was tested for displacement of the [^{3}H]-PN 200-110, and the optimal concentration to determine non-specific binding. The saturation concentration of [^{3}H]-PN 200-110 was also trialled, with 10nM being the highest concentration used in the trials, and 2nM determined to be high enough for saturation. Filters were tested for filtration of the membranes after incubation with and without pre-wetting. Similarly, the number of washes of the filters was trialled at 2, 5 and 10 washes. A 50mM Tris, a 50mM HEPES buffer, a 10mM Tris, and a 10mM HEPES (all with in mM EGTA 5, EDTA 1, $MgCl_2$ 4, Ascorbic Acid 1) buffer were trialled for incubation of the homogenate with the radioligand (all made to pH 7.4 with NaOH). Various dilutions of membrane protein were also trialled. Finally, fresh tissues and frozen ventricles were compared to confirm that receptor affinity and density were not significantly altered by freezing and storing the tissues.

3.7.2 Experimental Protocol

For each experiment two ventricles were pooled to obtain sufficient membrane for five points on a saturation curve. Two ventricles were thawed and then homogenized at 24 000 rpm by a Heidolph DIAX 600 in modified Tris incubation buffer (in mM Tris HCl 50, EGTA 5, EDTA 1, $MgCl_2$ 4, Ascorbic Acid 1, Trizma Base 50; pH 7.4 adjusted with NaOH). The homogenate was centrifuged at 1000g, and pellet discarded. The supernatant was centrifuged at 10 000g and the supernatant discarded. After resuspension in Tris incubation buffer, the membrane protein content was determined by Bradford assay using bovine serum albumin as the standard. The membrane was then diluted to 1mg/mL protein. Membrane (200μg) was incubated with increasing concentrations of [^{3}H]-PN 200 110 (0.1-2nM) and non-specific binding was determined by the addition of 0.1mM nifedipine. Samples were incubated

for 60 min at 35°C, and halted with the addition of 4mL ice-cold Tris incubation buffer. Samples were vacuum filtered over Whatman GFB filters and washed four times with ice-cold Tris wash buffer (in mM Tris 50, pH 7.4). Filters were incubated overnight with scintillant and counted the next morning. Prism was used to calculate non-linear curve fits and scatchard analyses of the data. Bmax was calculated using Prism and is defined as the density of the ligand receptor. Kd was also calculated using Prism and is defined as the affinity of the ligand [^{3}H]-PN 200 110 for the DHPR.

3.8 Reverse Transcriptase Polymerase Chain Reaction (RT-PCR) Experiments

3.8.1 Preliminary Experiments

Preliminary experiments were undertaken with each primer used in the study to determine whether the mRNA would be amplified. The assay was run as per the protocol below, but the solutions were run through a maximum number of amplification cycles to check for primer dimers and successful amplification of the bands (size of the band was checked against the ladder to ensure the correct location). Once each primer had successfully amplified the mRNA, the procedure was repeated until 20 cycles, then the solutions removed every 2 cycles to determine the optimal number of cycles.

3.8.2 Experimental Protocol

Animals were euthanased with an overdose of sodium pentobarbitone and the hearts rapidly excised. The ventricles were dissected free in cold TPSS and placed in

RNA*later*™ (Ambion) RNA stabilisation reagent for storage at -20 °C. RNA extraction was performed with the QIAGEN RNeasy® Mini Kit, utilising no more than 30 mg of tissue per sample obtained from the apex of the left ventricle. The tissue was lysed using a polytron rotor-stator homogeniser in a proprietary buffer containing guanidinium thiocyanate to liberate RNA prior to the extraction procedure. Lysates were then incubated with QIAGEN Proteinase K (>60 mAU/mL) for 10 min at 55 °C to ensure sample disruption was complete. RNA was consequently isolated via binding to a silica-gel-based membrane during a number of centrifugation procedures as recommended by the manufacturer's instruction. Total RNA samples were then stored at -80 °C in 2 μL aliquots until RT-PCR could be performed.

RT-PCR was performed by the two-tube method using QIAGEN Omniscript™ Reverse Transcriptase and QIAGEN HotStarTaq™ DNA Polymerase. Total RNA samples were thawed on ice and added to a reverse transcription reaction mixture, with a final volume of 20 μL and comprised of: 1x Buffer RT (supplied by QIAGEN); 0.5 mM dATP; 0.5 mM dCTP; 0.5 mM dGTP; 0.5 mM dTTP; 1 μM oligo $dT_{(15)}$; 10 units RNAsin® RNAse inhibitor (Promega); and 4 units Omniscript™ Reverse Transcriptase. Tubes containing the reaction mixture were incubated in a thermocycler (Corbett Research PC-960C) for 60 min at 37 °C to facilitate cDNA synthesis, followed by an inactivation step of 5 min at 93 °C and subsequent rapid cooling on ice. PCR reaction mixtures were consequently prepared using 2 μL of the reverse transcription product as template, with a final volume of 50 μL and comprised of: 1x PCR buffer (supplied by QIAGEN); 200 μM dATP; 200 μM dCTP; 200 μM dGTP; 200 μM dTTP; 0.2 μM each DHPR primer (TCC AGT TTA TAC TAC TTT GGC TGG T sense; ACT GAG GGC TCA TGT TTT GG antisense), SERCA

primer (GGT GCT GAA AAT CTC CTT GC sense; CTT TTC CCC AAC CTC AGT CA antisense), GAPDH primer (TTA GCA CCC CTG GCC AAG G sense; CTT ACT CCT TGG AGG CCA TG antisense) or β-Actin (AGC CAT GTA CGT AGC CAT CC sense; TCT CAG CTG TGG TGG TGA AG antisense); and 2.5 units HotStarTaq™ DNA Polymerase. All reactions were performed with 1.5 mM $MgCl_2$ contained in the 1x PCR buffer. Using the thermocycler, tubes were incubated initially for 15 min at 95°C to activate the HotStarTaq™ DNA Polymerase. Reaction tubes initially underwent 40 cycles to determine effectiveness of the primer. Subsequently, new reaction tubes underwent a number of cycles of amplification (empirically determined to be within the linear range of amplification), consisting of 15 s at 94 °C, 30 s at 55 °C and 60 s at 72 °C. A final program of 10 min at 72 °C was conducted to ensure all amplified product was fully extended. PCR product was visualised following gel electrophoresis by ethidium bromide staining and UV transillumination in an AlphaImager 2200 MultiImage cabinet. Spot densitometry was performed using the supplied software and the ratio of SERCA or DHPR band intensity to GAPDH band intensity for each sample calculated to allow a semi-quantitative comparison. The ubiquitous β-actin was also used as a housekeeper gene.

3.8.3 Primer Design

Where possible, primers were obtained from previously published articles. The primers were then tested using BLAST on the pubmed website. If primers were not obtained from published articles, the RNA gene sequence was identified using Entrez Nucleotide (http://www.ncbi.nlm.nih.gov:80/entrez/query.fcgi?db=Nucleotide), and run through a primer design program. The designed primers were tested for binding accuracy using BLAST (http://www.ncbi.nlm.nih.gov:80/BLAST/). Primers were

ordered from Invitrogen Life Technologies (Musgrave, Victoria, Australia), were desalted purity and had a 55% GC content.

3.9 Data Analysis

Raw data was first compiled in Microsoft Excel 97, collated and any mathematical transformations applied to the data. Final results were expressed as mean ± SEM. Means and SEM were transferred to a data plotting program (Sigma Plot or Prism) used for graphical purposes or further analyses. Either a two-tailed, unpaired Student's t-test was used for statistical comparisons, or a two-way ANOVA where indicated. A P level of <0.05 was considered to be statistically significant. For contractile and action potential data, a single stimuli was used from each dosage or time point to obtain this data. An EC_{50} or IC_{50} was calculated as the concentration that produces 50 % of the maximal response (EC for a positive inotropic response, IC for a negative inotropic response). A pD_2 was calculated as the negative log of the EC_{50} or IC_{50}. The strain potency used to compare potencies and affinities of drugs in both strains was calculated by dividing the EC_{50}, IC_{50}, Kd, Bmax or pixel intensity/unit area for *mdx* mice by the corresponding C57 value.

3.10 Drugs and Chemicals

All laboratory chemicals were purchased from Sigma Chemical Company, St. Louis, MO, USA except where otherwise indicated. Bay K 8644 **(**Bayer, Leverkusen) was dissolved in 100% ethanol at a stock concentration of 10^{-2} M and diluted once further in 50% ethanol and subsequently in milliQ water**.** Nifedipine was dissolved in 100% DMSO at a stock concentration of 10^{-2} M, and diluted once further in 50% DMSO

and subsequently in milliQ water. (±)–Verapamil hydrochloride and diltiazem hydrochloride were dissolved in milliQ water. Hot [^{3}H] PN 200-110 (Amersham Pharmacia Biotech, Buckingham Shire, England) had an activity of 71 Ci/mMol which was taken into account when expressing counts per minute as fmol/mg. Cyclopiazonic Acid was dissolved in DMSO as a 10mM solution, and further dilutions made in milliQ water. Ryanodine was dissolved in ethanol as a 1μM stock and further dilutions made in milliQ water; Caffeine was dissolved 0.1M HCl as a 0.5M solution and further dilutions made in milliQ water; Dantrolene was dissolved in milliQ water in a stock concentration of 1μM and further dilutions made with milliQ water from this stock. All RT-PCR reagents were purchased from Qiagen.

CHAPTER 4 – RESULTS

4.1 Morphometry

Whole mouse mass was significantly higher in C57, which is not surprising given the nature of the myopathy in *mdx.* Left atrial mass was not significantly different between the strains, but ventricular mass was heavier in C57 (P<0.001). Masses of tissues were still significantly higher when normalised for body mass. Ventricular tissues were used only for radioligand or molecular biology experiments. In the radioligand experiments, the amount of protein was standardised, so consideration of the difference in weight was not necessary. Similarly, for RT-PCR experiments mRNA was normalised to a housekeeper gene. The number of *mdx* used in the current study is much higher than C57, because *mdx* tissues were routinely used for assay development since the *mdx* were more readily available. Table 4.1 shows numbers of each species of mass and associated body and heart masses.

Table 4.1 Number and masses of mice used throughout the dissertation

	n	***Whole mouse mass (g)***	***Left atrial mass (mg)***	***Ventricle mass (g)***
mdx	215	25.0±0.3	18.5±0.9	0.135±0.002
C57	138	26.1±0.3*	19.1±0.8	0.157±0.003**

***P<0.01; **P<0.001 *mdx* compared to C57**

4.2 Calcium Influx Mechanisms

In this section the mechanisms of calcium influx into the myocardium in *mdx* were examined through a series of microelectrode and contractility experiments. These

experiments examined the action potentials in *mdx* and C57 and contractile responses to the L-type calcium channel drugs that act at the dihydropyridine, phenylalkylamine and benzothiazepine receptors. A series of radioligand experiments were undertaken to determine the affinity of a radiolabelled DHPR antagonist for its receptor and the number of DHPRs present. Finally RT-PCR experiments were utilised to determine DHPR mRNA expression.

4.2.1 Calcium Channel Agonist and Antagonist Concentration-Response Curves

4.2.1.1 Basal Measurements

Figure 4.1 shows an indicative recording of a single contraction in the absence of any drug. In *mdx* left atria, the basal force of contraction was lower in *mdx* (1.50±0.17mN) compared to C57 (1.91±0.18mN; $P<0.05$) with a subsequent concentration-response curve to calcium chloride revealing a reduced efficacy (*mdx* 3.44±0.21 mN, C57 4.11±0.3 mN; $P<0.005$ Fig 4.2A) and potency (pD_2 values *mdx* 3.40±0.08, C57 3.15±0.10; $P<0.05$). A longer relaxation time (Time to 90% relaxation; TR_{90}) was also evident in left atria from *mdx* mice (*mdx* 45.3±1.6ms (n=24); C57 39.0±1.7ms (n=24): Table 4.2 $P<0.01$), with no difference in time to peak force and dF/dt observed between *mdx* and C57 mice at basal forces.

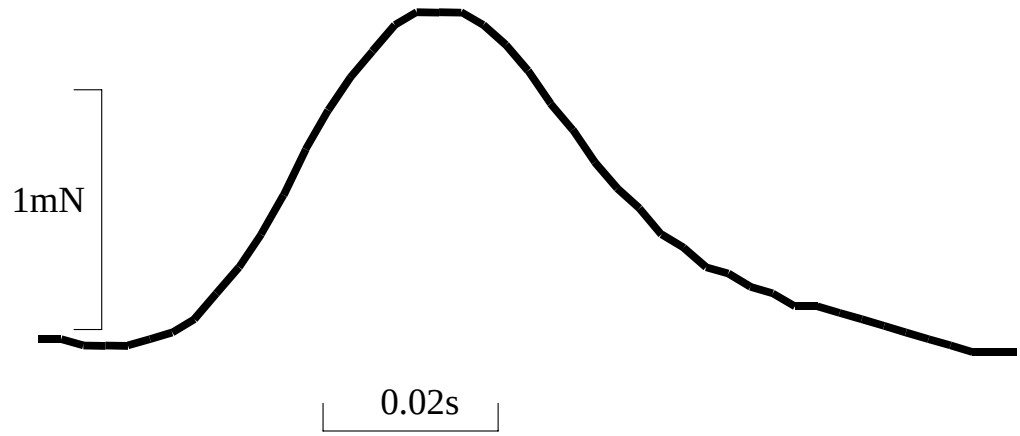

Figure 4.1 An indicative contraction from a C57 mouse. *Mdx* contractions had the same shape and approximate timecourse.

4.2.1.2 Response to the Calcium Channel Antagonists

All calcium channel antagonists reduced the force of contraction in left atria as expected. Nifedipine reduced the force of contraction similarly in left atria from both *mdx* and C57 but the potency was significantly reduced in left atria from *mdx* (pD_2 values: *mdx* 7.46±0.07; C57 7.75±0.10, $P<0.05$ Fig. 4.2). As expected the reduction in force was associated with a significant reduction in dF/dt upon exposure to the maximum concentration of nifedipine (*mdx* Basal 11.45±1.68 mN/s; max. effect 3.83±0.72 mN/s, $P<0.01$: C57 Basal 8.74±1.35 mN/s; max. effect 3.24±0.67 mN/s, $P<0.05$) without affecting the time to peak force. Nifedipine caused a further delay in relaxation in *mdx* only (Table 4.2). A strain potency ratio was calculated by dividing the potency of *mdx* by the potency for C57. The strain potency ratio for nifedipine was 1.9.

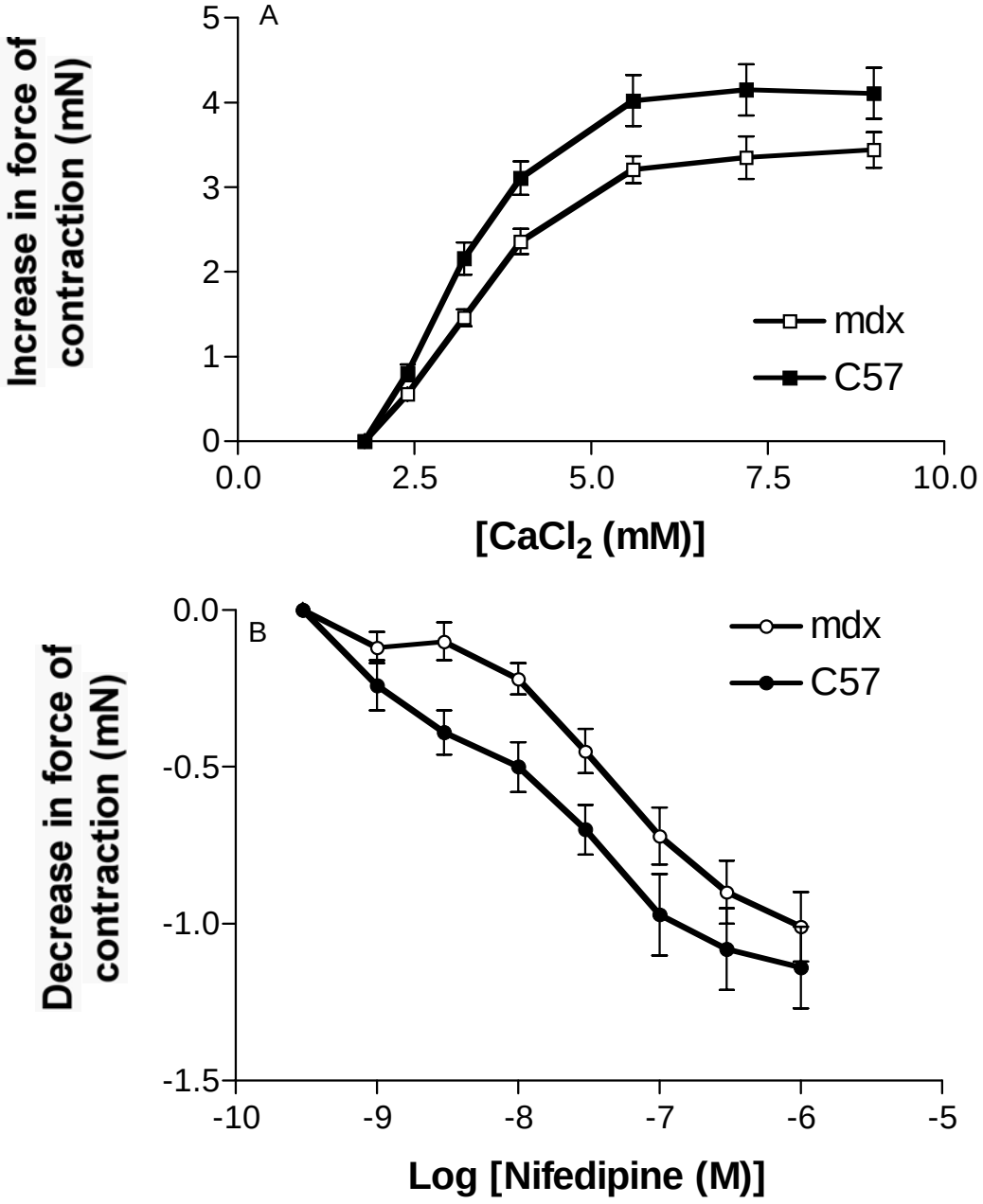

Figure 4.2 The effects of nifedipine on left atria, and the effects of extracellular calcium. A Response to extracellular calcium (n=24). B Effect of nifedipine on left atria contractile force. Basal force of contraction for *mdx* 1.50±0.17mN (n=10); for C57 1.91±0.18mN (n=8) measured prior to the CRC to nifedipine.

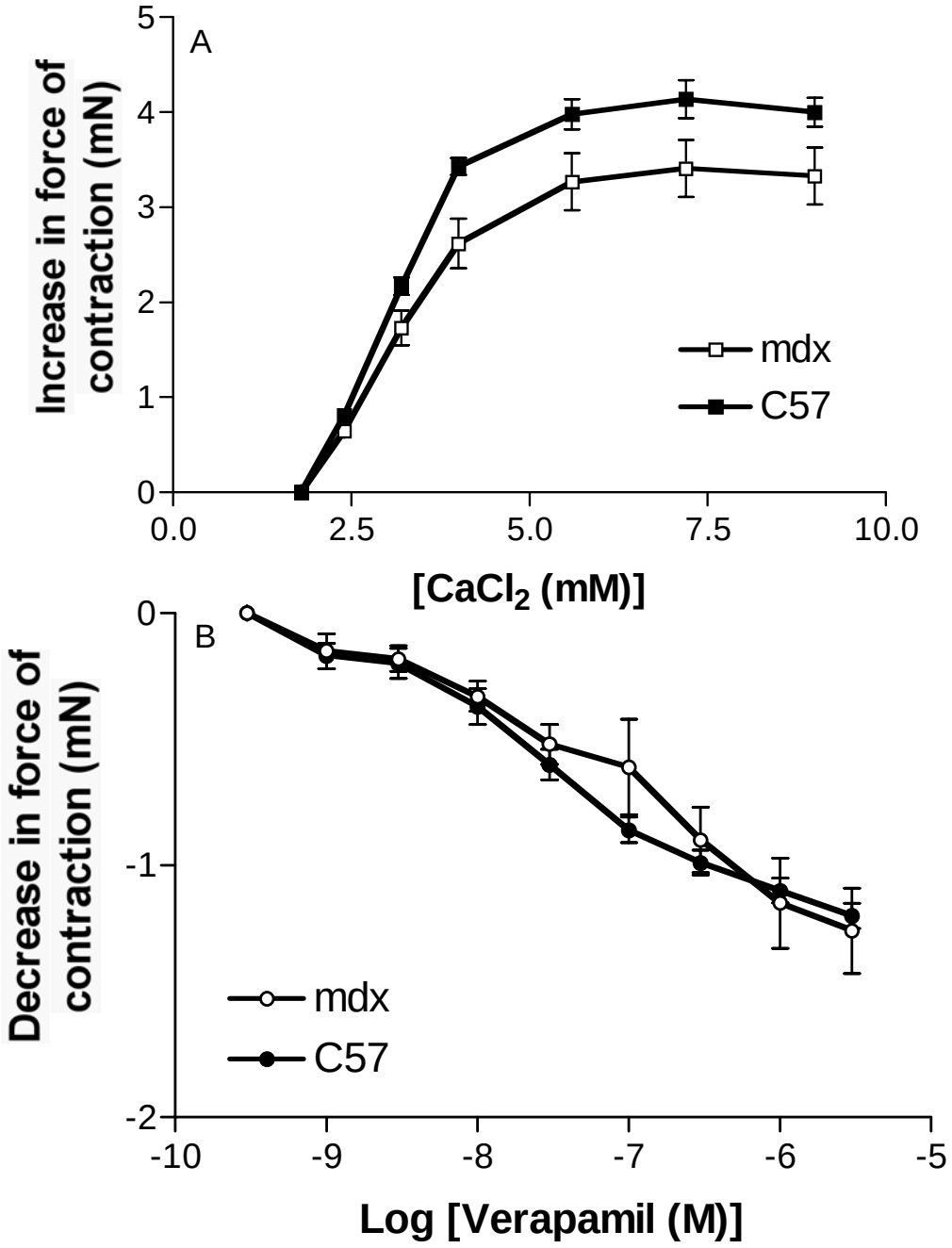

Figure 4.3 The effects of verapamil on left atria, and the effects of extracellular calcium. A Response to extracellular calcium (n=24). B Effect of verapamil on left atria contractile force. Basal force of contraction for *mdx* 1.84±0.07mN (n=10); for C57 1.76±0.09mN (n=8) measured prior to the CRC to verapamil.

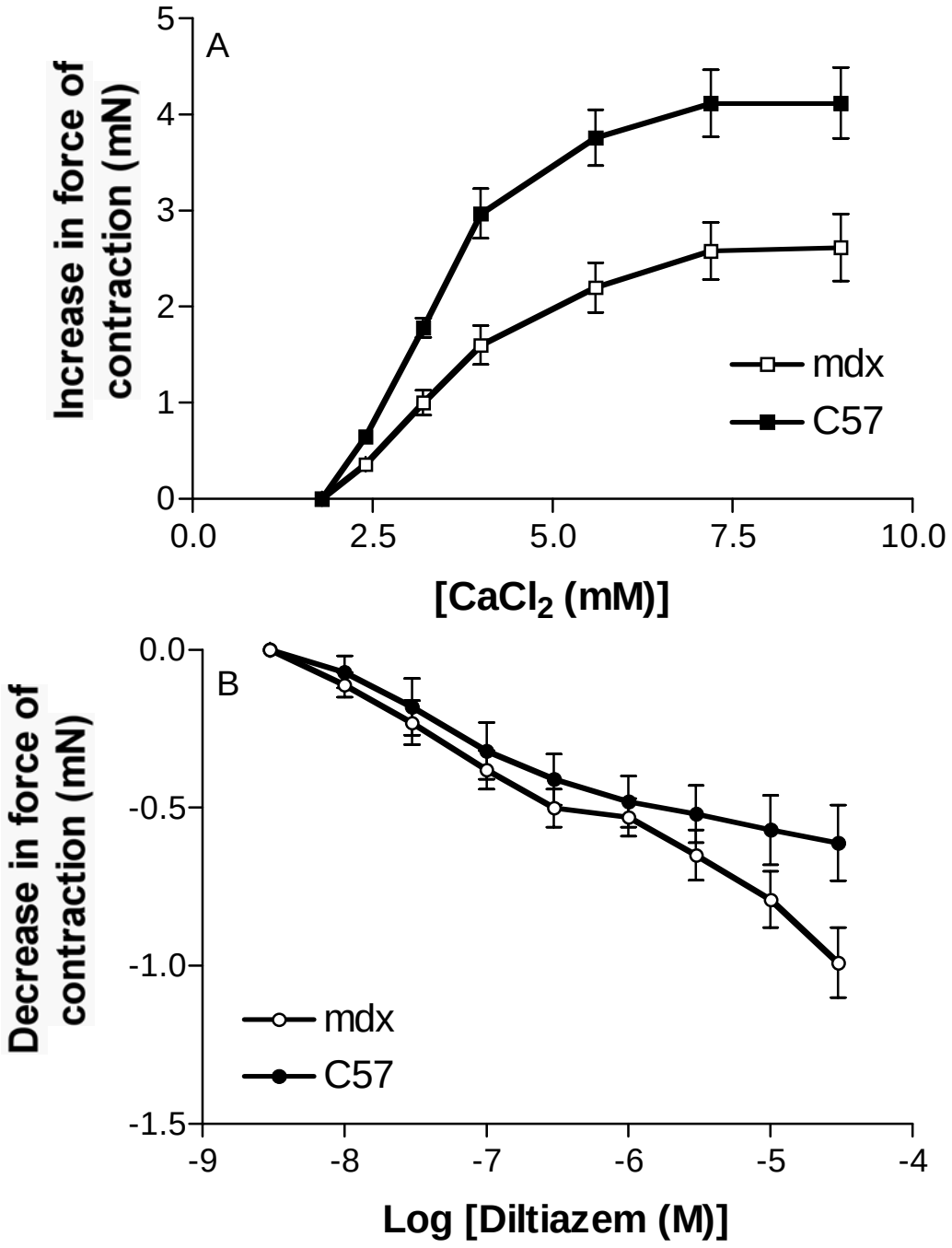

Figure 4.4 The effects of diltiazem on left atria, and the effects of extracellular calcium. A Response to extracellular calcium (n=24). B Effect of diltiazem on left atria contractile force. Basal force of contraction for *mdx* 1.37±0.09mN (n=5); for C57 1.49±0.12mN (n=8) measured prior to the CRC to diltiazem.

In contrast, there was an increase in sensitivity for verapamil in left atria from *mdx* compared to C57 (pD_2 *mdx* 7.50±0.10, pD_2 C57 7.03±0.08; P<0.05), with no difference in efficacy (Fig. 4.3). This increase in potency is due to a significant difference at only one concentration in the concentration-response curve that occurred at 50% of the maximum effect. The reduction in force was associated with a reduction in dF/dt upon exposure to the maximum concentration of verapamil, without any affect on relaxation time. In comparison, no difference in potency was observed for diltiazem in left atria between *mdx* and C57 (pD_2 *mdx* 7.11±0.35, pD_2 C57 6.71±0.20), although a lower efficacy was evident (Figure 4.4). Diltiazem produced a significant reduction in force that was associated with a reduction in dF/dt upon exposure to the maximum concentration, and a significant prolongation of relaxation time (Table 4.2).

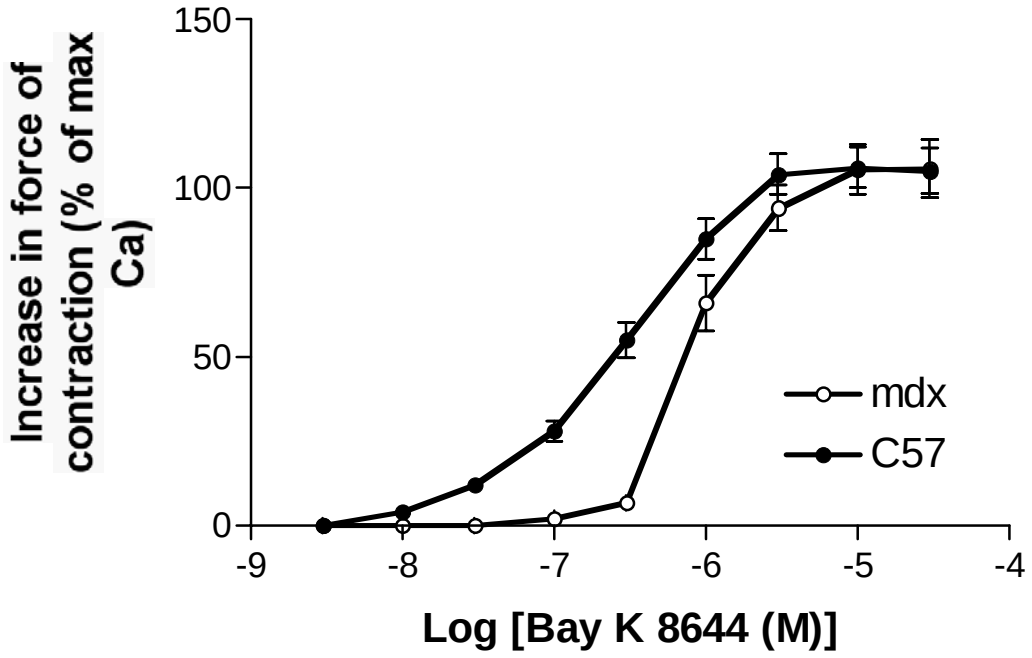

Figure 4.5 Response to Bay K 8644 in isolated *mdx* (○) and C57 (●) left atria. Concentration-response curve to Bay K 8644 in left atria (n=8) as a change in force of contraction. pD2 for *mdx* 6.10±0.03, pD2 for C57 6.53±0.05 (P<0.05). See text for basal forces.

Table 4.2 Effect of L-type calcium channel antagonists on Time to 90% Relaxation (TR_{90} in ms) in the tissue bath studies.

	C57		*mdx*	
	Basal	***Antagonist***	***Basal***	***Antagonist***
Nifedipine	39.8±2.1	44.9±1.7	41.9±1.7	49.9±3.8*
Diltiazem	38.6±1.8[a]	49.2±4.1*	46.8±1.3	55.8±2.1*
Verapamil	38.7±1.2[b]	41.8±2.5	47.2±1.8	47.6±1.8

*** P<0.05 antagonist vs. basal within strain, [a] P<0.05 *mdx* vs. C57 basal, [b] P<0.01 *mdx* vs. C57 basal; n=6-8. Antagonists values are shown at their maximally effective concentrations, with respect to inhibition of force of contraction.**

4.2.1.3 Response to Bay K 8644

Bay K 8644 elicited a strong positive inotropic effect in both strains producing a similar efficacy to calcium. Although the efficacy (as a percent of calcium chloride) was not different between the two strains, a reduced potency (pD_2 values *mdx* 6.10±0.03; C57 6.53±0.05, P<0.05 Fig 4.5) was again evident in *mdx*. The strain potency ratio for Bay K 8644 was 2.7, which is similar to the ratio obtained for nifedipine. Importantly, a similar potency difference was evident if the positive inotropic response was not normalised as a percentage of calcium chloride. The TR_{90}, time to peak force & dF/dt at the maximum concentration of Bay K 8644 were not significantly different (Table 4.3) between the strains. At the maximum concentration of Bay K 8644, *mdx* time to peak force was significantly longer (P<0.05). Time to peak force in C57 left atria was unaffected by the maximum concentration of Bay K 8644. Relaxation time in the presence of the highest concentration of Bay K 8644 was not significantly different to relaxation time in the absence of drug in either strain, despite a trend towards this parameter being longer in *mdx* with Bay K 8644 present. The solvent ethanol elicited a weak negative inotropic effect at the maximum solvent

concentration, but this was overcome completely by the pronounced positive inotropic effect of Bay K 8644.

4.2.2 Microelectrode and Contractility Experiments

4.2.2.1 Basal Measurements

There was no significant difference in basal force of contraction in left atria between *mdx* and C57 mice in the microelectrode and contractility series of experiments. While no difference was evident in time to peak force and dF/dt (data not shown), a longer relaxation time (measured as time to 90% relaxation) was evident in left atria from *mdx* mice (C57 39.0±1.7ms (n=24); *mdx* 45.3±1.6ms (n=24): P<0.01).

Table 4.3 Contractile parameters in response to Bay K 8644 $1x10^{-4.5}$M.

	TR_{90} (ms)		*TTPF* (ms)	
	Basal	Max	Basal	Max
mdx	28.8±0.7	31.4±1.6	30.4±0.6	32.9±0.8[a]
C57	28.3±1.0	28.1±0.9	30.5±1.1	31.4±1.4

No parameters were significantly different between the strains (n=8 for both *mdx* and C57). [a]TTPF (Time to peak force) was significantly prolonged by the maximum concentration of Bay K 8644 in *mdx* only.

Prior to the administration of drugs, there was no difference between *mdx* and C57 in the amplitude of the action potentials or the resting membrane potential (Table 4.4). The action potential duration (APD) at 20% (APD_{20}) and 50% (APD_{50}) repolarisation were not significantly different between *mdx* and C57 left atria, although at 90% (APD_{90}) repolarisation action potentials were shorter in the *mdx* left atria in the diltiazem group only (P<0.05).

4.2.2.2 Response to the Calcium Channel Antagonists

All calcium channel antagonists reduced force of contraction in a concentration and time-dependent manner (Fig 4.6, 4.7, 4.8) as expected. This was associated with a significant reduction in dF/dt upon exposure to the maximum concentration of drug tested (Table 4.2).

The reduction in force of contraction was statistically significant ($P<0.01$) for the concentration of antagonist required to produce the maximum negative inotropic effect for all three antagonists. None of the antagonists, at either the equipotent IC_{50} or concentration for maximum response, produced significantly different negative inotropic responses between *mdx* and C57 left atria when expressed as a percentage reduction in force of contraction. Diltiazem delayed relaxation in *mdx* and C57 mice, evident by an increased TR_{90} ($P<0.05$), whereas nifedipine delayed relaxation in *mdx* only ($P<0.05$) (Table 4.2). None of the antagonists affected time to peak force (Table 4.5) in either *mdx* or C57 mice at any concentration.

Nifedipine decreased APD_{20} in C57 but not *mdx* ($P<0.05$), however APD_{50} and APD_{90} remained unaltered in *mdx* and C57 (Fig. 4.6). The reduction in APD_{20} was only 1 ms and so can not be clearly observed in Fig. 4.6 due to the current line thickness. The reproducibility of the data resulted in such a small difference reaching statistical significance. Verapamil did not significantly alter APD_{20}, APD_{50} or APD_{90} in either *mdx* or C57 (Fig. 4.7), whereas diltiazem prolonged the APD at 20, 50 and 90% of repolarisation in both strains ($P<0.05$), with no difference evident between the strains (Fig. 4.8).

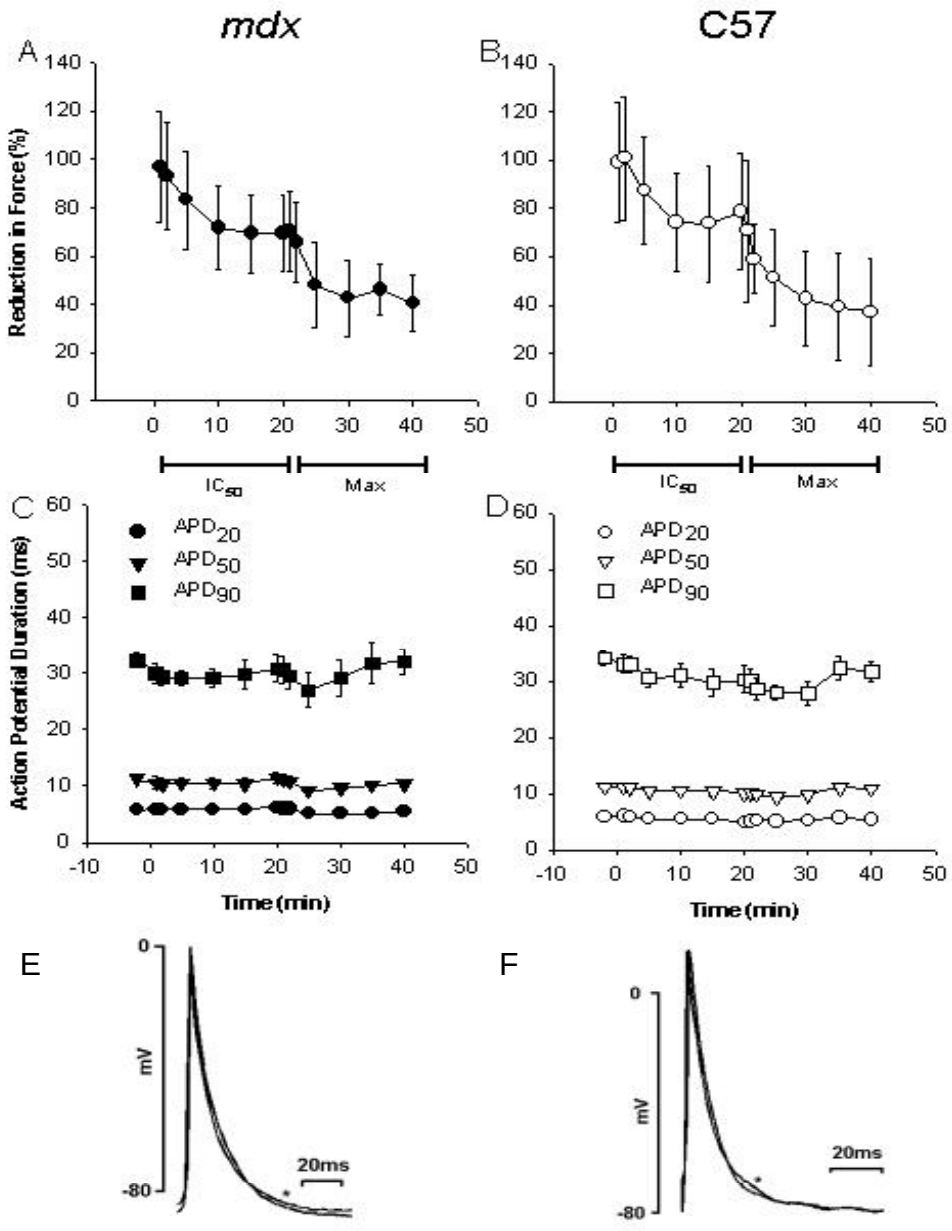

Figure 4.6 The effects of nifedipine on left atrial force of contraction and action potential duration. AB Reduction of force as percent of basal (n=6-8). CD Action potential duration at 20, 50 and 90% repolarisation. EF Original recording of a representative action potential during control period and 20 min after initial exposure to the concentration for maximum effect (*).

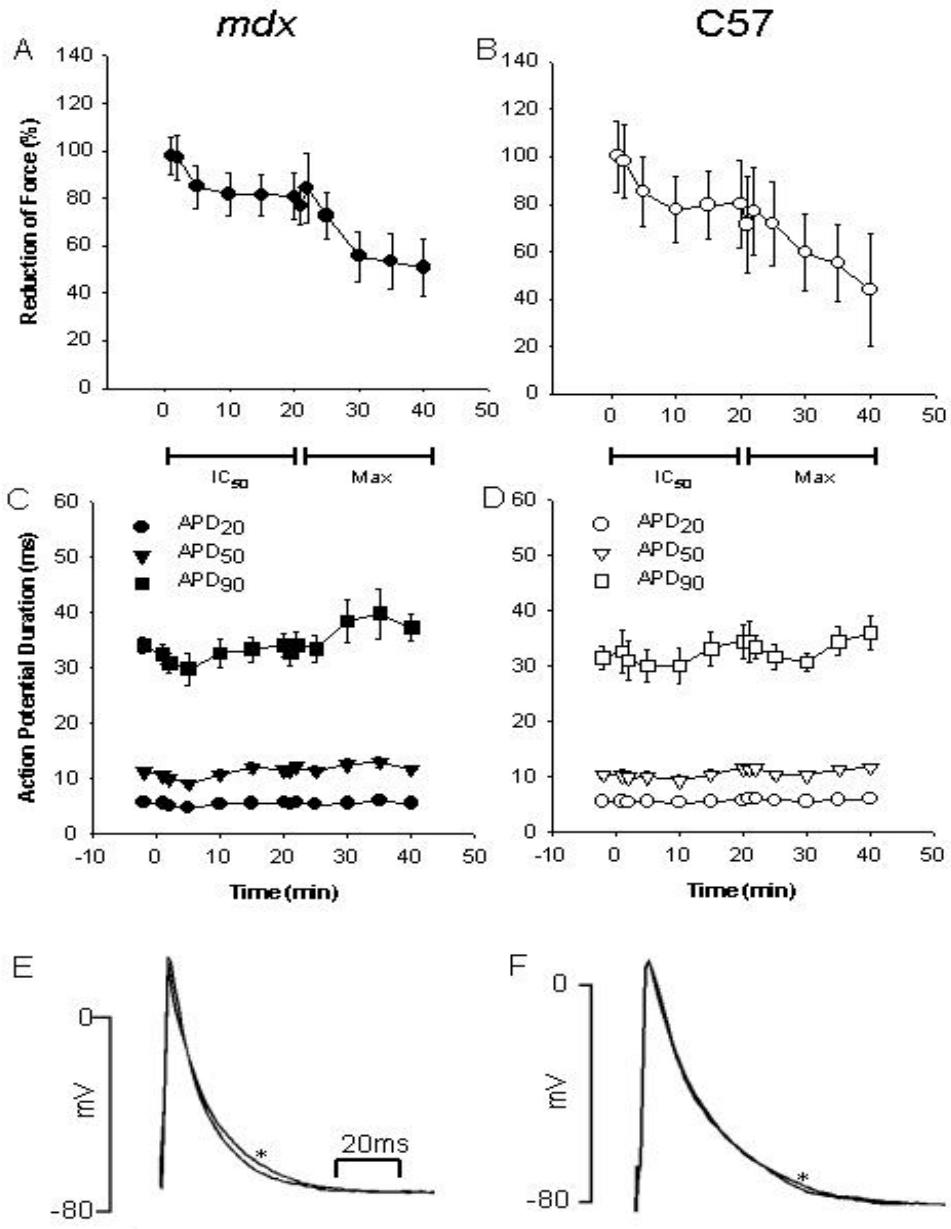

Figure 4.7 The effects of verapamil on left atrial force of contraction and action potential duration. AB Reduction of force as percent of basal (n=6-8). CD Action potential duration at 20, 50 and 90% repolarisation. EF Original recording of a representative action potential during control period and 20 min after initial exposure to the concentration for maximum effect (*).

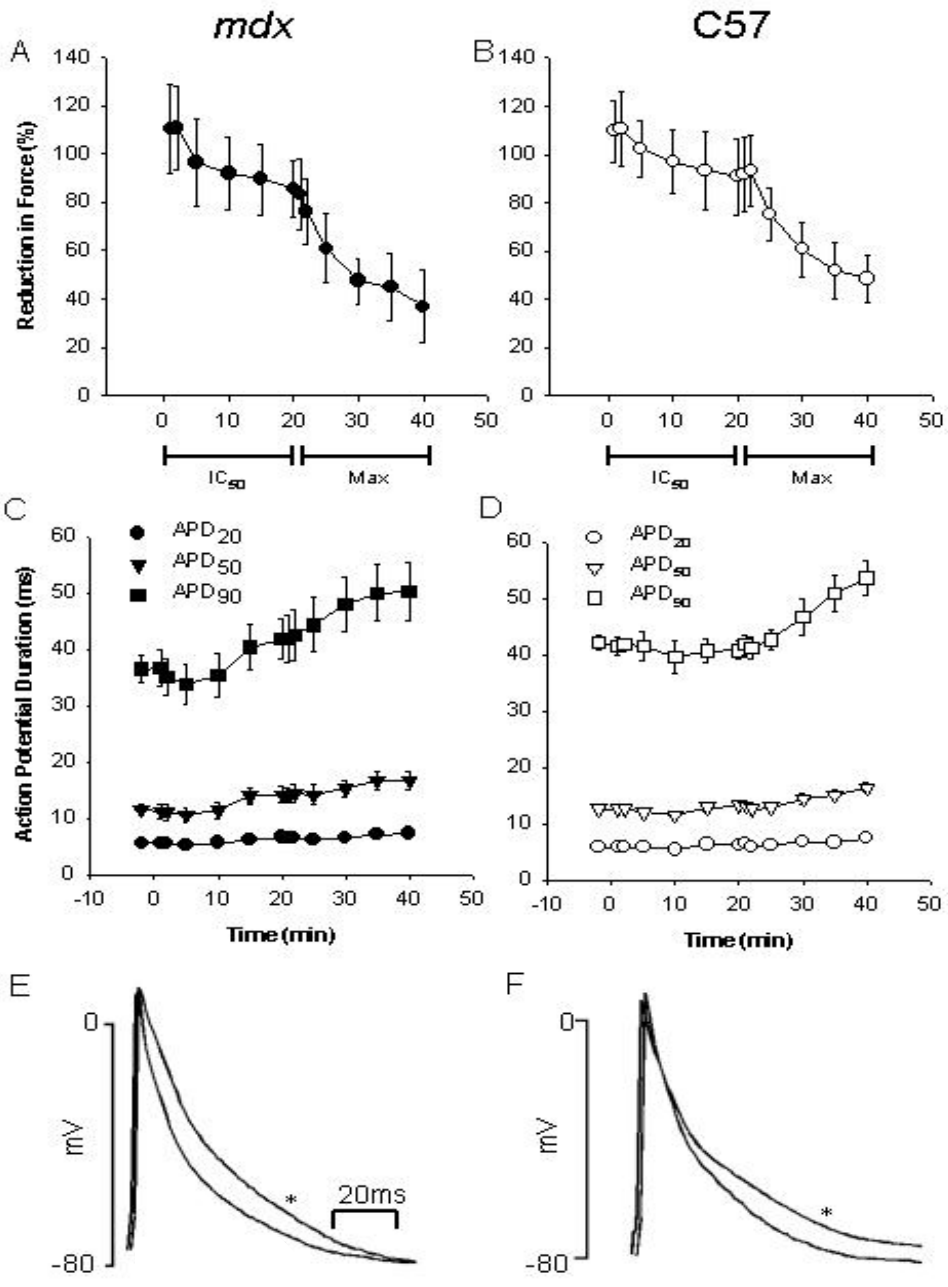

Figure 4.8 The effects of diltiazem on left atrial force of contraction and action potential duration. AB Reduction of force as percent of basal (n=6-8). CD Action potential duration at 20, 50 and 90% repolarisation. EF Original recording of a representative action potential during control period and 20 min after initial exposure to the concentration for maximum effect (*).

Table 4.4 Basal electrophysiological parameters

	RMP (mV)	*APA (mV)*	*Force (mN)*	*dF/dt (mN/ms)*	*TTPF (ms)*
mdx	-73.7±0.5	91.8±0.9	0.9±0.1	8.7±0.7	40.9±0.3
C57	-74.9±0.5	93.3±1.1	1.1±0.1	9.0±0.6	38.9±0.3

Table 4.5 Comparison of Ca^{2+} channel antagonist effects on contraction time course parameters in *mdx* and C57 left atria

	dF/dt (mN/ms)		*TTPF (ms)*	
	Mdx	***C57***	***Mdx***	***C57***
NFD IC_{50}	8.04±1.21	7.00±1.65	38.00±1.68	38.00±1.93
NFD Max	3.83±0.72**	3.24±0.67*	38.43±1.57	36.29±1.02
DTZ IC_{50}	10.57±2.19	9.44±2.59	43.00±1.45	42.83±3.14
DTZ Max	4.09±0.96**	4.80±1.13*	42.67±1.26	39.67±1.58
VRL IC_{50}	6.29±1.22*	11.93±2.18	40.17±1.46	40.14±1.32
VRL Max	4.93±0.42**	7.91±1.19*	37.00±0.69*	40.57±1.85
Control mean	11.49±1.36	11.74±1.51	40.19±0.69	38.79±1.00

n=6-8 *P<0.05, **P<0.01 basal vs. Maximum effect

4.2.3 Radioligand Binding Experiments

4.2.3.1 Assay Development

Since the radioligand assay had not been previously undertaken in our laboratory, a series of preliminary experiments were undertaken to optimise the assay. Incubation time was the first parameter evaluated. Tissues were incubated with a constant amount of radioligand (2nM [^{3}H]-PN 200 110 ± nifedipine for non-specific binding), and tubes removed at selected time intervals and counted (Fig 4.9). An incubation period of 60 min was determined to be sufficient as equilibrium was evident at 30 min

and remained relatively stable up to 150 min. Nifedipine was evaluated

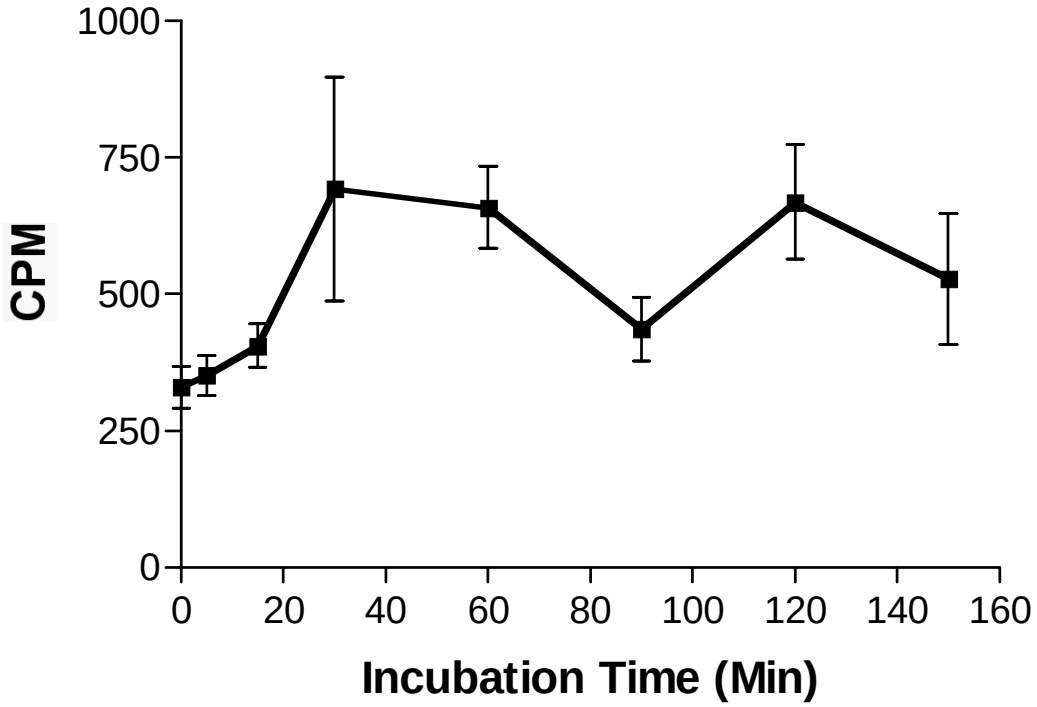

Figure 4.9 Determination of incubation time (2 separate counts from n=2). A constant concentration of [^{3}H]-PN 200 110 (2nM) was used for each of the time periods. An incubation time of 60min was determined to be sufficient to obtain a clear equilibrium response.

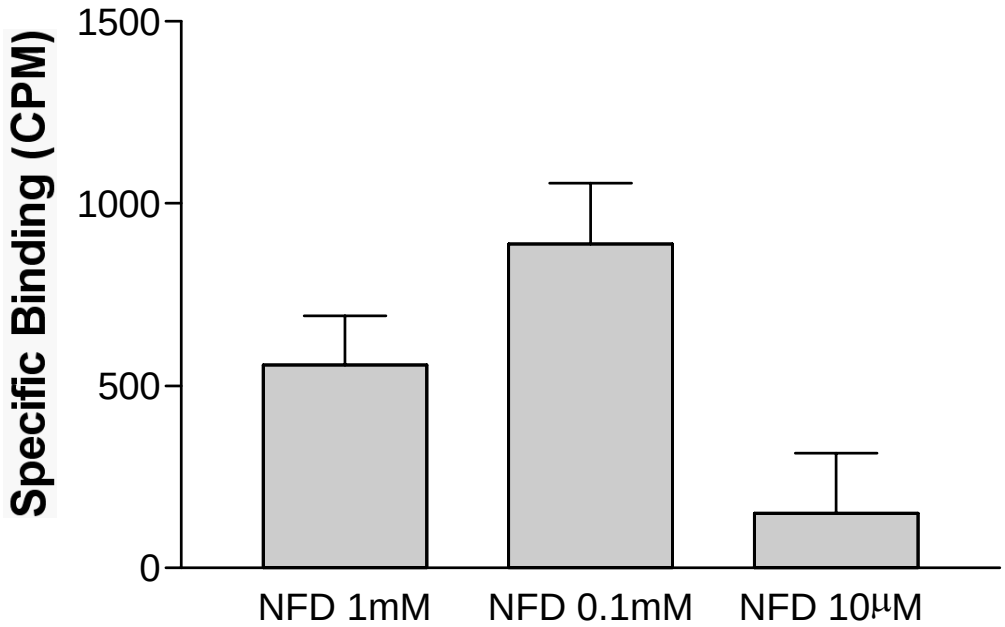

Figure 4.10 Determination of antagonist concentration for non-specific binding. Specific Binding in response to decreasing concentrations of nifedipine used to displace [^{3}H]-PN 200 110 (2 separate counts from n=2).

for displacement of the radioligand for non-specific binding (Fig 4.10) by two experiments using three different concentrations of nifedipine to displace the [^{3}H]-PN 200 110. A final concentration of 0.1mM nifedipine was determined to be the optimal concentration to displace the non-specifically bound radioligand. The temperature of incubation was evaluated. Room temperature (25°C) was compared to approximate physiological temperature (35°C) for an incubation period of 1hr (Fig 4.11). The specific binding was much higher at 35°C, so this temperature was used for further studies. Overnight incubation with scintillant was also considered, the trial revealing that overnight incubation greatly improved penetration of the scintillant into the filter, and higher counts of the radioligand. The amount of final membrane protein used in the incubation was also trialled, with 1mg/mL determined to be optimal protein for the final protocol.

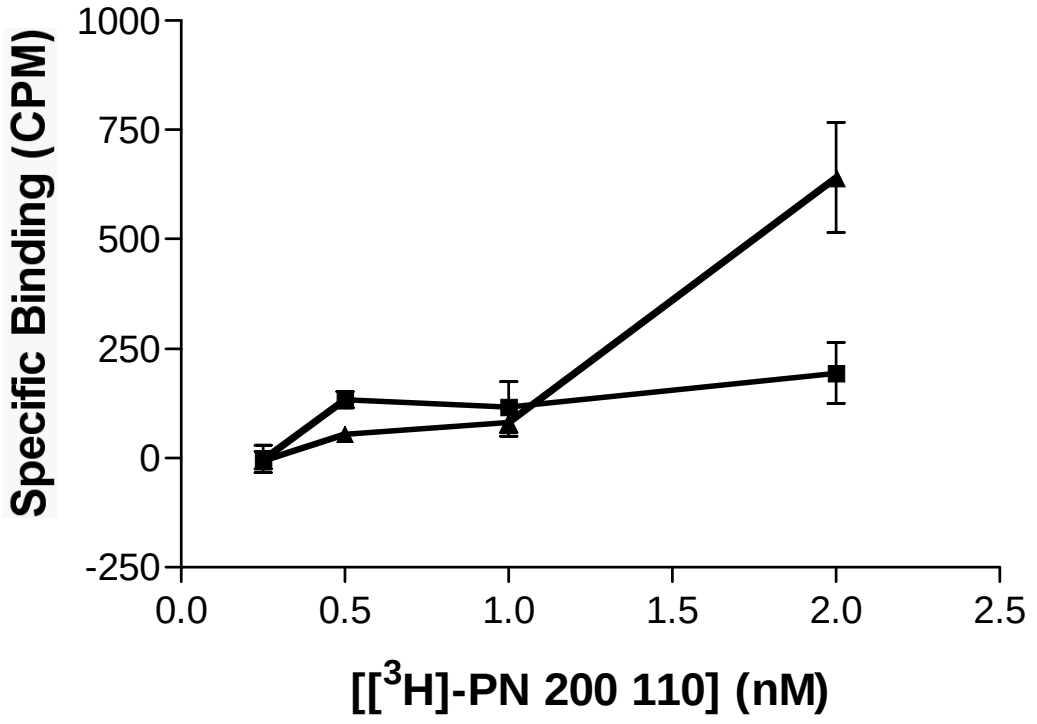

Figure 4.11 Determination of incubation temperature. Specific Binding at 25°C (ν) compared to 35°C (σ) n=4. Specific binding was much greater at 35°C with higher concentrations of PN200-110, so this temperature was used for incubation.

4.2.3.2 Comparison of *mdx* and C57 Ventricular Homogenates

Radioligand binding experiments revealed a significantly greater number of DHPRs in *mdx* (B_{max} 99.2±7.0 fmol/mg) compared to C57 (B_{max} 74.5±9.4 fmol/mg; Fig. 4.12, P<0.05) with a strain ratio (B_{max} *mdx* /B_{max} C57) of 1.3. The affinity of [^{3}H]-PN 200 110 was also significantly reduced in *mdx* (K_d 0.3897±0.07nM) compared to C57 (K_d 0.2572±0.09nM) (Fig. 4.12, P<0.05). The strain potency ratio (K_d *mdx* /K_d C57) was 2.0, a similar ratio to that observed in the functional tissue bath studies utilising nifedipine and Bay K 8644 (Table 4.6).

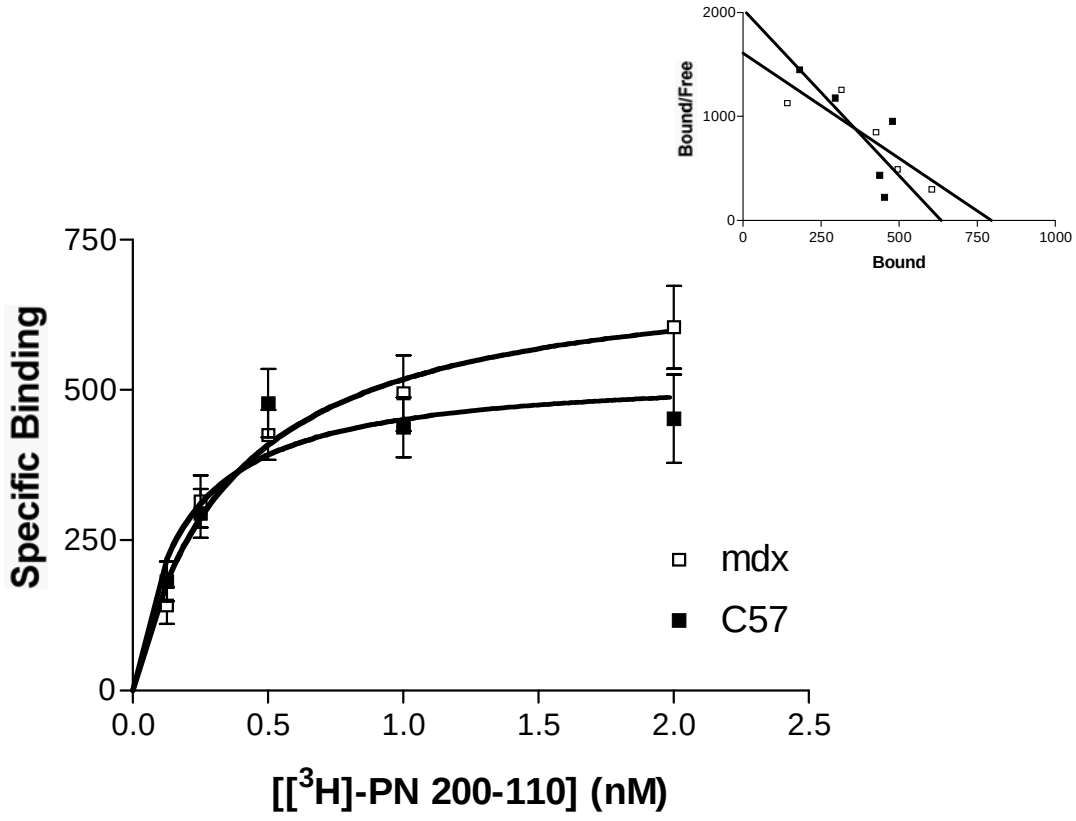

Figure 4.12 Saturation binding curve showing the mean of all experiments from *mdx* and C57 ventricular homogenates in response to increasing concentrations of [^{3}H]-PN 200 110 (0.1-2nM). Non-specific binding was determined by the addition of 0.1M nifedipine. Inset: Scatchard analysis of the saturation curve revealed a B_{max} of 107.4±6.5 fmol/mg and a Kd of 0.3897±0.07 nM (n = 15 experiments; 30 ventricles) for *mdx* and a B_{max} of 78.6±10.6 fmol/mg and a K_d of 0.2572±0.09 nM (n = 19 experiments; 38 ventricles) for C57. There is a significant difference between *mdx* and C57 in both Bmax (P<0.05) and K_d (P<0.05).

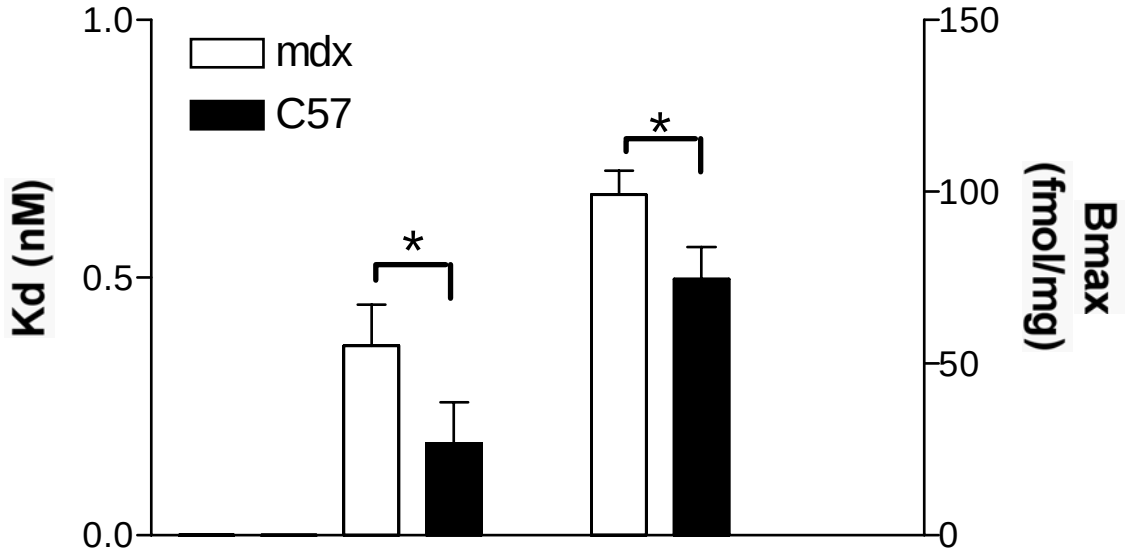

Figure 4.13 K_d and B_{max} from the scatchard plots in Figure 4.11. Both K_d and B_{max} were significantly different between *mdx* and C57.

4.2.4 RT-PCR

4.2.4.1 Comparison of *mdx* and C57 Dihydropyridine mRNA

Ventricular DHPR mRNA was significantly higher ($P<0.005$) in *mdx* compared to C57 (Fig. 4.14) when corrected for the amount of total mRNA by using the GAPDH samples. The original gel photos are presented in figures 4.15 and 4.16. The strain ratio for ventricular mRNA was 2.3 (Table 4.6). The left atrial DHPR mRNA was also higher in *mdx* compared to C57, although this did not quite reach statistical significance ($P=0.07$). The strain ratio for atrial mRNA for DHPRs was 2.0. The ubiquitous β-Actin was also used as a housekeeper gene and produced qualitatively similar data. The mRNA for DHPR was not statistically different between *mdx* atria and ventricles nor C57 atria and ventricles.

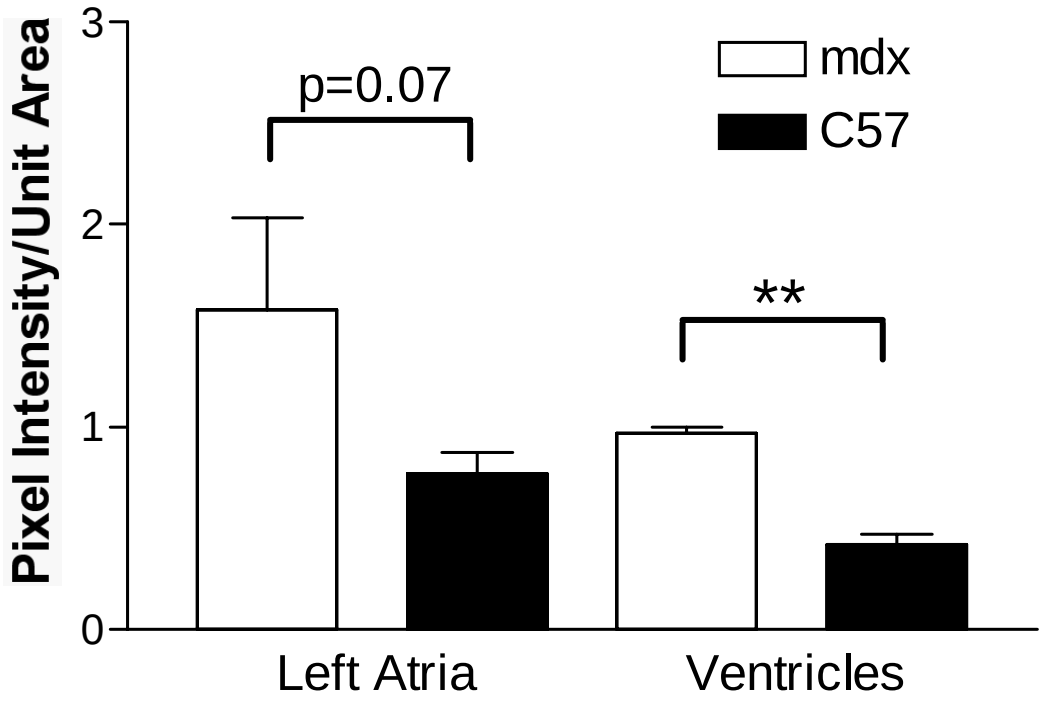

Figure 4.14 RT-PCR results from *mdx* (open; n=4) and C57 (filled; n=4) dihydropyridine receptor mRNA from ventricles and left atria. Band intensity was normalised to the amount of mRNA present by comparing each DHPR sample to its corresponding GAPDH sample. Ventricular mRNA was significantly higher in *mdx* (P<0.05) compared to C57. Analysis by two-way ANOVA revealed the *mdx* data set to be significantly different (P<0.05) to the C57 data set.

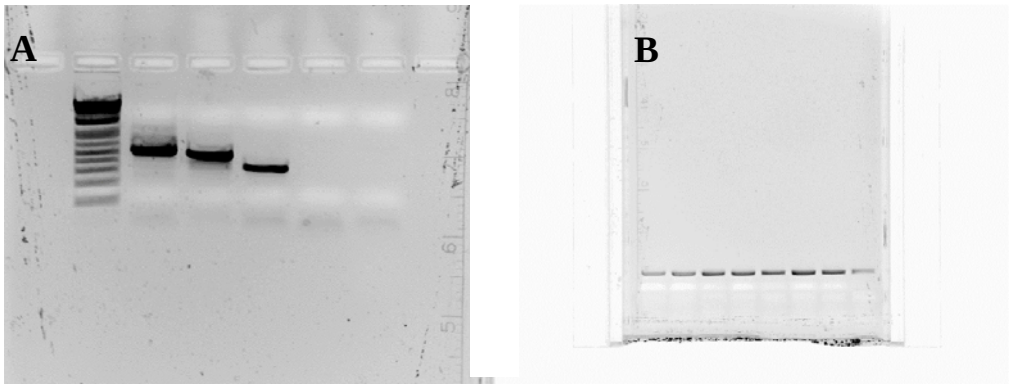

Figure 4.15 Max and linear range gel electrophoresis photos inverted so that mRNA bands are black. A Primers after 40 cycles to test binding to RNA. Primers shown are ladder, GAPDH and SERCA. B Linear range gel for DHPR. A linear range was undertaken with a combination of *mdx* and C57 samples mixed, so that a number of cycles could be determined where differences in expression could be detected.

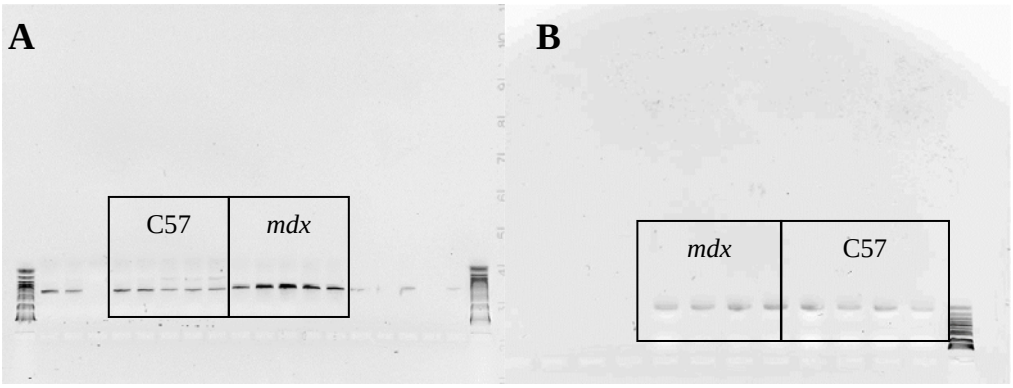

Figure 4.16 DHPR gel electrophoresis with colours inverted so bands are black. A DHPR mRNA in ventricles. B DHPR mRNA from *mdx* and C57 atria.

Table 4.6 Strain Potency Ratios for L-type calcium channel data

	Tissue		***Mdx/C57***
Potency	**Atrial**	**NFD EC_{50}**	1.9
	Atrial	**Bay K 8644 EC_{50}**	2.7
	Ventricular	**RLB Kd**	1.5
Density	**Ventricular**	**RLB Bmax**	1.3
	Atria	**DHPR RT-PCR**	2.0
	Ventricular	**DHPR RT-PCR**	2.3

The strain potency ratio was calculated by dividing the *mdx* EC_{50}, Kd, Bmax or total mRNA by the C57 EC_{50}, Kd, Bmax or total mRNA respectively. The strain ratio shows that each of the indicators of DHPR regulation is increased in *mdx*.

4.3 SR Calcium Release

To determine the role of the SR and active sequestration and extrusion mechanisms in dystrophin-deficient myocardium, rapid cooling contractures were undertaken. The rapid cooling contracture experiments evaluated SR function, SERCA function and NCX extrusion from dystrophin-deficient atria and compared that to control atria. A concentration-response curve was also undertaken to cyclopiazonic acid, a compound that blocks the activity of SERCA. A series of force-frequency experiments examined the function of the RyR and the SR in *mdx* compared to C57.

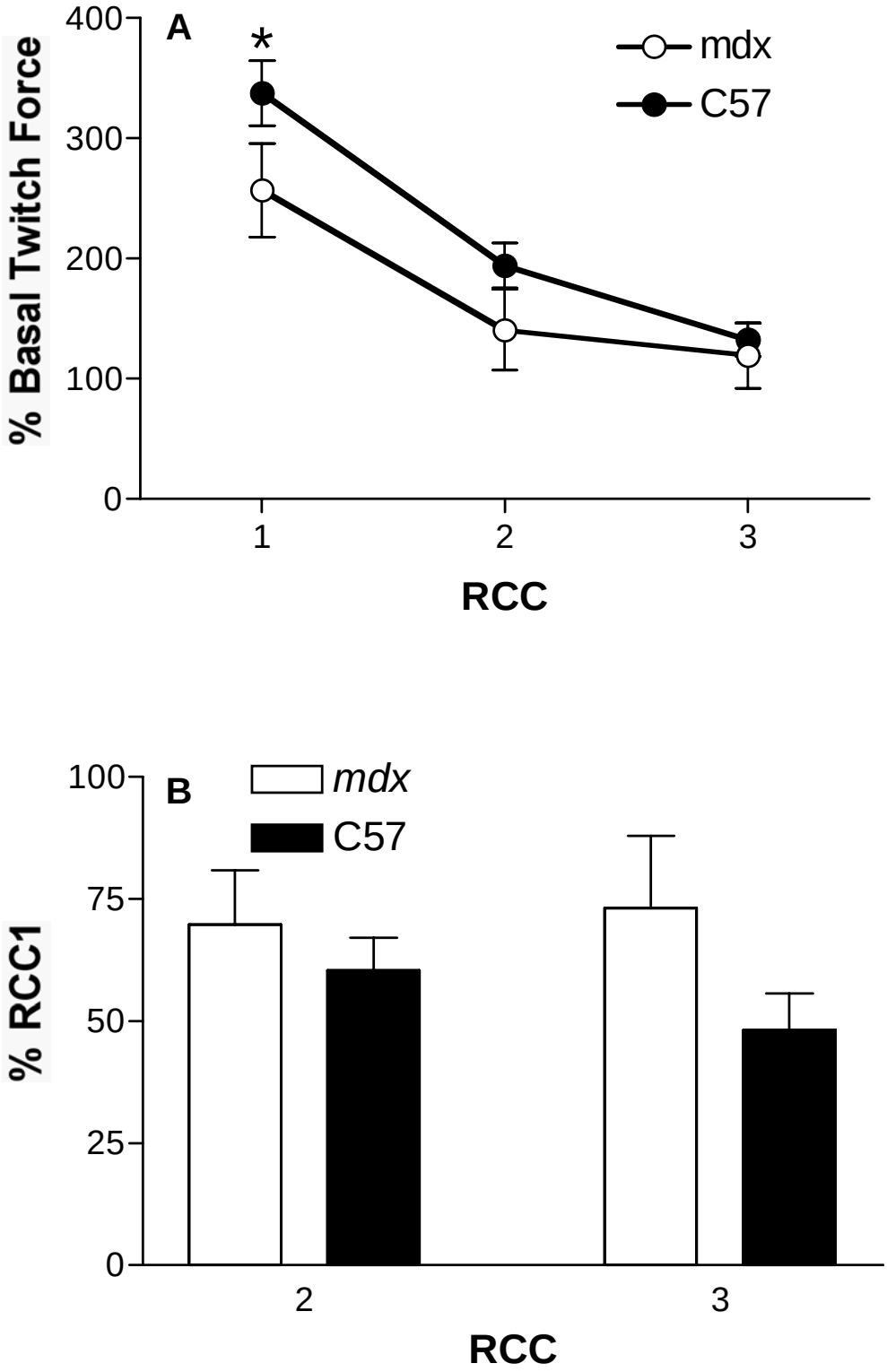

Figure 4.17 Rapid Cooling Contractures from left atria of *mdx* and C57. A Rapid cooling contractures as a percentage of normal twitch force. The calcium content of the SR was released by rapidly exchanging warm TPPS with ice-cold calcium free TPPS. The C57 (●; n=10) data set was significantly different to *mdx* (○; n=9: P<0.05) using two-way ANOVA. The RCC data set was highly significant (P<0.0001) using two-way ANOVA. B RCC2 and RCC3 are presented as a percentage of the RCC1, thus providing a. measure of SERCA function. RCC3 is non-significantly higher in *mdx* (n=10), compared to C57 (n=9; P=0.06).

4.3.1 Rapid Cooling Contractures

4.3.1.1 Basal Measurements

All basal measurements were recorded at the commencement of the experiment, before the rapid cooling contractures and in the absence of any drug. Basal contractility was lower in *mdx* (1.33±0.08mN) relative to C57 (1.56±0.16mN; P=0.05). Basal time to 90% relaxation (TR_{90}) was not significantly different between *mdx* (44.8±3.0ms) and C57 (41.5±3.0ms), although a higher mean TR_{90} was observed in *mdx*.

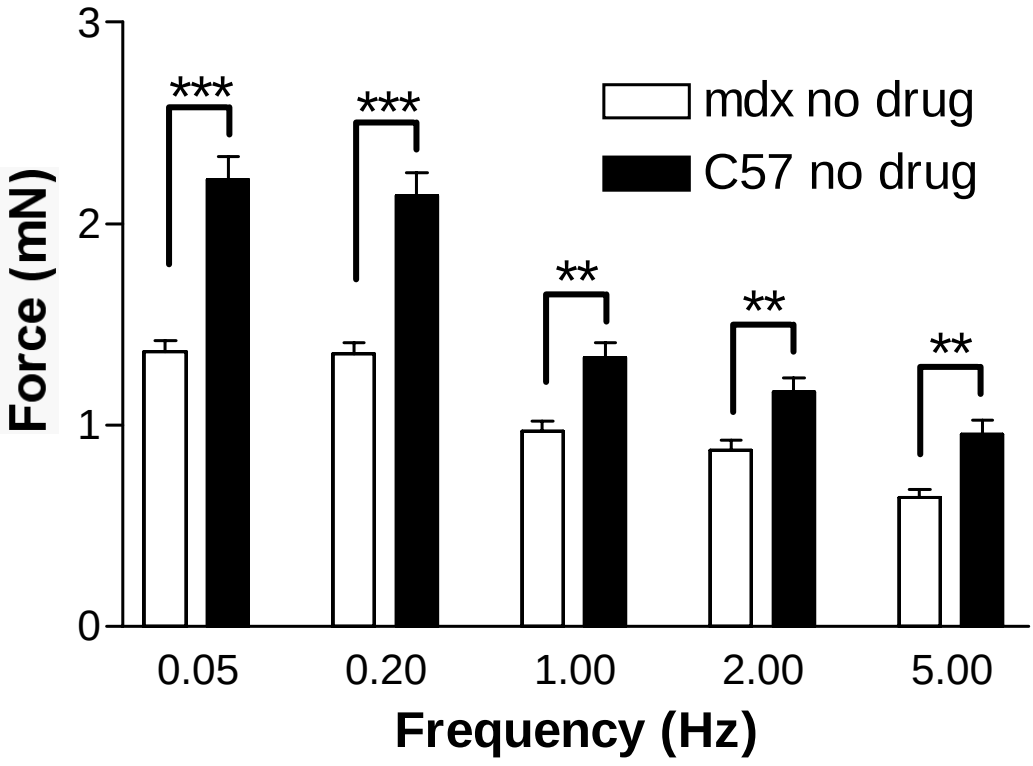

Figure 4.18 Basal contractility of *mdx* and C57 left atria at increasing frequencies (data pooled from control experiments and is shown in Fig 4.19, 4.20, 4.21). Contractility was measured at 0.05, 0.2, 1, 2 and 5 Hz. *Mdx* (n=21) consistently showed a significant reduction in force production compared to C57 (n=31) left atria. ***=P<0.001, **=P<0.01.

4.3.1.2 Rapid Cooling Contractures

The first rapid cooling contracture (RCC) was significantly smaller in *mdx* (1.53±0.26mN) compared to C57 (2.21±0.24mN: $P<0.01$) as shown in Figure 4.17 as a percentage of basal twitch force. The second RCC was not significantly different between the strains (Figure 4.17), but the third RCC when taken as a percentage of the first (therefore a measure of SERCA function) was larger in *mdx*.

4.3.2 Force-Frequency Relationships

At all frequencies tested, in the absence of any drug, the *mdx* left atria produced significantly less force than the C57 left atria ($P<0.01$; Fig. 4.18). However, addition of increasing concentrations of ryanodine progressively eliminated any difference in force between the *mdx* and C57s over all of the frequencies tested. With the blockade of sarcoplasmic reticulum calcium release by the addition of 1nM ryanodine, a positive staircase developed, with no difference in force production between strains (Fig. 4.19), in spite of a normally lowered efficacy and potency to calcium in *mdx* (see Fig. 4.2). The forces produced in the presence of ryanodine are quite low, indicating that the drug is successfully blocking SR release, as expected. The force frequency curve in the presence of dantrolene (Fig. 4.20) always maintained a negative staircase. The significantly lower force of contraction by the *mdx* myocardium in the absence of dantrolene, was maintained with the addition of dantrolene 0.1, 1 and 10μM at 0.05 and 0.20Hz. However, at the higher frequencies (1, 2 and 5Hz) this significant difference was lost.

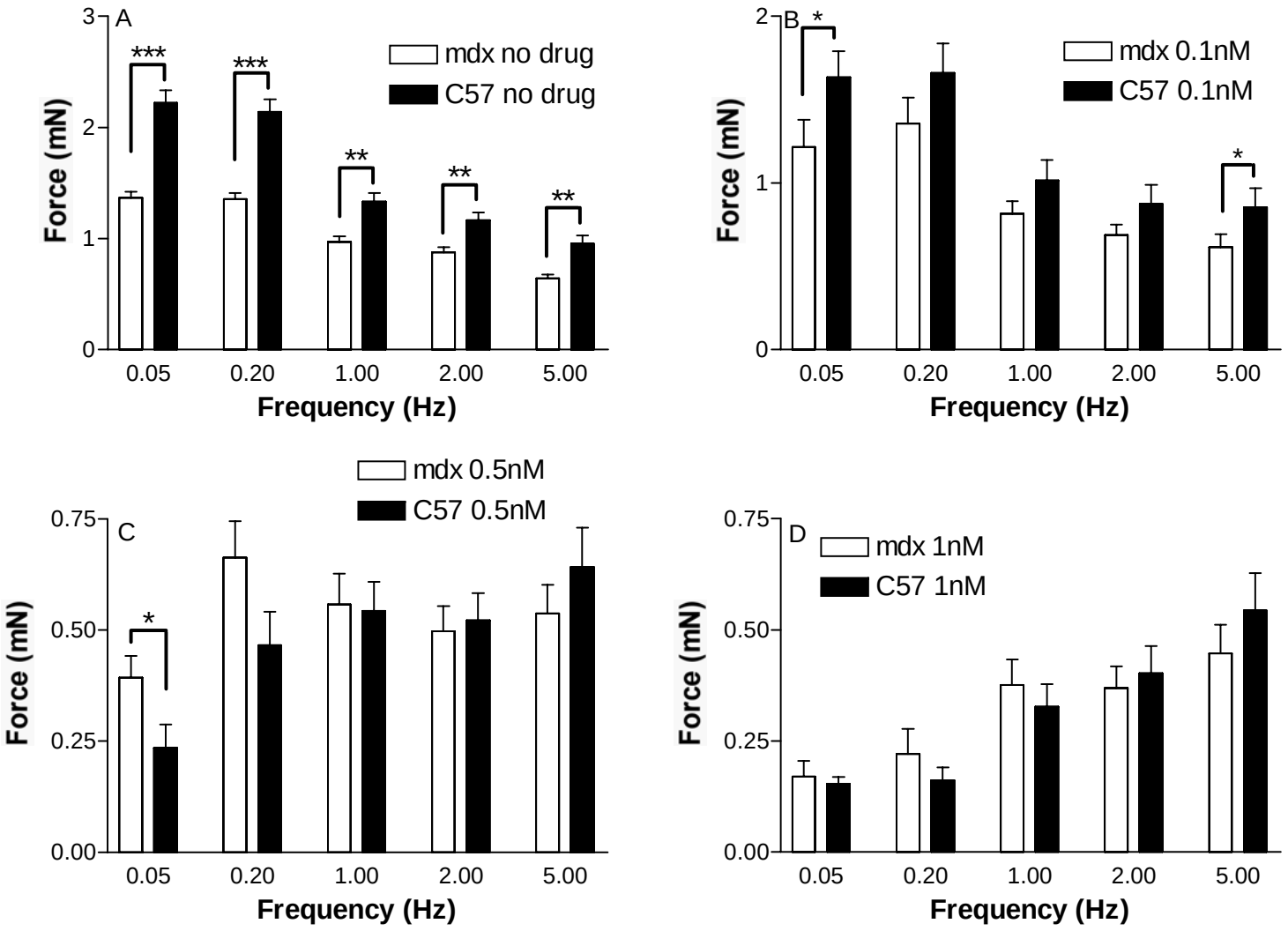

Figure 4.19 Force-frequency relationship in the presence of ryanodine. A force-frequency relationship in the absence of any drug *mdx* n=21, C57 n=31. ***=P<0.001; **=P<0.01. B Force-frequency in the presence of 0.1nM ryanodine. The *mdx* data set is significantly different to the C57 data set (P<0.005) using two-way ANOVA. C Force-frequency in the presence of 0.5nM ryanodine. D Force-frequency in the presence of 1nM ryanodine.

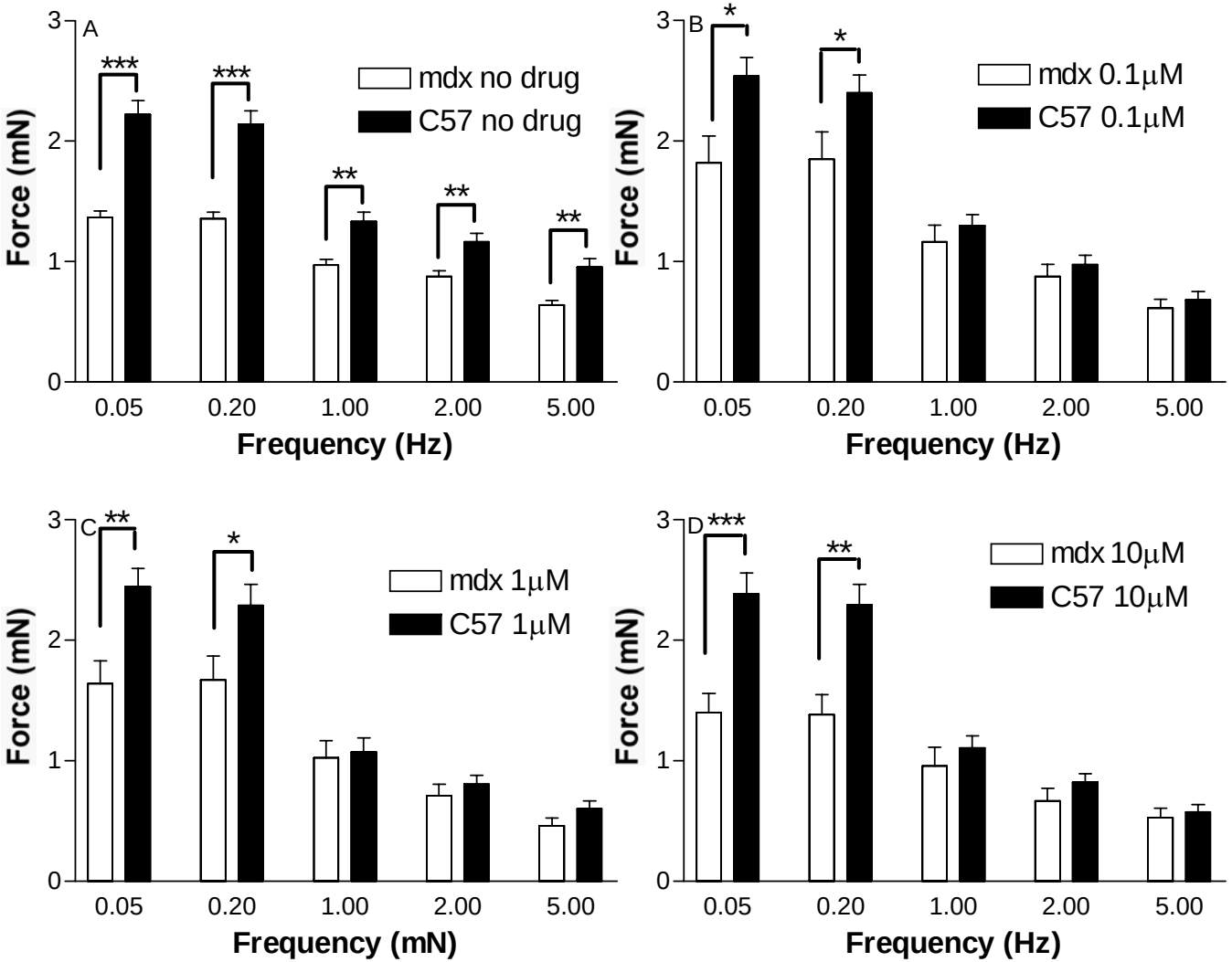

Figure 4.20 Force-frequency relationship in the presence of dantrolene. A is in the absence of any drug. In the presence of dantrolene 0.1 (B), 1 (C) and 10μM (D), both 0.05 and 0.2Hz were significantly different between *mdx* (n=8) and C57 (n=8). *P<0.05, **P<0.005, ***P<0.001.

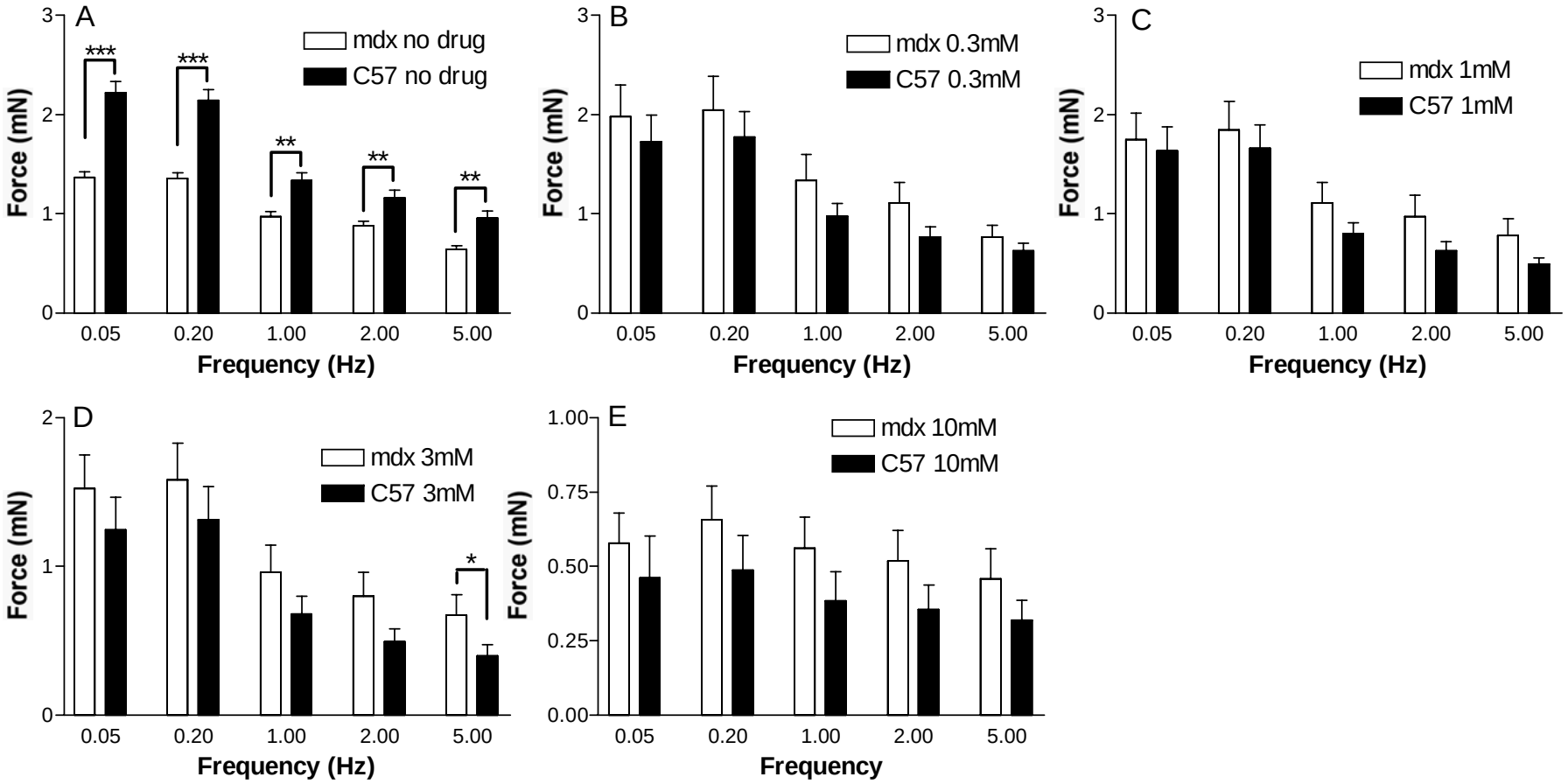

Figure 4.21 Force-frequency relationship in the presence of caffeine. The only significant difference between *mdx* (n=6) and C57 (n=8) in the presence of caffeine was at 5Hz with 3mM caffeine present. A negative staircase was observed at all concentrations of caffeine applied, although the staircase began to plateau at 10mM caffeine. B In the presence of 0.3mM caffeine the *mdx* data set is significantly different to the C57 data set using two-way ANOVA (P<0.005). C In the presence of 1mM caffeine the *mdx* data set is significantly different to the C57 data set using two-way ANOVA (P<0.005). D In the presence of 3mM caffeine the *mdx* data set is significantly different to the C57 data set using two-way ANOVA (P<0.0001). E In the presence of 10mM caffeine the *mdx* data set was significantly different to the C57 data set using two-way ANOVA (P<0.0005).

Force of contraction was reduced in the presence of higher concentrations of caffeine (Fig. 4.21), indicating that caffeine was blocking SR release and/or uptake. The negative staircase property of the left atria was maintained with all the concentrations of caffeine, although at 10mM caffeine, the force was not significantly different at 0.05Hz compared to 5Hz in either strain. Interestingly, there was a trend for the *mdx* to produce higher force than the C57 with caffeine present. This became significant at 5Hz with 3mM caffeine present.

4.4 Calcium Sequestration and/or Reuptake

4.4.1 Cyclopiazonic Acid

The efficacy of CPA was not significantly different between the strains (Fig. 4.22A) while the *mdx* showed a non-significant decrease in potency (EC_{50}s: *mdx* 12.3±3.1mM, C57 6.8±2.0mM; P=0.08). CPA significantly lengthened relaxation time in both *mdx* and C57, as was expected due to its inhibition of SERCA. Time to 90% relaxation (TR_{90}) was significantly greater in *mdx* (45.5±0.3ms) compared to C57 (38.5±0.3ms) at the lowest concentrations of CPA tested (P<0.05), but this effect disappeared at higher concentrations as inhibition of SERCA prolonged relaxation in both *mdx* and C57 (Fig. 4.22B).

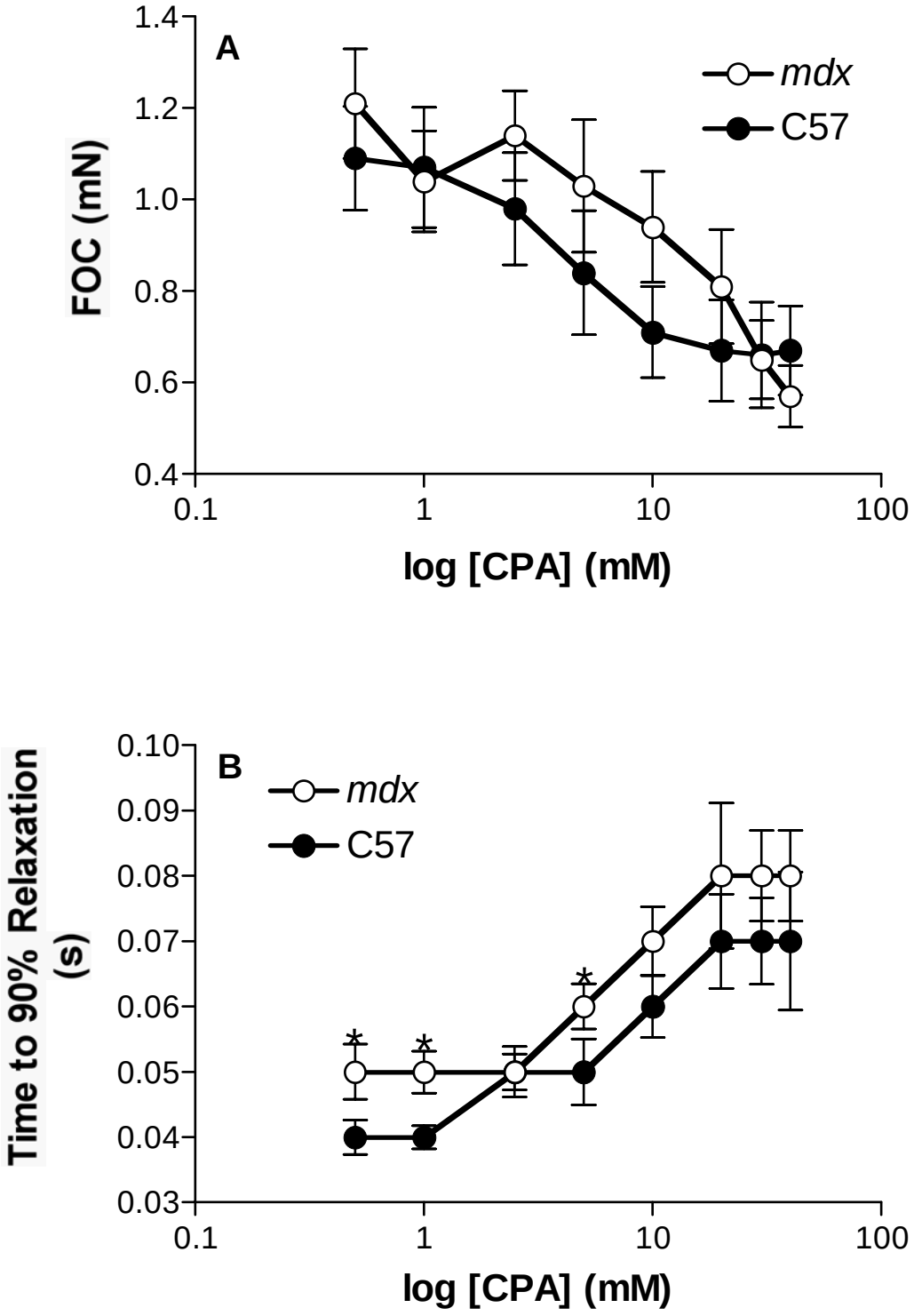

Figure 4.22 Left atrial force of contraction and time to 90% relaxation in response to cyclopiazonic acid. A *Mdx* (○, n=10) response was reduced compared to C57 (●, n=9), although the difference was not significant. Potency and efficacy were not significantly different between the two strains, although CPA tended towards a lower potency in *mdx*. B Time to 90% relaxation in response to CPA. Due to an inhibition of SERCA, relaxation time was prolonged and this was particularly evident in *mdx* (○, n=10) at 0.3, 1 and 5 mM CPA compared to C57 (●, n=9) ($P<0.05$). The *mdx* data set are significantly different to the C57 data set using two-way ANOVA ($P<0.0005$).

4.4.2 SERCA RT-PCR

RT-PCR experiments from ventricle revealed a significantly higher expression of SERCA mRNA in dystrophic tissue (*mdx* 2.47±0.3 intensity/pixel unit area; n=5; C57 1.15±0.05 intensity/pixel unit area; n=5: $P<0.05$ see Figure 4.23). The original gel photos are shown in Figure 4.24.

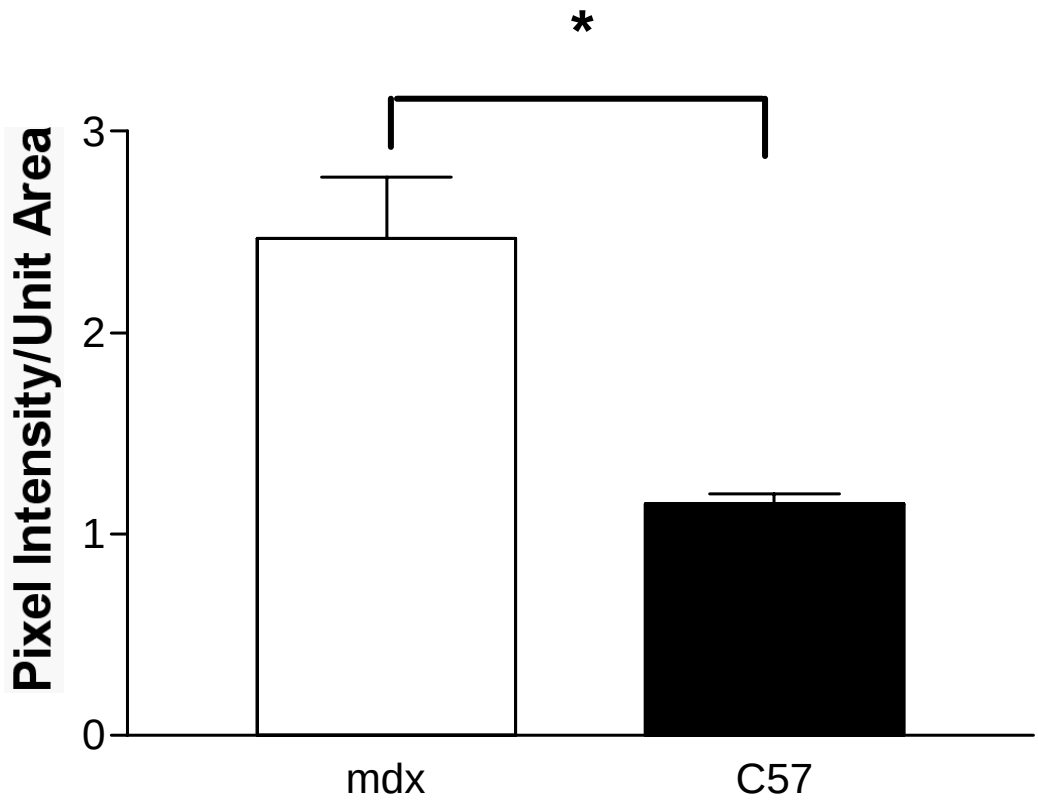

Figure 4.23 SERCA mRNA expression as pixel intensity per unit area. The intensities were normalised to GAPDH protein levels for each sample. The intensities were also normalised to be per pixel, so that variations in band size were taken into account. The mRNA for SERCA in *mdx* (n=5) is upregulated compared to control mice (n=5) $P<0.05$.

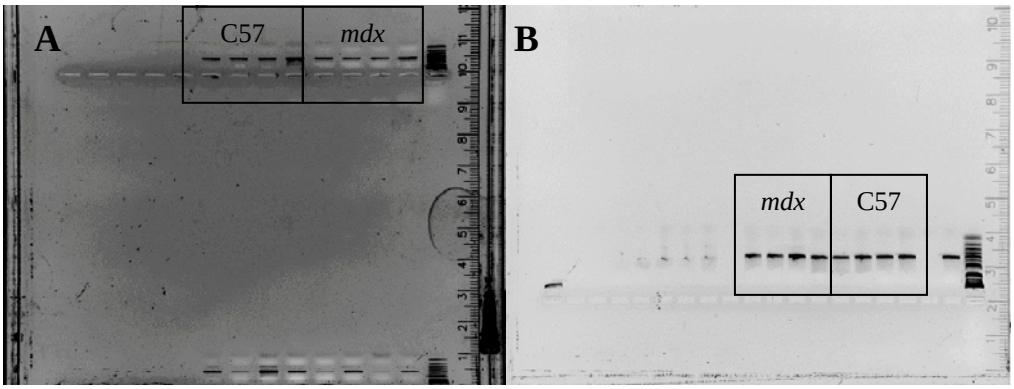

Figure 4.24 SERCA gel electrophoresis of mRNA with colours inverted so that bands are black. A GAPDH expression. B SERCA mRNA expression.

CHAPTER 5 – DISCUSSION

5.1 Functional differences between *mdx* and C57 cardiac tissues

At the completion of the equilibration period for each experiment basal measurements were taken to compare drug responses to those in the absence of drug. This allowed basal measurements of the myopathy of *mdx* at 12-14 weeks of age to be assessed. In the tissue bath experiments a calcium concentration-response curve was undertaken immediately after the equilibration period, so that the maximum force production for each atrium could be determined. These experiments revealed that the initial basal force of contraction and the potency of and efficacy to calcium were reduced in left atria of *mdx* mice, in spite of an elevation of intracellular calcium (Dunn & Radda, 1991). This reduction in myocardial contractile force has been shown previously in our laboratory (Lu & Hoey 2000a) and in others (Sapp *et al.*, 1996). A possible mechanism for the reduction in potency and capacity to generate force in response to extracellular calcium represents a reduction in myofilament sensitivity to calcium. Such weakness may be a protective mechanism against the weaker sarcolemmal membrane (Kanai *et al.*, 2001), since dystrophin has now been shown to play a mechanical stabilization role in cardiomyocytes (Hainsey *et al.*, 2003) similar to its established role in skeletal muscle. Chronically elevated calcium, to a similar level as that observed in dystrophic cardiomyocytes, can cause a significant reduction in myofilament sensitivity (Holt & Christensen, 1997), although this has not yet been shown for dystrophin-deficient cardiomyocytes.

Action potentials of *mdx* are reported as being shorter in *mdx* mice (Pacioretty *et al.*, 1992; Perloff *et al.*, 1984), however the current study was unable to verify this phenomena. Differences in experimental methodologies such as the horizontal placement of the atria in the microelectrode apparatus may contribute to this finding. The resting membrane potential, action potential amplitude and maximum upstroke velocity were unaffected by a lack of dystrophin. A shorter action potential indicates that either the calcium channels are unlikely to remain open for a longer period of time, or that repolarisation is markedly increased. The shorter cardiac action potential has been attributed to activation of a large transient outward potassium current (Alloatti *et al*., 1995). The mechanisms underlying such a large transient outward current are unclear, although an increase in resting intracellular calcium may cause a larger transient K^+ current, which in turn may promote premature repolarisation of the action potential, leading to earlier inactivation of the voltage dependent L-type calcium channel (Sperelakis *et al.*, 1996).

A delayed relaxation of the *mdx* left atria has been observed in the current study and previously (Sapp *et al.*, 1996). This prolonged relaxation may be due to an increase in intracellular calcium due to dysfunctional sequestration, or extrusion of calcium from the cytosol. However, delayed relaxation time and the longer action potential duration that are usually seen but not observed in *mdx* may be linked, as K^+ channels may play a role in both of these observations (Cingolani *et al.*, 1990).

5.2 Contractility and Microelectrode Studies

The tissue bath studies examined the left atria of *mdx* and C57, their force of contraction, and their responses to drugs that alter L-type calcium channel function. The tissue bath protocols were well established in our laboratory, and data generated by these protocols had been published previously (Lu and Hoey, 2000a and b) indicating the reliability and suitability of these methods.

In the microelectrode studies the contractility of *mdx* and C57 left atria, along with the action potential characteristics were measured concurrently. Three different classes of calcium channel antagonists and one class of agonist were tested to determine their effect on the cardiac action potential in the *mdx* model of dystrophin-deficiency.

5.2.1 Concentration-Response Curve to Bay K 8644

Bay K 8644 exerts positive inotropic actions by binding to the cardiac DHPR of the L-type calcium channel to enhance sarcolemmal calcium influx that in turn triggers greater CICR (Schramm *et al.*, 1983). In the current study a marked positive inotropic effect was observed in response to Bay K 8644 in both *mdx* and C57, indicating that the drug was effective in depolarising the L-type calcium channel. Bay K 8644 produced a similar efficacy to extracellular calcium in both *mdx* and C57, showing that it is an efficient positive inotrope.

Although the efficacy as a percentage of calcium chloride was not different between *mdx* and C57, the left atria from *mdx* were less sensitive to Bay K 8644 compared to C57. There was also a significantly lower potency observed in *mdx*. This was the first indication that there may have been a conformational change in the DHPR that

affected its affinity for DHPR drugs. The strain potency ratio was 2.7, indicating a change in affinity of the drug for the receptor. This potency shift was also observed when the positive inotropic response was not normalised as a percent of calcium (ie absolute force), indicating that this potency change was due to modification of the DHPR, and not the lowered force production in *mdx*. Time to peak force was significantly longer in *mdx* in the presence of Bay K 8644 than the time to peak force without the drug present. This is merely a reflection of the larger force production in the cardiac tissue with the positive inotrope present. The time to peak force was not significantly longer in the presence of Bay K 8644 in C57 than without the drug being present, despite a trend towards this occurring.

One study has used Bay K 8644 previously in dystrophic myocardium (Sadeghi *et al.*, 2002). Sadeghi (2002) measured Ca^{2+} currents from neonatal cardiomyocytes and observed that calcium channels in *mdx* myocytes were stimulated 2.3-fold more by Bay K 8644 than channels in control myocytes. The authors suggest that this increase is due to allosteric changes in the channel (Sadeghi *et al.*, 2002) allowing the channel to be open longer. This increase is similar to the potency change observed in the current study and suggestive of a conformational change of the DHPR.

5.2.2 Effects of the Calcium Channel Antagonists

The L-type calcium channel antagonists reduce the influx of calcium by blocking the α_1-subunit of the channel. The calcium channel antagonists were effective in reducing the influx of calcium via the L-type calcium channel. This is demonstrated by a negative inotropic response to each of the calcium channel antagonists, in a time- and dose-dependent manner. The tissue bath studies revealed differences in potency and

efficacy for the calcium channel antagonists in left atria between *mdx* and C57 mice. In the microelectrode studies, the drugs were tested at equipotent doses, the IC_{50}s were calculated from the tissue bath studies and used to determine the effects of these drugs on the action potential in *mdx* cardiac tissue. The concentration that produced the maximum effects in the tissue bath studies was also used. Therefore, for all of the drugs used in the microelectrode study, higher doses were used for *mdx* left atria compared to C57. When these equipotent doses were administered, there was no difference in action potential attributes (except for diltiazem), or the negative inotropic effect of the calcium channel antagonists.

In the tissue baths, the left atria displayed a decrease in sensitivity to the DHPR antagonist nifedipine that was similar to the reduction in potency to the DHPR agonist Bay K 8644. There are various explanations for this effect, such as: i) modulation of the DHPR results from the long-term exposure to an intracellular calcium overload (Dunn & Radda, 1991), or ii) in response to nifedipine there is an increase in activity of a putative sarcolemmal leak channel as has been observed in skeletal muscle (Turner *et al.*, 1991). If sarcolemmal leak channels are present in cardiomyocytes, and if these channels behave similarly, it is possible that influx of calcium via these channels may cause earlier inactivation of the L-type channels. Sadeghi *et al.*, (2002) observed that inactivation of the L-type calcium channel from *mdx* neonatal cardiomyocytes was delayed. This therefore suggests that the first hypothesis is more probable, however the physiological behaviour of neonatal cardiomyocytes may not necessarily mimic adult cardiomyocytes. Nifedipine also caused a further delay in relaxation of the *mdx* left atria. This effect cannot be accounted for via the effect on the L-type calcium channel, as blockade of the channel reduces intracellular calcium

levels, therefore relaxation should occur earlier. This effect may be due to an influence on the potassium channels. Another DHPR antagonist nicardipine has been shown to inhibit the repolarising potassium current and the Na^+/Ca^{2+} exchange that extrudes calcium from the cell post-contraction (Richard *et al.*, 1988). Since the structure of nifedipine closely resembles nicardipine, it is possible that it affected these mechanisms similarly.

There was an increase in sensitivity to verapamil in the left atria from *mdx* compared to C57, although this was only due to one point on the curve, so it is of questionable physiological significance. There was no parallel dextral shift of the curve to signify a change in potency of the phenylalkylamine receptor. It is known that nifedipine can block the calcium current regardless of whether the channel is in the open or the inactivated state (steady depolarisation, without requiring pulses), and as such is considered more voltage-dependent than use-dependent (Bers & Perez-Reyes, 1999). Verapamil, on the other hand, appears to block the channel preferentially in the open state (ie requiring depolarising pulse) and as such is use-dependent. Thus, these differences in mechanism may also explain the observed differences in response to the two agents.

Although the binding sites for all three classes of calcium channel antagonists are found on the α_1-subunit of the L-type calcium channel (Catterall & Striessnig, 1992), the DHPR seems to be exclusively extracellular (Kass & Arena, 1989; Kass *et al.*, 1991) whilst the phenylalkylamine and benzothiazepine sites have both intracellular (Hescheler *et al.*, 1982) and extracellular (Wegener & Nawrath, 1995; Adachi-Akahane *et al.*, 1993) components in ventricular myocytes and functional interaction

has been reported between sites (Kanda *et al.*, 1998). It is also possible that a difference in receptor location on the L-type calcium channel in *mdx* myocardium may explain the lowered potency for nifedipine.

The marked increase in APD observed in response to diltiazem may be due to an action of the drug on K^+ channels. While the APD is shortened by diltiazem in rabbit ventricular tissues that naturally have a longer APD (Miyazaki *et al.,* 1996), no reports could be found on its electrophysiological effects in mouse or rat cardiac tissues that have a much shorter APD. In contrast, phenylalkylamines have been shown to inhibit the cardiac delayed rectifier potassium current and the sodium-activated potassium current, which would provide a basis for prolongation of the APD (Waldegger *et al.*, 1999; Berger *et al.*, 1991; Mori *et al.*, 1998), although only slight prolongation was evident in response to verapamil in our studies. This prolongation may be due to an inhibition of NCE (mitochondrial sodium/potassium exchange), which would reduce the ATP available for SERCA for relaxation of the myocardium (Schwartz, 1992). Diltiazem is unique in the calcium channel antagonists in inhibiting the NCE in this manner. Kuo *et al.,* (2002) have shown improvement in cardiomyopathy by blocking overactive NCE in the cardiomyopathic hamster. The function of the NCE in *mdx* is unknown.

An *in vivo* study to determine the efficacies of nifedipine, diltiazem and verapamil in γ-sarcoglycan deficient dystrophic hamsters observed that only diltiazem halted morbidity and mortality associated with dystrophic pathobiology (Johnson & Bhattacharya, 1993). In the same study, diltiazem effectively reduced the intracellular calcium overload in cardiac tissues, although effects on contractility or action

potential duration of myocardium were not examined. A reduction in calcium deposits in dystrophic hamster myocardium post treatment with diltiazem has also been observed histologically (Bhattacharya *et al*., 1982). It is probable that this protection is due to an effect on the NCE as well as the reduction in calcium influx through blockade of the L-type calcium channel. Therefore there may be therapeutic potential from administration of calcium channel antagonists in conditions of calcium overload, including the dystrophinopathies.

5.3 Radioligand Binding Studies

To date, no previous studies have measured DHPR density or affinity in *mdx* myocardium. Given the change in potency in the tissue bath studies to the DHPR drugs, it was an important set of experiments to determine whether this change was due to a change in the density of the channels, or a conformational change of the receptor, or both. In the radioligand studies, the *mdx* mice showed a significant increase in DHPRs, which could account for an increased influx of calcium into the cell, although the functionality of the receptors remains to be determined. The *mdx* mouse had a significantly reduced affinity for the DHPR agonist [^{3}H]-PN 200 110. These results are clearly consistent with a reduced potency of nifedipine and Bay K 8644 in the organ bath experiments, and suggest that both upregulation of the receptors occurs, and a conformational change of the receptor reducing its affinity for DHPR drugs.

Receptor regulation is a commonly observed phenomenon in cardiovascular disease states. For example, congestive heart failure is associated with a reduction in β-

adrenoceptor affinity, concurrent with β-adrenoceptor downregulation, as evidenced by an increased K_d and lower B_{max} measured in radioligand binding studies (Brodde, 1991). Similarly, regulation of the L-type calcium channel occurs in response to other disease processes. Hyperthyroidism has been shown to downregulate the L-type calcium channel (Watanabe *et al.*, 2003), and electrical remodelling involving the L-type calcium channel is an early manifestation of arrhythmia (Bosch *et al.*, 2003). The DHPRs have been shown to downregulate in end stage heart failure (Takahashi *et al.*, 1992). As radioligand binding studies utilizing antagonists are not dependent on receptor stimulus and agonist efficacy, the K_d is determined solely by receptor affinity and is unaffected by the receptor density (B_{max}). The increased K_d observed with [^{3}H]-PN200 110 in the current study shows a lowered receptor affinity and thus presumably altered conformation that would explain the lowered potency observed with Bay K 8644 and nifedipine.

A possible mechanism that could affect the affinity of DHPRs is changes in the cell membrane potential, with depolarisation of the cardiac resting membrane potential causing an increase in DHPR affinity and thus presumably hyperpolarisation causing a decrease in DHPR affinity (Bean, 1984). However, microelectrode studies in left atria of *mdx* and C57 mice utilising the same conditions as those in the tissue bath studies, did not show any difference in resting membrane potential, eliminating this as a basis for the difference in DHPR affinity in the tissue bath studies. Furthermore, the difference in receptor affinity was maintained in the radioligand binding studies, where the influence of the membrane potential is eliminated. This provides clear evidence that a change in receptor affinity is not due to changes in membrane potential.

Another influence affecting DHPR affinity is the concentration of free calcium. Using [^{3}H]-PN 200 110 in radioligand binding studies, Peterson and Catterall (1995) showed that divalent ions cause a biphasic effect on the affinity of DHPRs, with a low free calcium causing an increase in affinity, while a high free calcium causes a significant decrease in affinity. It is therefore, highly feasible that the calcium overload observed in *mdx* myocytes is a mediator responsible for the lowered affinity state of the DHPRs observed in the atrial contractility studies. However, in DHPR radioligand binding studies, calcium is not added to the incubation buffer and chelators such as EGTA are also present. This then eliminates any acute effects of calcium on modifying the affinity state of the DHPRs within such studies. Given that a lowered affinity for [^{3}H]-PN 200 110 was still observed, this may suggest that the chronic *in vivo* elevation of intracellular calcium and/or the primary lack of dystrophin may cause a more rigid conformational change in DHPRs, that is subsequently maintained in isolated membranes.

5.4 Dihydropyridine Receptor RT-PCR

Given the increase in DHPR density shown in radioligand binding studies, it is important to measure mRNA levels of the DHPR. These experiments showed a 2 fold and a 2.3 fold increase in atria and ventricles respectively, which supports the radioligand binding data. DHPRs have been shown to become upregulated in other conditions, including chronic adrenergic stimulation (Maki *et al.*, 1996). While a comparison to previous values in *mdx* myocardium is not possible, Pereon *et al.*, (1997) showed an elevation in DHPR mRNA expression in *mdx* diaphragm, however,

this was not associated with an elevation in DHPR protein expression measured by [^{3}H]-PN 200-110 binding. This anomaly was explained by elevated protein degradation in *mdx* diaphragm, a muscle that shows marked deterioration (Stedman *et al.*, 1991). In comparison, adult rat ventricular myocytes incubated in the presence of high intracellular calcium showed a two-fold increase in DHPR mRNA, providing evidence that a dystrophin-deficiency mediated increase in intracellular calcium could be the basis for the increased DHPR expression (Davidoff *et al.*, 1997).

5.5 Upregulation of the L-type Calcium Channel

This dissertation provides strong evidence for upregulation of the L-type calcium channel, resulting in an increase in channel density. This change is associated with a conformational change of the receptor that lowers its affinity for DHPR drugs. An increase in L-type calcium current has been shown in *mdx* smooth muscle, where this increase is responsible for sustained tone in *mdx* colon (Mule & Serio, 2001). In other models of cardiomyopathy that are not due to dystrophin-deficiency (myocardial infarction induced by left coronary artery ligation), an elevation of intracellular calcium and an increased number of L-type calcium channels has been observed (Gopalakrishnan *et al.*, 1991). Furthermore, in the presence of an intracellular calcium overload, mRNA for the channel subunit containing the DHPR binding site has been reported to increase twofold (Davidoff *et al.*, 1997). Like the *mdx* mouse, heart failure in the γ-sarcoglycan deficient cardiomyopathic hamster is due to a loss of the dystrophin associated glycoprotein complex (Palmieri *et al.*, 1981) and intracellular calcium is also elevated (Wagner *et al.*, 1989), further indicating a causal relationship between dystrophin dysfunction and an intracellular calcium overload. Studies on the

hamster, however, are divided on whether there is a change in the affinity or density of cardiac L-type calcium channels. An increase in numbers of DHPR and phenylalkylamine binding sites has been reported (Wagner *et al.*, 1989), although contrasting reports (Howlett & Gordon 1987; Sen *et al.*, 1990) observe no change in density or affinity of these sites. The data for the influence of the L-type calcium channel in the pathogenesis of the cardiomyopathic hamster remain divided.

The current study is the first to show a decrease in the affinity of the DHPR binding site, along with a significant increase in DHPR binding sites in *mdx* cardiomyocytes, both of which may explain the accompanying functional data which revealed a decrease in potency to nifedipine and Bay K 8644 in isolated atria. While indirect consequences of dystrophin deficiency causing an intracellular calcium overload may explain the alteration in DHPR affinity and density, it is also possible that the dystrophin deficiency may result directly in altered receptor conformation. Brand *et. al.* (1985) showed that DHPRs are located in transverse tubules (T tubules) of the myocyte, which is also the site where the majority of the cardiac dystrophin is located (Bers, 1991; Peri *et al.*, 1994). Furthermore, dystrophin has been suggested to play a role in anchoring cardiac DHPRs, or modulating their activity (Meng *et al.*, 1996). Therefore, the deficiency of dystrophin could result in a direct defect in the DHPR that in turn may contribute to the observed reduction of potency of DHP drugs in *mdx* cardiac tissues and a compensatory increase in DHPRs. Davidoff *et al.*, (1997) observed a direct relationship between an intracellular calcium overload in rat cardiomyocytes, and an increase in DHPRs. Those experiments showed that elevated extracellular calcium in the incubation medium of the cardiomyocytes, caused a marked increase in DHPR mRNA, binding sites for [^{3}H]-PN 200 110, an increased

Kd, and an increase in L-type calcium current after three days of intracellular calcium overload (Davidoff *et al.,* 1997). These findings mirror those of the current study, of a reported intracellular calcium overload leading to an increase in DHPR mRNA, binding sites for [^{3}H]-PN 200 110, an increased Kd, along with further functional changes. It therefore seems logical to hypothesise that a lack of dystrophin leads to intracellular calcium overload as an initiating event for the observed changes in the current study.

Clearly, if an elevation of DHPRs is evident, then an alteration in the L-type calcium current should occur concurrently. It has already been shown that cultured neonatal cardiac myocytes from 1 to 4 day old *mdx* mice show a reduction in inactivation of the L-type calcium current, a change that could potentially elevate intracellular calcium, although no difference in peak current was evident in that particular study (Sadeghi *et al.*, 2002). However, there are significant differences in T-tubule development and ion channel function between cultured neonatal cardiomyocytes and adult myocytes (Nuss & Marban, 1994), and such differences could be further exacerbated in *mdx* mice, as the *mdx* do not show significant pathology until about 21 days of age (McArdle *et al.*, 1995). To date only Alloatti *et al.,* (1995) has published details on the adult *mdx* cardiac L-type calcium current, in which no significant differences in current were observed, however the authors did not provide details on perfusion or pipette solutions to indicate if the concentration of intracellular calcium was regulated during the experiment, yet this can have a major impact on current (Xiao *et al.*, 1994).

Following a moderate increase in calcium bound to the calcium-binding protein calmodulin, the association between the inhibitory domain of the L-type channel and the catalytic subunit is disrupted to allow the catalytic subunit to phosphorylate a wide range of substrates. Also elevation of intracellular calcium causes the L-type calcium channel β-subunit (Jahn *et al*., 1988) to be phosphorylated by the calcium-/calmodulin-dependent protein kinase II (CaM kinase) which results in an increased influx of calcium through the channel (Armstrong *et al*., 1988). Through these processes the calcium current can be increased by small increases in intracellular calcium, but at greater levels of increased resting intracellular calcium such as those observed in DMD, inhibition of influx predominates. Thus the calcium current can be differentially regulated depending on the level to which intracellular calcium is elevated. Furthermore, when intracellular calcium is elevated, calcium entry via the L-type calcium channel will be further reduced largely due to a decrease in the electrochemical driving force for calcium entry (Sperelakis *et al.*, 1996). Further study is required to elucidate the L-type calcium channel kinetics of mature *mdx* mice and how this may affect both APD and intracellular calcium levels.

5.6 Differences in calcium handling between ventricles and atria

Dystrophic ventricular tissue shows hypertrophy whereas atria either do not show enlargement or there are scant reports to support these kinds of changes. The atria workload is minimal compared to ventricular as they are only required to pump blood to the ventricles. Any systemic disease state that affects the volume or pressure of circulation will have an affect on the ventricular tissue, but not necessarily atria.

In comparison with ventricular cardiomyocytes, atrial cells are characterised by the absence of a t-tubular system (Minajeva *et al.,* 1997). They contain only peripheral junctional SR connected to the sarcolemma and a higher proportion of corbular SR within the cytoplasm. Because corbular SR is not connected to the sarcolemmal membrane, calcium release from these stores must be triggered by a diffusible agent (Minajeva *et al.,* 1997). Atrial and ventricular fibres do, however, exhibit the same sensitivity to calcium (Minajeva *et al.,* 1997), and although they exhibit a lower density of ryanodine receptors, atrial cells have a very similar Kd and IC_{50} for ryanodine, and EC_{50} for calcium (Cote *et al.,* 2000). A 30% higher level of SERCA mRNA has been observed in atria (Minajeva *et al.,* 1997) compared to ventricle, and a lower expression of phospholamban. However, the structures necessitated by a functional SR network are present: Cl^- selective channels, Ca^{2+}-Mg^{2+}-ATPase and other calcium regulating proteins (Cote *et al.,* 2000). Both atria and ventricles of *mdx* exhibit fibrosis, focal degeneration and fatty infiltration (Bridges, 1986).

5.7 Function of the Sarcoplasmic Reticulum

The sarcoplasmic reticulum as the major store of calcium in the cardiomyocyte may contribute to the intracellular calcium overload. The rapid cooling contracture experiments enable comparison of SR calcium between dystrophic and normal tissues via the relative size of the contracture produced.

5.7.1 Altered Relaxation

The reduced contractility of *mdx* isolated cardiac muscle appears to be in some part due to defective intracellular calcium homeostasis (Alloatti *et al.*, 1995). The *mdx* left atria displayed a longer relaxation time in this study as previously reported (Sapp *et al.*, 1996), which is indicative of a reduction in calcium sequestration, storage and/or extrusion from the cell. The two main pathways for removal of calcium are SERCA and the NCX. In the cardiomyopathic hamster, which exhibits a cardiac sarcoglycan deficiency, the NCX is increased secondary to the intracellular calcium overload (Wagner *et al.*, 1989). Theoretically this would increase calcium extrusion at the resting membrane potential, and thus cannot be the basis for the elevation of intracellular calcium that is observed in *mdx*. A delayed relaxation is often associated with delayed repolarisation, however in *mdx* tissues, relaxation is delayed in spite of a shorter action potential.

5.8 Force-Frequency Experiments

At lower frequencies of stimulation, SR sequestration and function can be examined. As frequency is increased, active sequestration mechanisms have less time to restore calcium to the SR, but the voltage-dependent calcium channels are stimulated more frequently causing greater opening of the L-type calcium channels and hence greater net calcium influx. A negative staircase was observed in the murine myocardium with an impaired capacity to generate force being observed in *mdx* over a range of stimulation frequencies in the force-frequency experiments. Previously Alloatti *et al.*, (1996) demonstrated a decline in force of contraction in response to increasing frequencies that was more marked in *mdx* compared to C57 left atria. The current

study showed a similar relationship in *mdx,* with the left atria unable to produce similar forces to C57 atria over a range of frequencies. A similar negative staircase in rat cardiac tissue is related to a myofilament desensitisation mechanism (Morii *et al.*, 1996). Possible mechanisms to explain this include a reduced time for SR calcium loading or a loss of myofilament sensitivity to calcium as reported in rat cardiac tissue (Morii *et al.*, 1996). Mechanisms for a loss of myofilament sensitivity include altered responsiveness due to effects of ions and chemicals such as Mg^{2+}, H^{+}, phosphocreatine and inorganic phosphate (Donaldson, *et al.*, 1978; Fabiato & Fabiato, 1978; Kentish, 1986). In particular, an increase in stimulation frequency may cause an decrease in intracellular pH (Bountra *et al.*, 1988).

5.8.1 Response to Ryanodine

When low concentrations of ryanodine were applied to the tissues, no difference in force of contraction relative to basal for each strain was evident, suggesting no difference in calcium release. When high doses of ryanodine were applied, SR release of calcium was inhibited, as evident by lower forces produced by the left atria. In this situation, L-type calcium current becomes that major pathway for calcium to activate the contractile apparatus. Under these conditions the L-type calcium current can be observed by the contractile properties of the tissue, because L-type calcium current is the only source of calcium available to the cell. In ryanodine treated animals where the cardiac tissue was stimulated at low frequencies, calcium from the SR has been shown to leak from the SR back into the cytoplasm from where it is extruded via NCX, which results in lower steady-state forces (Meyer *et al.*, 2001). This phenomenon was observed in the current study. In species with a negative force-frequency relationship such as mouse, ryanodine has been shown to convert the force-

frequency relationship to a positive staircase, indicating that unmasking the sarcolemma contribution to the force-frequency relationship isolates a positive force-frequency relationship in all species (Prabhu, 1998). Thus, on the addition of ryanodine, force-frequency relationship amplification is consistent with an increased importance of sarcolemmal calcium influx (Prabhu, 1998).

When 1nM Ryanodine was added to the tissue bath to remove the contribution of the SR in releasing calcium for contractions, the force-frequency curve shows a positive staircase, indicative of L-type calcium influx becoming the predominant pathway to elevate cytosolic calcium. Low force of contraction is also observed in the presence of 1nM Ryanodine, as there is no SR contribution to contractility of the myocardium. Force in the presence of 1nM Ryanodine was restored to equivalent of C57, indicating a greater influx of calcium via the L-type calcium channels in *mdx*, since the *mdx* myocardium cannot contract with similar force at the same level of cytosolic calcium. This functional finding once again lends support to the notion that the L-type calcium channels are upregulated in *mdx* myocardium.

5.8.2 Response to Caffeine

Caffeine was effective in inhibiting calcium release from the SR, as is evident from a decreased contractile force in both the control and *mdx* tissues. On the addition of caffeine, SR calcium release was inhibited, therefore L-type calcium current became the predominant source of calcium for contraction of the left atria. On the addition of the lowest concentration of caffeine, the *mdx* began to produce forces similar to those in C57, despite a normally reduced response to extracellular calcium. This is indicative of a greater flow of calcium through the L-type calcium channels. Because

caffeine is a methylxanthine, it also inhibits the enzyme phosphodiesterase allowing accumulation of cyclic AMP. Cyclic AMP increases the open time of the L-type calcium channels, thereby increasing sarcolemmal influx, as well as inhibiting SR calcium release. This effect is observed at the highest concentration of caffeine used where there is a trend for the *mdx* to produce greater force than the C57. This provides further functional data to support that *mdx* have a greater density of L-type calcium channels.

5.8.3 Response to Dantrolene

The force of contraction produced in both *mdx* and C57 with dantrolene present is indicative of the compound not blocking SR calcium release. Forces are maintained at levels observed in the absence of any drug, even in the presence of the highest concentration of dantrolene. A negative staircase remained, suggesting that L-type influx is not necessarily predominating at higher frequencies. There is a similar force-frequency relationship in the presence of the highest concentration of dantrolene to the force-frequency relationship in the absence of drug, indicating that dantrolene did not block SR release. In other studies, dantrolene has been shown to be ineffective in blocking the cardiac ryanodine receptor (Zhao *et al*., 2002), but concentrations five times higher than the concentration used in the current study have shown a mild negative inotropic effect (Meissner *et al*., 1996). In rat myocardium dantrolene has been shown to produce a negative inotropic response in a low extracellular calcium solution, but not in high calcium (Fratea *et al*., 1997). The high calcium levels in dystrophic myocardium may thus be affecting the response to dantrolene. Dantrolene did not alter the force-frequency effect in rat myocardium or any SR calcium modulation mechanisms (uptake, release, postrest recovery) (Fratea *et al*., 1997). It is

plausible that a similar lack of effect was observed in the current study. The only study that observed the effects of dantrolene on murine myocardium showed that dantrolene was not effective in suppressing arrhythmia in a murine model (Brooks *et al*., 1989) which may suggest that dantrolene is not effective in blocking SR calcium release in murine myocardium.

Dantrolene has been used in a clinical trial in boys with DMD. No cardiac changes were observed, however dantrolene reduced serum creatine kinase in the trial (Bertorini *et al.*, 1991). The skeletal muscles showed a trend towards "a lessening of muscle deterioration" however no statistical differences were observed (Bertorini *et al.*, 1991). The trial used only 7 patients with varying ages from 6 to 13 years of age, and one concentration of dantrolene was used. The study used 2 years prior to treatment as control. This study may have provided more clear evidence had the trial been placebo based and blinded.

5.9 Rapid Cooling Contractures

The amplitude of RCCs is a useful indicator of releasable SR calcium in intact cardiac muscle (Bers & Bridge, 1989). The first RCC in *mdx* is significantly smaller than control, when expressed in absolute force (mN), and when expressed as a percentage of normal twitch force. This indicates that either: i) the SR in *mdx* is releasing less calcium, ii) that the SR is leaky and/or cannot sequester and store calcium effectively, or iii) that the myocardium is unable to contract in response to a similar amount of calcium released as the C57. The tissue bath experiments in the current study have shown that the third hypothesis is most probable, as *mdx* left atria are unable to

contract with similar forces to control in response to extracellular calcium. RCC2 and RCC3 are smaller than RCC1 in both *mdx* and C57, but not significantly different between the strains. Using the SERCA specific inhibitor, the potency of CPA was not significantly different between the strains suggesting that SERCA function is comparable between the dystrophic and normal left atria. Therefore sequestration does not appear to be dysfunctional in *mdx* left atria. The difference between RCC1 and RCC2 is attributed to the activity of the NCX (Bers & Bridge, 1989). In the current study, the percent change between *mdx* and C57 is almost identical when the decreased force production of *mdx* is taken into consideration. This suggests that NCX is functioning normally in *mdx* left atria.

5.10 CPA Concentration-Response Curve

Relaxation time is increased in *mdx* atria (Sapp *et al.*, 1996) and DMD ventricles (Kovick *et al.*, 1975; Goldberg *et al.*, 1980). The current study showed no functional change in the level of SERCA, therefore the increased relaxation time may be attributed to changes in sarcolemmal calcium extrusion, or calcium binding proteins. Interestingly, Kargacin & Kargacin (1996) found no change in SERCA or the sensitivity of SERCA for calcium in skeletal muscle of *mdx* mice. They did, however, suggest that some SERCA units may be non-functional in dystrophic muscle. This could occur if some of the pump protein is partially degraded in the face of elevated calcium levels in dystrophin-deficient muscle or the continual degeneration and regeneration of dystrophic muscle causes expression of immature non-functional protein to be expressed in the SR membrane (Kargacin & Kargacin, 1996). Mule &

Serio (2001) observed no differences in SERCA by CPA-induced inhibition in colon of *mdx*.

Phospholamban has been shown to significantly lengthen relaxation time in cardiomyocytes (Zvaritch *et al.*, 2000) and to decrease SERCA affinity for calcium (Kimura *et al.*, 1996). The level of expression of the intraluminal SR calcium binding proteins is altered in *mdx* myocardium. In *mdx* skeletal muscle SR, Culligan *et al.*, (2002) observed a 20% reduction in the calcium binding capacity due to a reduction in calsequestrin-like binding proteins. Thus it is plausible that the lusitropic effect observed in *mdx* cardiac tissues may be due to changes in intraluminal SR calcium binding proteins. While active sequestration by SERCA appears to be functioning normally in *mdx* myocardium, if the binding proteins were not retaining the calcium in the SR, this calcium may contribute to the calcium overload and loss of sensitivity of the contractile proteins.

5.11 SERCA RT-PCR

SERCA in cardiac muscle of the laminin deficient dystrophic (dy/dy C57BL6J) mouse has been shown to be unchanged compared to control cardiomyocytes (Lucas-Heron *et al*., 1987). Where SERCA mRNA has been successfully upregulated in mouse overexpression models, protein level was only moderately changed above the endogenous expression (Periasamy & Huke, 2001). The authors suggest that there may be powerful post-transcriptional mechanisms working to maintain a physiological SERCA level. In the current study, SERCA mRNA was increased,

although no functional evidence supported this change. It appears that mRNA changes observed in *mdx* SERCA are not translated into functional changes.

In *mdx* heart, a study has shown decreased SERCA mRNA in 5 month old mice (Rohman *et al.,* 2003). Given that changes in intracellular calcium lead to regulation of calcium handling proteins (Davidoff *et al.,* 1997), it is not surprising that changes such as these are observed. SERCA mRNA levels have been shown to be increased (De Boer *et al.*, 2001) and decreased (Mittman *et al.*, 1998) in various models of cardiomyopathy, but protein levels in failing myocardium have been shown to be unchanged (Schwinger *et al.*, 1995; Munch *et al.*, 1998). The current study using *mdx* at 12-14 weeks of age showed an increase in SERCA mRNA but no functional change. It is postulated that mRNA is increased in response to the high intracellular calcium at this age, but protein levels remain unchanged.

CHAPTER 6 – IMPLICATIONS AND CONCLUSIONS

6.1 Conclusions From the Current Study

The current study aimed to elucidate potential mechanisms for the intracellular calcium overload that contributes to the pathogenesis of the myocardium in dystrophin-deficient conditions. The major findings from the current study were alterations in the potency, affinity and density of the DHPRs in *mdx*. Drugs active at the DHPR were approximately 2-fold less potent in *mdx* myocardium. In contracting left atrial preparations using both a DHPR agonist and antagonist, a potency difference of 2.7 and 1.9 respectively was evident. This finding was reinforced in purified ventricular membranes using radioligand binding studies which gave a similar potency difference of 2.0 and indicated an upregulation of DHPRs by 1.3 fold. RT-PCR studies provided further supportive evidence of receptor upregulation by increased mRNA expression in both atria and ventricles by 2.0 and 2.3 fold respectively. At various levels of complexity, utilising a range of techniques, clear evidence is provided to show that dystrophin deficiency in the *mdx* mouse results in DHPR upregulation in the myocardium and a reduction in receptor affinity.

It is postulated that this increase in calcium channels is a contributor to the calcium overload in dystrophic myocardium. Yet the major calcium regulating mechanism, sequestration of calcium into the SR, appears to be unaffected in *mdx*. This is an interesting finding considering the delayed relaxation observed in this study and others (Sapp *et al.*, 1996). A shorter action potential in *mdx* previously (Alloatti *et al.*,

1995) would suggest that prolonged L-type Ca^{2+} influx is not responsible for delayed relaxation either. Therefore it is probable that this effect is due to alternate mechanisms, such as SR storage. Since the calcium binding proteins of the SR have been shown to be dysfunctional in dystrophic skeletal muscle, future cardiac studies should examine these particular proteins. SERCA mRNA was shown to be upregulated, a finding that was not supported with any functional changes. There was a trend towards there being a greater amount of SERCA in the CRC to CPA, but this was not statistically significant. The RCCs suggested that SERCA function was equivalent in *mdx* to that in C57. The consensus of data supports *mdx* SERCA levels being equivalent to C57 in the heart. It is probable that mRNA changes are not translated to protein.

Interestingly, the potency of calcium is also lowered when conducting a concentration-response curve to extracellular calcium. This reduction in potency to calcium and capacity to generate force is indicative of a reduced sensitivity of the contractile proteins to calcium. One possible explanation for this is that a chronically elevated intracellular calcium such as that observed in dystrophic muscles could cause a significant reduction in myofilament sensitivity (Holt & Christensen, 1997).

6.2 Implications of the Findings

The current study has shown a significant defect in myocardial calcium handling that could contribute significantly to the pathogenesis of dystrophin-deficient disorders. The L-type calcium channels are upregulated in *mdx* myocardium, and as such represent a pathway for calcium overload which contributes to necrosis of

cardiomyocytes. The study has also shown a potency shift to DHP compounds due to a proposed conformational change in the dihydropyridine receptor. Thus treatment protocols need to be adjusted according to these findings.

Currently boys with DMD are routinely administered positive inotropic drugs to increase cardiac output. Based on the findings of the current study indicating inherent calcium overload, this practice may be detrimental to the patient. Skeletal myopathy is the overt clinical sign in DMD, yet cardiac and respiratory insufficiency account for almost all mortality associated with the disease. The current study would suggest that administration of a calcium channel antagonist when cardiomyopathy is first apparent, or even earlier may be of some benefit in reducing calcium-dependent pathogenesis. Similarly, the calcium channel antagonists have the added advantage of reducing the incidence of arrhythmias, which may become life-threatening in DMD. A reduction in intracellular calcium may also be of advantage in terms of skeletal muscle myopathy, since an increase in intracellular calcium seems to be an important step in the pathogenesis associated with the development of the myopathy. Previously, an *in vivo* trial of diltiazem improved dysfunctional calcium handling in a mouse model of hypertrophic cardiomyopathy due to a disruption of the sarcomere (Semsarian *et al.*, 2002). Early administration of diltiazem restored calcium handling protein levels to normal and prevented development of pathology (Semsarian *et al.*, 2002). Therefore the early administration of drugs that reduce intracellular calcium overload may have therapeutic potential in dystrophin-deficient conditions.

Administration of a calcium channel blocker prior to cardiomyopathy may be able to inhibit the observed increase in density of the DHPR. Further studies are warranted to

determine whether this event can be inhibited, and at what age these changes occur. Similarly, a reduction in intracellular calcium may be linked with prevention of apoptosis and cellular necrosis. The potential for prevention of the pathogenesis in DMD needs to be elucidated.

6.3 Future Research Directions

6.3.1 Longitudinal Study

A longitudinal study needs to be undertaken in *mdx* to confirm the age at which cardiac changes are observed, and to correlate these changes with alterations in calcium handling. The current study has observed a particular pathobiology at one age only. It is unknown when the onset of these changes occur, and whether these changes are maintained as the animal ages. Similarly, it remains unknown whether the primary defect of a lack of dystrophin causes changes in the L-type calcium channels, or whether these changes are secondary to other changes that lead to an intracellular accumulation of calcium. The lack of sarcolemmal integrity associated with the loss of dystrophin must lead to mechanical changes of the myocardium. It is unknown at what age the *mdx* begins to manifest cardiomyopathy associated with dystrophin-deficiency. Similarly, it is unknown to what extent utrophin is able to upregulate in *mdx* cardiac tissues, and to what degree of function utrophin is able to compensate. The *mdx* mouse remains a poorly understood model of dystrophin-deficiency, especially in terms of pathogenesis of cardiac abnormalities.

6.3.2 Calcium Channel Antagonists

Future work should entail a controlled drug trial of the calcium channel antagonists in the *mdx* model of dystrophin-deficiency. With the observed upregulation of the L-type calcium channel in *mdx,* it is expected that an antagonist to this channel would be beneficial in reducing the calcium dependent proteolysis in the myocardium. Calcium channel blockers have further advantages in reducing the possibility of arrhythmia in boys with DMD, and reducing cardiac workload, thus delaying heart failure associated with dystrophin-deficiency and respiratory insufficiency. Since the current study has observed an upregulation of the DHPR utilising several different techniques and at different levels of complexity, it is hypothesised that an *in vivo* controlled drug trial of a DHPR antagonist would reduce the intracellular calcium overload associated with dystrophin-deficiency. Given that this in turn may restore sensitivity of the contractile proteins, a marked reduction in contractility caused by the calcium channel antagonists may not occur. Similarly, since calcium overload is an initiating event in terms of cellular necrosis and apoptosis, a reduction in this calcium may have the potential to reverse or at least delay this pathogenesis.

6.3.3 Patch Clamp and L-type Calcium Current

Patch clamp data needs to be obtained for *mdx* and C57 cardiomyocytes at 12-14 weeks of age to confirm that the L-type current is increased compared to normal at this age. This study attempted to obtain L-type calcium currents by patch clamping dystrophin-deficient and normal cardiomyocytes (see Appendix) but was unsuccessful. Future work should examine the current magnitude from *mdx* and C57 cardiomyocytes for comparison and examine open probability, conductance and

inactivation of the L-type calcium channel. An antagonist to the DHPR should also be tested, to determine the potency of these drugs in reducing the L-type current. Based on the observations of the current study, it is hypothesised that the L-type current is larger in *mdx* compared to C57, and that a higher concentration of DHPR antagonist would be required to reduce the current in *mdx* by a similar extent to that observed in C57 cardiomyoctes. It would also be interesting to combine the longitudinal study with a patch clamp study, to observe changes in L-type current by age.

6.3.4 The Sodium/calcium Exchanger as a Potential Contributor to Calcium Overload

The role of the sodium/calcium exchanger in dystrophic myocardium is as yet unknown. As the primary mechanism mediating calcium efflux from the cytoplasm, it deserves attention as a potential contributor to calcium overload in dystrophin-deficient myocardium. Also, since the protein is located on the sarcolemma, where dystrophin is absent, there is potential for dysfunction of the NCX in the absence of dystrophin. Similarly, in the presence of an intracellular calcium overload, there is a potential for changes in expression of the NCX in an attempt to maintain homeostasis.

6.3.5 Calcium Binding Proteins

In *mdx* skeletal muscle, the calcium sequestration proteins of the SR have been shown to be dysfunctional (Culligan *et al.*, 2002). The function of the calcium sequestration proteins in cardiac SR has not been reported. Data from the current study support functional SERCA, and a leaky SR. A study needs to evaluate the function of the cardiac SR calcium binding proteins.

6.3.6 Myofilament Sensitivity to Calcium

The current study and previous studies (Lu & Hoey 2000 a & b; Sapp *et al.*, 1996) have observed a decrease in force production by the myocardium of dystrophin-deficient mice. This reduced ability to produce force exists despite an increased intracellular calcium concentration. It is hypothesised that a chronic calcium overload produces conformational changes in Troponin to reduce the sensitivity of the myofilaments to calcium. A study of skinned cardiac myofilaments could determine whether or not the myofilaments are desensitised.

6.4 Conclusion

The current study has shown substantial evidence to support both a decrease in affinity of the DHPR in *mdx* due to a conformational change of the DHPR, and an increase in DHPR density. The decrease in affinity is supported by tissue bath data using an agonist and antagonist at the DHPR, and radioligand binding studies using [^{3}H]-PN 200 110. An increase in receptor density is supported by radioligand binding studies, and DHPR mRNA levels. Both of these changes are also supported in functional data, whereby blocking SR calcium release and causing L-type calcium current to become the primary source of intracellular calcium caused a restoration of force in *mdx* atria, despite a usually impaired force of contraction.

A decrease in affinity of the DHPR may be due to a conformational change due to an interaction with the DAGPC. Alternatively, a loss of sarcolemmal integrity due to the absence of dystrophin may be the primary cause of intracellular calcium overload, and

an increase in DHPRs occurs secondary to this calcium overload. A conformational change of the DHPR could represent a calcium-induced change due to initial calcium overload. If this hypothesis is correct, the lack of dystrophin may be the initial event in a cycle of abnormal calcium handling, whereby the myocardium attempts to maintain intracellular calcium homeostasis by increasing L-type calcium channels, however this leads to further dysfunctional calcium handling. Eventually calcium-dependent proteolytic enzymes are activated and cellular necrosis begins to diminish the function of the myocardium.

The reduced force of contraction observed in *mdx* myocardium may represent a diminished calcium sensitivity of the myofilaments, caused by chronic calcium overload, a hypothesis that needs to be tested.

The delayed relaxation observed in *mdx* can not be attributed to dysfunctional SERCA. The current study has shown a trend towards the upregulation of SERCA, rather than a downregulation which could account for a delayed relaxation. The potential mechanisms for this observation remain a loss of the SR calcium binding proteins, a mechanism that has been observed in skeletal muscle, a leaky SR or a leaky sarcolemma which is also feasible given the location of dystrophin.

Regardless of the basis for the delayed relaxation, the use of calcium channel antagonists in treating dystrophinopathy-related cardiomyopathy requires further research. Calcium influx via the calcium channels in *mdx* appears to be a substantial contributor to the lack of calcium homeostasis and resultant calcium overload.

REFERENCES

Adachi-Akahane S, Amano Y, Okuyama R & Nagao T (1993) Quaternary diltiazem can act from both sides of the membrane in ventricular myocytes. *Jpn J Pharmacol* **61** 263-266.

Ahn AH & Kunkel LM (1993) The structural and functional diversity of dystrophin. *Nat Genet* **3 (4)** 283-291.

Alcantara MA, Villarreal MT, Del Castillo V, Gutierrez G, Saldana Y, Maulen I, Lee R, Macias M & Orozco L (1999) High frequency of de novo deletions in Mexican Duchenne and Becker muscular dystrophy patients. Implications for genetic counseling. *Clin Genet* **55 (5)** 376-380.

Alderton JM & Steinhardt RA (2000) Calcium influx through calcium leak channels is responsible for the elevated levels of calcium-dependent proteolysis in dystrophic myotubes. *J Biol Chem* **275 (13)** 9452-9460.

Alloatti G, Pia Gallo M, Penna C & Levi RC (1995) Properties of cardiac cells from dystrophic mouse. *J Mol Cell Cardiol* **27** 1775-1779.

Anand R & Emery AE (1982) Verapamil and calcium-stimulated enzyme efflux from skeletal muscle. *Clin Chem* **28 (7)** 1482-1484.

Anderson JE, McIntosh LM & Poettcker R (1996) Deflazacort but not prednisone improves both muscle repair and fiber growth in diaphragm and limb muscle in vivo in the *mdx* dystrophic mouse. *Muscle Nerve* **19 (12)** 1576-1585.

Anderson JL, Head SI, Rae C & Morley JW (2002) Brain function in Duchenne muscular dystrophy. *Brain* **125 (1)** 4-10.

Armstrong D, Erxleben C, Kalman D, Lai Y, Nairn A & Greengard P (1988) Intracellular calcium controls the activity of DHP-sensitive calcium channels through protein phosphorylation and its removal. *J Gen Physiol* **92,** 10a.

Backman E & Nylander E (1992) The heart in Duchenne muscular dystrophy: a non-invasive longitudinal study. *European Heart Journal* **13** 1239-1244.

Bakker AJ, Head SL, Williams DA & Stephenson DG (1993) Ca^{2+} levels in myotubes grown from skeletal muscle of dystrophic *(mdx)* and normal mice. *J Physiol* **460** 1-13.

Barry WH (2000) Na^{+}- Ca^{2+} exchange in failing myocardium: Friend or foe? *Circ Res* **87** 529-531.

Baudet S, Shaoulian R & Bers DM (1993) Effects of thapsigargin and cyclopiazonic acid on twitch force and sarcoplasmic reticulum Ca^{2+} content of rabbit ventricular muscle. *Circ Res* **73** 813-819.

Bean BP (1984) Nitrendipine block of cardiac calcium channels: high affinity binding to the inactivated state. *Proc Nat Acad Sci* **81** 6388-6392.

Berger F, Borchard U, Hafner D, Kammer T & Weis T (1991) Inhibition of potassium outward currents and pacemaker current in sheep cardiac Purkinje fibres by the verapamil derivative YS 035. *Naunyn-Schmiedebergs Arch Pharmacol* **344** (6) 653-661.

Bers DM (2002) Cardiac excitation-contraction coupling. *Nature* **415** 198-205.

Bers DM (1991) Excitation-contraction coupling and cardiac contractile force. In: Symposium CF, editor. The physiological basis of Starling's law of the heart. *Kluwer Academic Publisher* 17-32.

Bers DM & Bridge JHB (1989) Relaxation of rabbit ventricular muscle by Na-Ca exchange and sarcoplasmic reticulum calcium pump. *Circ Res* **65,** 334-342.

Bers DM & Perez-Reyes E (1999) Ca channels in cardiac myocytes: structure and function in Ca influx and intracellular Ca release. *Cardiovasc Res* **42 (2)** 339-360.

Bertorini TE, Bhattacharya SK, Palmieri GMA, Chesney CM, Pifer D & Baker B (1982) Muscle calcium and magnesium content in Duchenne muscular dystrophy. *Neurology* **32** 1088-1092.

Bertorini TE, Cornelio F, Bhattacharya SK, Palmieri GM, Dones I, Dworzak F & Brambati B (1984) Calcium and magnesium content in fetuses at risk and prenecrotic Duchenne muscular dystrophy. *Neurology* **34 (11)** 1436-1440.

Bertorini TE, Palmieri GMA, Griffin JW, Igarashi M, Hinton A & Karas JG (1991) Effect of dantrolene in Duchenne muscular dystrophy. *Muscle Nerve* **14** 503-507.

Bhattacharya SK, Palmieri GM, Bertorini TE & Nutting DF (1982) The effects of diltiazem in dystrophic hamsters. *Muscle Nerve* **5 (1)** 73-78.

Bia BL, Cassidy PL, Young ME, Rafael JA, Leighton B, Davies KE, Radda GK & Clarke Kieran (1999) Decreased myocardial nNOS, increased iNOS and Abnormal ECGs in mouse models of Duchenne muscular dystrophy. *J Mol Cell Cardiol* **31** 1857-1862.

Bies RD, Friedman D, Roberts R, Perryman MB & Caskey CT (1992) Expression and localization of dystrophin in human cardiac Purkinje fibers. *Circulation* **86 (1)** 147-153.

Bittner RE, Schofer C, Weipoltshammer K, Ivanova S, Streubel B, Hauser E, Freilinger M, Hoger H, Elbe-Burger A & Wachtler F (1999) Recruitment of bone-marrow-derived cells by skeletal and cardiac muscle in adult dystrophic *mdx* mice. *Anat Embryl* **199** 391-396.

Bodensteiner JB & Engel AG (1978) Intracellular calcium accumulation in Duchenne

dystrophy and other myopathies: a study of 567,000 muscle fibers in 114 biopsies. *Neurology* **28 (5)** 439-446.

Boland BJ, Silbert PL, Groover RV, Wollan PC & Silverstein MD (1996) Skeletal, cardiac and smooth muscle failure in Duchenne muscular dystrophy. *Paediatric Neurology* **14 (1)** 7-12.

Bolanos-Jimenez F, Bordais A, Behra M, Strahle U, Sahel J & Rendon A (2001) Dystrophin and Dp71, two products of the DMD gene, show a different pattern of expression during embryonic development in zebrafish. *Mech Dev* **102 (1-2)** 239-241.

Bosch RF, Scherer CR, Rub N, Wohrl S, Steinmeyer K, Haase H, Busch AE, Seipel L & Kuhlkamp V (2003) Molecular mechanisms of early electrical remodeling: transcriptional downregulation of ion channel subunits reduces $I_{Ca,L}$ and I_{to} in rapid atrial pacing in rabbits. *J Am Coll Cardiol* **41 (5)** 858-869.

Bountra C, Kaila K & Vaughan-Jones RD (1988) Effect of repetitive activity upon intracellular pH, sodium and contraction in sheep cardiac Purkinje fibres. *J Physiol Lond* **398** 341-360.

Brandt NR, Kawamoto RM & Caswell AH (1985) Dihydropyridine binding sites on transverse tubules isolated from triads of rabbit skeletal muscle. *J Recept Res* **5 (2-3)**155-170.

Braun U, Paju K, Eimre M, Seppet E, Orlova E, Kadaja L, Trumbeckaite S, Gellerich FN, Zierz S, Jocjush H & Seppet EK (2001) Lack of dystrophin is associated with altered integration of the mitochondria and ATPases in slow-twitch muscle cells of *mdx* mice. *BBA* **1505** 258-270.

Bridges LR (1986) The association of cardiac muscle necrosis and inflammation with the degenerative and persistent myopathy of *mdx* mice *J Neurol Sci* **72 (2-3)** 147-57.

Brodde O-E (1991) β_1 and β_2-adrenoceptors in the human heart: properties, function, and alterations in chronic heart failure. *Pharmacol Rev* **43** 203-242.

Brooks RR, Carpenter JF, Jones SM & Gregory CM (1989) Effects of dantrolene sodium in rodent models of cardiac arrhythmia. *Eur J Pharmacol* **164 (3)** 521-530.

Brown RH (1997) Dystrophin-associated proteins and the muscular dystrophies. *Annu Rev Med* **48** 457-466.

Bulfield G, Siller WG, Wight PAL & Moore KJ (1984) X chromosome-linked muscular dystrophy *(mdx)* in the mouse. *Proc Natl Acad Sci USA* **81** 1189-1192.

Burrow KL, Coovert DD, Klein CJ, Bulman DE, Kissel JT, Rammohan KW, Burghes AH & Mendell JR (1991) Dystrophin expression and somatic reversion in prednisone-treated and untreated Duchenne dystrophy. CIDD Study Group. *Neurology* **41 (5)** 661-666.

Camacho SA, Wikman-Coffelt J, Wu ST, Watters TA, Botvinick EH, Sievers R, James TL, Jasmin G & Parmley WW (1988) Improvement in myocardial performance without a decrease in high-energy phosphate metabolites after isoproterenol in Syrian cardiomyopathic hamsters. *Circulation* **77 (3)** 712-719.

Carlson CG & Officer T (1996) Single channel evidence for a cytoskeletal defect involving acetylcholine receptors and calcium influx in cultured dystrophic (*mdx*) myotubes. *Muscle Nerve* **19 (9)** 1116-1126.

Catterall WA & Striessnig J (1992) Receptor sites for Ca^{2+} channel antagonists. *Trends Pharmacol Sci* **13** 256-262.

Caviedes R, Caviedes P, Liberona JL & Jaimovich E (1994) Ion channels in a skeletal muscle cell line from a Duchenne muscular dystrophy patient. *Muscle Nerve* **17** 1021-1028.

Chamberlain JS (2002) Gene therapy of muscular dystrophy. *Hum Mol Genet* **11 (20)** 2355-2362.

Chen F, Spicher K, Jiang M, Birnbaumer L & Wetzel GT (2001) Lack of muscarinic regulation of Ca^{2+} channels in G_{i2} alpha gene knockout mouse hearts. *Am J Physiol* **280 (5)** H1989-H1995.

Chu V, Otero JM, Lopez O, Sullivan MS, Morgan JP, Amende I & Hampton TG (2002) Electrocardiographic findings in *mdx* mice: A cardiac phenotype of Duchenne muscular dystrophy. *Muscle Nerve* **26** 513-519.

Cingolani HE, Wiedmann RT, Lynch JJ, Wenger HC, Scott AL, Siegl PKS & Stein RB (1990) Negative Lusitropic effect of DPI 201-106 and E4031. Possible role of prolonging actions potential duration. *J Moll Cell Cardiol* **22** 1025-1034.

Cohn RD, Durbeej M, Moore SA, Coral-Vazquez R, Prouty S & Campbell KP (2001) Prevention of cardiomyopathy in mouse models lacking the smooth muscle sarcoglycan-sarcospan complex. *J Clin Invest* **107 (2)** R1-R7.

Collet C, Allard B, Tourneur Y & Jacquemond V (1999) Intracellular calcium signals measured with indo-1 in isolated skeletal muscle fibres from control and *mdx* mice. *J Physiol* **520 (2)** 417-429.

Cooper BJ, Winand NJ, Stedman H, Valentine BA, Hoffman EP, Kunkel LM, Scott MO, Fischbeck KH, Kornegay JN, Avery RJ, Williams JR, Schmickel RD & Sylvester JE (1988) The homologue of the Duchenne locus is defective in X-linked muscular dystrophy of dogs. *Nature* **334 (6178)** 154-156.

Cooper PJ, Ward M-L, Hanley PJ, Denyer GR & Loiselle DS (2001) Metabolic consequences of a species difference in Gibbs free energy of Na^+/Ca^{2+} exchange: rat versus guinea pig. *Am J Physiol* **280** R1221-R1229.

Cote K, Proteau S, Teijeira J & Rousseau E (2000) Characterization of the sarcoplasmic reticulum K^+ and Ca^{2+} - release channel-ryanodine receptor – in human atrial cells. *J Moll Cell Cardiol* **32** 1-13.

Coulton GR, Curtin NA, Morgan JE & Partridge TA (1988) The *mdx* mouse skeletal muscle myopathy: II. Contractile properties. *Neuropathology and Applied Neurobiology* **14** 299-314.

Cowan J, MacDessi J, Stark A & Morgan G (1980) Incidence of Duchenne muscular dystrophy in New South Wales and Australian Capital Territory. *J Med Genet* **17** 245-249.

Cox GA, Cole NM, Matsumura K, Phelps SF, Hauschka SD, Campbell KP, Faulkner JA & Chamberlain JS (1993) Overexpression of dystrophin in transgenic *mdx* mice eliminates dystrophic symptoms without toxicity. *Nature* **364 (6439)** 725-729.

Cox GF & Kunkel LM (1997) Dystrophies and heart disease. *Current opinions in Cardiology* **12** 329-343.

Cox DA & Matlib MA (1993) A role for the mitochondrial Na^+-Ca^{2+} exchanger in the regulation of oxidative phosphorylation in isolated heart mitochondria. *J Biol Chem* **15 268 (2)** 938-947.

Crosbie RH, Heighway J, Venzke DP, Lee JC & Campbell KP (1997) Sarcospan, the 25-kDa transmembrane component of the dystrophin-glycoprotein complex. *J Biol Chem* **272** 31221-31224.

Cullen MJ & Mastaglia FL (1980) Morphological changes in dystrophic muscle. *Br Med Bull* **36 (2)** 145-152.

Culligan K, Banville N, Dowling P & Ohlendieck K (2002) Drastic reduction of calsequestrin-like proteins and impaired calcium binding in dystrophic *mdx* muscle. *J Appl Physiol* **92** 435-345.

Culligan K & Ohlendieck K (2002) Abnormal calcium handling in muscular dystrophy. *Basic Appl Myol* **12 (4)** 147-157.

Cziner DG & Levin RI (1993) The cardiomyopathy of Duchenne's muscular dystrophy and the function of dystrophin. *Med Hypotheses* **40** 169-173.

Dangain J & Neering IR (1993) Effect of caffeine and high potassium on normal and dystrophic mouse EDL muscles at various developmental stages. *Muscle Nerve* **16 (1)** 33-42.

Danilou G, Comtois AS, Dudley R, Karpati G, Vincent G, Des Rosiers C & Petrof BJ (2001) Dystrophin-deficient cardiomyocytes are abnormally vulnerable to mechanical stress-induced contractile failure and injury. *FASEB J* **15** 1655-1657.

Davidoff AJ, Maki TM, Ellingsen O & Marsh JD (1997) Expression of calcium channels in adult cardiac myocytes is regulated by calcium. *J Mol Cell Cardiol* **29 (7)** 1791-1803.

Davies KE (1997) Challenges in Duchenne muscular dystrophy. *Neuromuscul Disord* **7 (8)** 482-486.

Davies JE, Winokur TS, Aaron MF, Benza RL, Foley BA & Holman WL (2001) Cardiomyopathy in a carrier of Duchenne's muscular dystrophy. *J Heart Lung Transplant* **20** 781-784.

Dawson DM (1966) Leakage of enzymes from denervated and dystrophic chicken muscle. *Arch Neurol* **14 (3)** 321-325.

De Backer F, Vandebrouck C, Gailly P & Gillis JM (2002) Long-term study of Ca^{2+} homeostasis and of survival in collagenase-isolated muscle fibres from normal and *mdx* mice. *J Physiol* **542.3** 855-865.

De Boer RA, Henning RH, Suurmeijer AJ, Pinto YM, Olthof E, Kirkels JH, van Gilst WH, Crijns HJ & van Veldhuisen DJ (2001) Early expression of natriuretic peptides and SERCA in mild heart failure: association with severity of the disease. *Int J Cardiol* **78 (1)** 5-12.

Deconinck N, Tinsley J, De Backer F, Fisher R, Kahn D, Phelps S, Davies K & Gillis JM (1997) Expression of truncated utrophin leads to major functional improvements in dystrophin-deficient muscles of mice. *Nat Med* **3 (11)** 1216-1221.

De La Porte S, Morin S & Koenig J (1999) Characteristics of skeletal muscle in *mdx* mutant mice. *Int Rev Cytol* **191** 99-148.

De Paoli P, Cerbai E, Koidl B, Kirchengast M, Sartiani L & Mugelli A (2002) Selectivity of different calcium antagonists on T- and L-type calcium currents in guinea-pig ventricular myocytes. *Pharmacol Res* **46 (6)** 491-497.

Divet A & Huchet-Cadiou C (2002) Sarcoplasmic reticulum function in slow- and fast-twitch skeletal muscles from *mdx* mice. *Pflugers Arch* **444** 634-643.

Donaldson SK, Best PM & Kerrick GL (1978) Characterization of the effects of Mg^{2+} on Ca^{2+} and Sr^{2+}-activated tension generation of skinned rat cardiac fibers. *J Gen Physiol* **71** 645-655.

Duarte JA, Soares JM & Appell HJ (1992) Nifedipine diminishes exercise-induced muscle damage in mouse. *Int J Sports Med* **13 (3)** 274-277.

DuBell WH, Gigena MS, Guatimosim S, Long X, Lederer WJ & Rogers TB (2002) Effects of PP1/PP2A inhibitor calyculin A on the E-C coupling cascade in murine ventricular myocytes. *Am J Physiol* **282 (1)** H38-48.

Dubowitz V & Heckmatt J (1980) Management of muscular dystrophy: Pharmacological and physical aspects. *Br Med Bull* **36 (2)** 139-144.

Dubrovsky AL, Angelini C, Bonifati DM, Pegoraro E & Mesa L (1998) Steroids in muscular dystrophy: where do we stand? *Neuromuscul Disord* **8 (6)** 380-384.

Dunn JF & Radda GK (1991) Total ion of skeletal and cardiac muscle in the *mdx* mouse dystrophy: Ca^{2+} is elevated at all ages. *J Neurol Sci* **103** 226-231.

Dupont-Versteegden E, McCarter RJ & Katz MS (1994) Voluntary exercise decreases progression of muscular dystrophy in diaphragm of *mdx* mice. *J Appl Physiol* **77 (4)** 1736-1741.

Eagle M, Baudouin SV, Chandler C, Giddings DR, Bullock R & Bushby K (2002) Survival in Duchenne muscular dystrophy: improvements in life expectancy since 1967 and the impact of home nocturnal ventilation. *Neuromuscul Disord* **12 (10)** 926-929.

Ebashi S, Toyokura Y, Momoi H & Sugita H (1959) High creatine phosphokinase activity in sera of progressive muscular dystrophy. *J. Biochem* **46** 103-104.

Ehrlich BE, Kaftan E, Bezprozvannaya S & Bezprozvanny I (1994) The pharmacology of intracellular Ca^{2+}-release channels. *Trends Pharmacol Sci* **15 (5)** 145-149.

Emery AE. (1991) Population frequencies of inherited neuromuscular diseases a world survey. *Neuromuscul Disord* **1** 19-29.

Emery AEH. (1993) *Duchenne muscular dystrophy 2nd Edn.* Oxford medical publications, Oxford.

Emery AE & Burt D (1980) Intracellular calcium and pathogenesis and antenatal diagnosis of Duchenne muscular dystrophy. *Br Med J* **280 (6211)** 355-357.

Ervasti JM & Campbell KP (1993) Dystrophin-associated glycoproteins: their possible roles in the pathogenesis of Duchenne muscular dystrophy. *Mol Cell Biol Hum Dis Ser* **3** 139-166.

Even PC, Decrouy A & Chinet A (1994) Defective regulation of energy metabolism in *mdx*-mouse skeletal muscles. *Biochem J* **304** 649-654.

Fabiato A & Fabiato F (1975) Contractions induced by a calcium-triggered release of calcium from the sarcoplasmic reticulum of single skinned cardiac cells. *J Physiol* **249 (3)** 469-495.

Fabiato A & Fabiato F (1978) Effects of pH on the myofilaments and the sarcoplasmic reticulum of skinned cells from cardiac and skeletal muscles. *J Physiol Lond* **276** 233-255.

Fanin M, Melacini P, Angelini C & Danieli GA (1999) Could utrophin rescue the myocardium of patients with dystrophin gene mutations? *J Mol Cell Cardiol* **31** 1501-1508.

Ferrari R, Cucchini F, Bolognesi R, Bachetti T, Boraso A, Bernocchi P, Gaia G & Visioli O (1994) How do calcium antagonists differ in clinical practice? *Cardiovasc Drugs Ther* **8 Suppl 3** 565-575.

Finsterer J & Stollberger C (2003) The heart in human dystrophinopathies. *Cardiology* **99 (1)** 1-19.

Fiolet JWT, Baartscheer A & Schumacher CA (1995) Intracellular [Ca^{2+}] and VO_2 after manipulation of the free-energy of the Na^{+}/Ca^{2+}-exchanger in isolated rat ventricular myocytes. *J Mol Cell Cardiol* **27** 1513-1525.

Fisher R, Tinsley JM, Phelps SR, Squire SE, Townsend ER, Martin JE & Davies KE (2001) Non-toxic ubiquitous over-expression of utrophin in the *mdx* mouse. *Neuromusc Disord* **11** 713-721.

Fong PY, Turner PR, Denetclaw WF & Steinhardt RA (1990) Increased activity of calcium leak channels in myotubes of Duchenne human and *mdx* mouse origin. *Science* **250 (4981)** 673-676.

Franco A Jr & Lansman JB (1990) Calcium entry through stretch-inactivated ion channels in *mdx* myotubes. *Nature* **344 (6267)** 670-673.

Fratea S, Langeron O, Lecarpentier Y, Coriat P & Riou B (1997) In vitro effects of dantrolene on rat myocardium. *Anesthesiology* **86 (1)** 205-215.

Fruen BR, Bardy JM, Byrem TM, Strasburg GM & Louis CF (2000) Differential Ca^{2+} sensitivity of skeletal and cardiac muscle ryanodine receptors in the presence of calmodulin. *Am J Physiol* **279 (3)** C724-C733.

Gardener-Medwin D (1980) Clinical features and classification of the muscular dystrophies. *Br Med Bull* **36 (2)** 109-115.

Gillis JM (1996) Membrane abnormalities and Ca^{2+} homeostasis in muscles of the *mdx* mouse, an animal model of the Duchenne muscular dystrophy: a review. *Acta Physiol Scand* **156** 397-406.

Gillis JM & Deconinck N (1998) The physiological evaluation of gene therapies of dystrophin-deficient muscles. *Adv Exp Med Biol* **453** 411-417.

Gnecchi-Ruscone T, Taylor J, Mercuri E, Peternostro G, Pocue R, Bushby K, Sewry C, Muntoni F & Camici PG (1999) Cardimyopathy in Duchenne, Becker and Sarcoglycanopathies: A role for coronary dysfunction? *Muscle Nerve* **22** 2549-2556.

Goldberg SJ, Feldman L, Reinecke C, Stern LZ, Sahn DJ & Allen HD (1980) Echocardiographic determination of contraction and relaxation measurements of the left ventricular wall in normal subjects and patients with muscular dystrophy. *Circulation* **62 (5)** 1061-1069.

Gopalakrishnan M, Triggle DJ, Rutledge A, Yong WK, Bauer JA & Ho-Lueng F (1991) Regulation of K^+ and Ca^{2+} channels in experimental cardiac failure. *Am J Physiol* **261** H1979-H1987.

Gordon T & Stein RB (1985) Temperature effects on the kinetics of force generation in normal and dystrophic mouse muscles. *Experimental Neurology* **89** 348-360.

Gurusinghe AD, Wilce MC, Austin L & Hearn MT (1991) Duchenne muscular dystrophy and dystrophin: sequence homology observations. *Neurochem Res* **16 (6)** 681-686.

Hain J, Onoue H, Mayrleitner M, Fleischer S & Schindler H (1995) Phosphorylation modulates the function of the calcium release channel of sarcoplasmic reticulum from cardiac muscle. *J Biol Chem* **270** 2074-2081.

Hainsey TA, Senapi S, Kuhn DE & Rafael JA (2003) Cardiomyopathy features associated with muscular dystrophy are independent of dystrophin absence in cardiovasculature. *Neuromusc Disord* **13** 294-302.

Hammerer-Lercher A, Erlacher P, Bittner R, Korinthenberg R, Skladal D, Sorichter S, Sperl W, Puschendorf B & Mair J (2001) Clinical and experimental results on cardiac troponin expression in Duchenne muscular dystrophy. *Clin Chem* **47 (3)** 451-458.

Hamplova-Peichlova J, Krusek J, Paclt I, Slavicek J, Lisa V & Vyskocil F (2002) Citalopram inhibits L-type calcium channel current in rat cardiomyocytes in culture. *Physiol Res* **51 (3)** 317-21.

Hara H, Nolan PM, Scott MO, Bucan M, Wakayama Y & Fishbeck KH (2002) Running endurance abnormality in *mdx* mice. *Muscle Nerve* **25** 207-211.

Haws CM & Lansman JB (1991) Developmental regulation of mechanosensitive calcium channels in skeletal muscle from normal and *mdx* mice. *Proc R Soc Lon* **245** 173 –177.

Head SI (1993) Membrane potential, resting calcium and calcium transients in isolated fibres from normal and dystrophic mice. *J Physiol* **469** 11-19.

Hegreberg GA, Camacho Z & Gorham JR (1974) Histopathologic description of muscular dystrophy of mink. *Arch Pathol* **97 (4)** 225-229.

Hescheler J, Pelzer D, Trube G & Trautwein W (1982) Does the organic calcium channel blocker D600 act from inside or outside on the cardiac cell membrane? *Pflugers Arch Eur J Physiol* **393** 287-291.

Hinton VJ, De Vivo DC, Nereo NE, Goldstein E & Stern Y (2000) Poor verbal working memory across intellectual level in boys with Duchenne dystrophy. *Neurology*. **54 (11)** 2127-2132.

Hjemdahl P & Wallen NH (1997) Calcium antagonist treatment, sympathetic activity and platelet function. *Eur Heart J* **18 Suppl A** 36-50.

Hockerman GH, Peterson BZ, Sharp E, Tanada TN, Scheuer T& Catterall WA (1997) Construction of a high-affinity receptor site for dihydropyridine agonists and antagonists by single amino acid substitutions in a non-L-type Ca^{2+} channel. *PNAS USA* **94 (26)** 14906-14911.

Hoffman, EP (2001) *Dystrophinopathies* Research Centre for Genetic Medicine, Washington.

Hoffman EP, Brown RJ & Kunkel LM (1987) Dystrophin: the protein product of the Duchenne muscular dystrophy locus. *Cell* **51** 919-928.

Hoffman LM, Maguire AM & Bennett J (1997) Cell-mediated immune response and stability of intraocular transgene expression after adenovirus-mediated delivery. *Invest Ophthalmol Vis Sci* **38 (11)** 2224-2233.

Hoffman EP & Dressman D (2001) Molecular pathophysiology and targeted therapeutics for muscular dystrophy. *Trends Pharmacol Sci* **22** (9) 465-470.

Hohenegger M & Suko J (1993) Phosphorylation of the purified cardiac ryanodine receptor by exogenous and endogenous protein kinases. *Biochem J* **296** 303-308.

Holt E & Christensen G (1997) Transient Ca^{2+} overload alters Ca^{2+} handling in rat cardiomyocytes: effects on shortening and relaxation. *Am J Physiol* **273 (2 Pt 2)** H573-H582.

Hoogerwaard EM, van der Wouw PA, Wilde AAM, Bakker ER, Ippel PF, Oosterwijk JC, Majoor-Krakauer DF, van Essen AJ, Leschot NJ & deVisser M (1999) Cardiac involvement in carriers of Duchenne and Becker muscular dystrophy. *Neromuscul Disord* **9** 347-351.

Hotchkiss RS, Osborne DF, Lappas GD & Karl IE (1995) Calcium antagonists decrease plasma and tissue concentrations of tumor necrosis factor-alpha, interleukin-1 beta, and interleukin-1 alpha in a mouse model of endotoxin. *Shock* **3 (5)** 337-342.

Howlett SE & Gordon T (1987) Calcium channels in normal and dystrophic hamster muscle: [^{3}H]nitrendipine binding studies. *Biochem Pharm* **36** 2653-2659.

Hunsaker RH, Fulkerson PK, Barry FJ, Lewis RP, Leier CV & Unverferth DV (1982) Cardiac function in Duchenne's muscular dystrophy. Results of 10-year follow-up study and noninvasive tests. *Am J Med* **73 (2)** 235-238.

Hunter S (1980) The heart in muscular dystrophy. *Br Med Bull* **36 (2)** 133-134.

Ikeda Y, Martone M, Gu Y, Hoshijima M, Thor A, Oh SS, Peterson KL & Ross J (2000) Altered membrane proteins and permeability correlate with cardiac dysfunction in cardiomyopathic hamsters. *Am J Physiol* **278** H1362-H1370.

Ishikawa Yuka, Bach JR, Ishikawa Yukitoshi & Minami R (1995) A management trial for Duchenne cardiomyopathy. *Am J Phys Med Rehabil* **74** 435-350.

Ishikawa Y, Bach JR & Minami R (1999) Cardioprotection for Duchenne's muscular dystrophy. *Am Heart J* **137 (5)** 895-902.

Jahn H, Nastainczyk W, Rohrkasten A, Schneider T & Hoffman F (1988) Site-specific phosphorylation of the purified receptor for calcium-channel blockers by cAMP- and cGMP-dependent protein kinases, protein kinase C, calmodulin-dependent protein kinase II. *Eur J Biochem* **178** 535-542.

Jasmin G, Solymoss B & Proschek L (1979) Therapeutic trials in hamster dystrophy. *Ann N Y Acad Sci* **317** 338-348.

Johnson PJ & Bhattacharya SK (1993) Regulation of membrane-mediated chronic muscle degerneration in dystrophic hamsters by calcium-channel blockers: diltiazem, nifedipine and verapamil. *J Neurol Sci* **115 (1)** 76-90.

Kakulas BA (1997) Problems and potential for gene therapy in Duchenne muscular dystrophy. *Neuromuscul Disord* **7 (5)** 319-324.

Kanai AJ, Pearce LL, Clemens PR, Birder LA, VanBibber MM, Choi SY, de Groat WC & Peterson J (2001) Identification of a neuronal nitric oxide synthase in isolated cardiac mitochondria using electrochemical detection. *PNAS USA* **98 (24)** 14126-14131.

Kamper A & Rodemann HP (1992) Alterations of protein degradation and 2-D protein pattern in muscle cells of *mdx* and DMD origin. *Biochem Biophys Res Commun* **189 (3)** 1484-1490.

Kanda S, Adachi-Akahane S & Nagao T (1998) Functional interaction between benzothiazepine- and dihydropyridine binding sites of cardiac L-type Ca^{2+} channels. *Eur J Pharm* **358** 277-287.

Kargacin ME & Kargacin GJ (1996) The sarcoplasmic reticulum calcium pump is functionally altered in dystrophic mice. *BBA* **1290** 4-8.

Karpati G (1990) The principles and practice of myoblast transfer. *Adv Exp Med Biol* **280** 69-74.

Kass RS & Arena JP (1989) Influence of pHo on calcium channel block by amlodipine, a charged DHP compound: Implications for location of the DHP receptor. *J Gen Physiol* **93** 1109-1127.

Kass RS, Arena JP & Chin S (1991) Block of L-type calcium channels by charged DHPs: Sensitivity to side of application and calcium. *J Gen Physiol* **98** 63-75.

Keep NH, Norwood FLM, Moores CA, Winder SJ & Kendric-Jones J (1999) The 2.0 a structure of the second calponin homology domain from the actin-binding region of the dystrophin homologue utophin. *JMB* **285** 1257-1264.

Kentish JC (1986) The effects of inorganic phosphate and creatine phosphate on force production in skinned muscles from rat ventricle. *J Physiol Lond* **370** 585-604.

Khan MA (1993) Corticosteroid therapy in Duchenne muscular dystrophy. *J Neurol Sci* **120 (1)** 8-14.

Kimura Y, Kurzydlowski K, Tada M & MacLennan DH (1996) Phospholamban regulates the Ca^{2+}-ATPase through intramembrane interactions. *J Biol Chem* **271,** 21726-21731.

Kingston HM, Harper PS, Pearson PL, Davies KE, Williamson R & Page D (1983) Localisation of gene for Becker muscular dystrophy. *Lancet* **2 (8360)** 1200.

Kissel JT, Burrow KL, Rammohan KW & Mendell JR (1991) Mononuclear cell analysis of muscle biopsies in prednisone-treated and untreated Duchenne muscular dystrophy. CIDD Study Group. *Neurology* **41 (5)** 667-672.

Kocic I, Dworakowska D & Dworakowski R (1998) Different aspects of the effects of thapsigargin on automatism, contractility and responsiveness to phenylephrine in cardiac preparations from rats and guinea pigs. *Pharm Res* **37 (4)** 273-280.

Koenig M, Hoffman EP, Bertelson CJ, Monaco AP, Feener C & Kunkel LM (1987) Complete cloning of the Duchenne muscular dystrophy (DMD) cDNA and preliminary genomic organization of the DMD gene in normal and affected individuals. *Cell* **50 (3)** 509-517.

Koenig M, Monaco AP & Kunkel LM (1988) The complete sequence of dystrophin predicts a rod-shaped cytoskeletal protein. *Cell* **53 (2)** 219-222.

Kornegay JN, Tuler SM, Miller DM & Levesque DC (1988) Muscular dystrophy in a litter of golden retriever dogs. *Muscle Nerve* **11** 1056-1064.

Kovick RB, Fogelman AM, Abbasi AD, Peter JB & Pearce ML (1975) Echocardiographic evaluation of posterior left ventricular wall motion in muscular dystrophy. *Circulation* **52 (3)** 447-454.

Kunkel L, Burns G, Aldrige J & Latt S (1985) Genetic analysis of Duchenne dystrophy. *Adv Exp Med Biol* **182** 287-294.

Kuo TA, Zhu L, Golden K, Marsh JD, Bhattacharya SK & Liu B-F (2002) Altered Ca^{2+} homeostatsis and impaired mitochondrial function in cardiomyopathy. *Mol Cell Biochem* **283** 119-127.

Kuznetsov AV, Winkler K, Wiedermann FR, von Bossanyi P, Dietzmann K & Kunz WS (1998) Impaired mitochondrial oxidative phosphorylation in skeletal muscle of the dystrophin-deficient *mdx* mouse. *Molecular and Cellular Biology* **183** 87-96.

Lachnit WG. Phillips M, Gayman KJ & Pessah IN (1994) Ryanodine and dihydropyridine binding patterns and ryanodine receptor mRNA level in myopathic hamster heart. *Am J Physiol* **267** H1205-H1213.

Lamb GD (2000) Excitation-contraction coupling in skeletal muscle: comparisons with cardiac muscle. *Clin Exp Pharmacol Physiol* **27 (3)** 216-224.

Lidov HG, Byers TJ, Watkins SC & Kunkel LM (1990) Localization of dystrophin to postsynaptic regions of central nervous system cortical neurons. *Nature* **348 (6303)** 725-728.

Loiselle DS (1987) Cardiac basal and activation metabolism. *Basic Res Cardiol* **82** 37-50.

Lu S & Hoey A (2000a) Changes in function of cardiac receptors mediating the effects of the autonomic nervous system in the muscular dystrophy (*mdx*) mouse. *J Mol Cell Cardiol* **32** 143-152.

Lu S & Hoey A (2000b) Age- and sex-associated changes in cardiac β_1-adrenoceptors from the muscular dystrophy (*mdx*) mouse. *J Mol Cell Cardiol* **32** 1661-1668.

Lu QL, Mann CJ, Lou F, Bou-Gharios G, Morris GE, Xue SA, Fletcher S, Partridge TA & Wilton SD (2003) Functional amounts of dystrophin produced by skipping the mutated exon in the *mdx* dystrophic mouse. *Nat Med* **9 (8)** 1009-1014.

Lucas-Heron B (1996) Absence of a calmitine-specific protease inhibitor in skeletal muscle mitochondria of patients with Duchenne's muscular dystrophy. *Biochem Biophys Res Comm* **225** 701-704.

Lucas-Heron B, Loirat MJ, Ollivier B & Leoty C (1987) Calcium-related defects in cardiac and skeletal muscles of dystrophic mice. *Comp Biochem Physiol* **86B:** 295-301.

Maier LS, Brandes R, Pieske B & Bers DM (1998) Effects of left vetricular hypertrophy on force Ca^{2+} handling in isolated rat myocardium. *Am J Physiol* **274** H1361-H1370.

Maki T, Gruver EJ, Davidoff AJ, Izzo N, Toupin D, Colucci W, Marks AR & Marsh JD (1996) Regulation of calcium channel expression in neonatal myocytes by catecholamines. *J Clin Invest* **97 (3)** 656-663.

Mallouk N, Jacquemond V & Allard B (2000) Elevated subsarcolemmanl Ca^{2+} in *mdx* mouse skeletal muscle fibres detected with Ca^{2+}-activated K^+ channels. *PNAS* **97 (9)** 4950-4955.

Mann CJ, Honeyman K, Cheng AJ, Ly T, Lloyd F, Fletcher S, Morgan JE, Partridge TA & Wilton SD (2001) Antisense-induces exon skipping and synthesis of dystrophin in the *mdx* mouse. *PNAS* **98** 42-47.

Mann CJ, Honeyman K, McClorey G, Fletcher S & Wilton SD (2002) Improved antisense oligonucleotide induced exon skipping in the *mdx* mouse model of muscular dystophy. *J Gene Med* **4** 644-654.

Marks AR (2001) Ryanodine receptors/calcium release channels in heart failure and sudden cardiac death. *J Mol Cell Cardiol* **33 (4)** 615-624.

Marx SO, Reiken S, Hisamatsu Y, Jayaraman T, Burkhoff D, Rosemblit N & Marks AR (2000) PKA phosphorylation dissociates FKBP12.6 from the calcium release channel (ryanodine receptor): defective regulation in failing hearts. *Cell* **101** 365-376.

Matsumura K, Tome FMS, Ionasescu V, Ervasti JM, Anderson RD, Romero NB, Simon D, Recan D, Kaplan J-C, Fardeau M & Campbell KP (1993) Deficiency of dystrophin-associated proteins in Duchenne muscular dystrophy patients lacking COOH-terminal domains of dystrophin. *J Clin Invest* **92** 866-871.

McArdle A, Edwards RHT & Jackson MJ (1995) How does dystrophin deficiency lead to muscle degeneration? Evidence from the *mdx* mouse. *Neuromuscul Disord* **5** 445-456.

McCance KL & Huether SE (1990) *Pathophysiology: The biological basis for disease in adults and children.* Mosby, St. Louis.

McCarter GC, Dentclaw WF, Reddy P & Steinhardt RA (1997) Lipofection of a cDNA plasmid containing the dystrophin gene lowers intracellular free calcium and calcium leak channel activity in *mdx* myotubes. *Gene Therapy* **4** 483-487.

McDearmon EL, Burwell AL, Combs AC, Renley BA, Sdano MT & McEvasti JM (1998) Differential heparin sensitivity of alpha-dystroglycan binding to laminins expressed in normal and dy/dy mouse skeletal muscle. *J Biol Chem* **273 (37)** 24139-24144.

McGeachie JK, Grounds MD, Partridge TA & Morgan JE (1993) Age-related changes in replication of myogenic cells in *mdx* mice: quantitative autoradiographic studies. *J Neurol Sci* **119 (2)** 169-179.

Megeney LA, Kablar B, Perry RLS, Ying C, May L & Rudnicki MA (1999) Severe cardiomyopathy in mice lacking dystrophin and MyoD. *PNAS USA* **96** 220-225.

Meissner A, Szymanska G & Morgan JP (1996) Effects of dantrolene sodium on intracellular Ca^{2+}-handling in normal and Ca^{2+}-overloaded cardiac muscle. *Eur J Pharmacol* **316 (2-3)** 333-342.

Melacini P, Fanin M, Danieli GA, Fasoli G, Villanova C, Angelini C, Vitiello L, Miorelli M, Buja GF & Mostacciuolo ML (1993) Cardiac involvement in Becker muscular dystrophy. *J Am Coll Cardiol* **22 (7)** 1927-1934.

Melacini P, Vianello A, Villanova C, Fanin M, Miorin M, Angelini C & Dalla Volta S (1996) Cardiac and respiratory involvement in advanced stage Duchenne muscular dystrophy. *Neuromuscul Disord* **6 (5)** 367-376.

Melacini P, Fanin M, Angelini A, Pegoraro E, Livi U, Danieli GA, Hoffman EP, Thiene G, Dalla Volta S & Angelini C (1998) Cardiac transplnatation in Duchenne muscular dystrophy carrier. *Neuromuscul Disord* **8** 585-590.

Mendell JR, Kissel JT, Amato AA, King W, Signore L, Prior TW, Sahenk Z, Benson S, McAndrew PE & Rice R (1995) Myoblast transfer in the treatment of Duchenne's muscular dystrophy. *N Engl J Med* **333 (13)** 832-838.

Meng H, Leddy JJ, Frank J, Holland P & Tuana BS (1996) The association of cardiac dystrophin with myofibrils/Z-disc regions in cardiac muscle suggests a novel role in the contractile apparatus. *J Biol Chem* **271 (21)** 12364-12371.

Metzger JM, Greaser ML & Moss RL (1989) Variations in cross-bridge attachment rate and tension with phosphorylation of myosin in mammalian skinned skeletal muscle fibers. Implications for twitch potentiation in intact muscle. *J Gen Physiol* **93 (5)** 855-883.

Meyer M, Trost SY, Bluhm WF, Knot HJ, Swamson E & Dillmann WH (2001) Impaired sacroplasmic reticulum function leads to contractile dysfunction and cardiac hypertrophy. *Am J Physiol* **280** H2046-H2050.

Miller RG & Hoffman EP (1994) Molecular diagnosis and modern management of Duchenne muscular dystrophy. *Neurol Clin* **12 (4)** 699-725.

Minajeva A, Kaasik A, Paju K, Seppet E, Lompre AM, Veksler V & Ventura-Clapier R (1997) Sarcoplasmic reticulum function in determining atrioventricular contractile differences in rat heart. *Am J Physiol* **273 (5 Pt 2)** H2498-H2507.

Mittmann C, Munstermann U, Weil J, Bohm M, Herzig S, Nienaber C & Eschenhagen T (1998) Analysis of gene expression patterns in small amounts of human ventricular myocardium by a multiplex RNase protection assay. *J Mol Med* **76 (2)** 133-140.

Mirit E, Gross C, Hasin Y, Palmon A & Horowitz M (2000) Changes in cardiac mechanics with heat acclimation: adrenergic signaling and SR-Ca regulatory proteins. *Am J Physiol* **279** R77-R85.

Miyazaki K, Adaniya H, Sawanobori T & Hiraoka M (1996) Electrophysiological effects of clentiazem, a new Ca^{2+} antagonist, on rabbit hearts. *J Cardiovasc Pharmacol* **27** (5) 612-621.

Miyazato H, Biro S, Setoguchui M, Maeda M, Tashiro T, Nakao S & Tanaka H (1997) Abnormal immunostaining for dystrophin in isoproterenol-induced acute myocardial injury in rats: Evidence for change in dystrophin in the absence of genetic defect. *J Mol Cell Cardiol* **29** 1217-223.

Moise NS, Valentine BA, Brown CA, Erb HN, Beck KA, Cooper BJ & Gilmour RF (1991) Duchenne's cardiomyopathy in a canine model: electrocardiographic and echocardiographic studies. *J Am Coll Cardiol* **17 (3)** 812-820.

Mori K, Kobayashi S, Saito T, Masuda Y & Nakaya H (1998) Inhibitory effects of class I and IV antiarrhythmic drugs in the Na^{+}-activated K^{+} channel current in guinea pig ventricular cells. *Naunyn-Schmiedebergs Arch Pharmacol* **358 (6)** 641-648.

Morii I, Kilhara Y, Konishi T, Inubushi T & Sasayama S (1996) Mechanism of the negative force-frequency relationship in physiologically intact rat ventricular myocardium: Studies by intracellular Ca^{2+} monitor with indo-1 and ^{31}P-Nuclear magnetic resonance spectroscopy. *Jpn Circ J* **60** 593-603.

Mule F & Serio R (2001) Increased calcium influx is responsible for the sustained mechanical tone in colon from dystrophic (*mdx*) mice. *Gastroenterology* **120 (6)** 1430-1437.

Munch G, Bolck B, Hoischen S, Brixius K, Bloch W, Reuter H & Schwinger RH (1998) Unchanged protein expression of sarcoplasmic reticulum Ca^{2+}-ATPase, phospholamban, and calsequestrin in terminally failing human myocardium. *J Mol Med* **76 (6)** 434-441.

Murphy WA, Totty WG & Carroll JE (1986) MRI of normal and pathologic skeletal muscle. *AJR Am J Roentgenol* **146 (3)** 565-574.

Murray JM, Davies KE, Harper PS, Meredith L, Mueller CR & Williamson R (1982) Linkage relationship of a cloned DNA sequence on the short arm of the X chromosome to Duchenne Muscular Dystrophy. *Nature* **300** 69-71.

Nakamura A, Yoshida K, Takeda S, Dohi N & Ikeda S (2002) Progression of dystrophic features and activation of mitogen-activated protein kinases and calcineurin by physical exercise, in hearts of *mdx* mice. *FEBS Lett* **520 (1-3)** 18-24.

Nakayama H & Kuniyasu A (1996) Identification of binding sites for calcium channel antagonists. *Jpn Heart J* **37 (5)** 643-650.

Nagy B & Samaha FJ (1986) Membrane defects in Duchenne dystrophy: protease affecting sarcoplasmic reticulum. *Ann Neurol* **20 (1)** 50-56.

Nario K & Satoh H (1996) Cardiac mechanical and electrophysiologic modulations of guinea-pig by caffeine and thapsigargin. *Gen Pharmacol* **27 (7)** 1227-1235.

Newsom-Davis J (1980) The respiratory system in muscular dystrophy. *Br Med Bull* **36 (2)** 135-138.

NHMRC (National Health and Medical Research Council) 1995, *Australian Code of Practice for the Care and Use of Animals for Scientific Purposes*, Australian Government Publishing Service, Canberra.

Niggli E (1999) Localized intracellular calcium signaling in muscle: calcium sparks and calcium quarks. *Annu Rev Physiol* **61** 311-335.

Nolan MA, Jones ODH, Pedersen RL & Johnston HM (2003) Cardiac assessment in childhood carriers of Duchenne and Becker muscular dystrophies. *Neuromuscul Disord* **13** 129-132.

Noll G, Wenzel RR, Shaw S & Luscher TF (1998) Calcium antagonists and

sympathetic nerve activation: are there differences between classes? *J Hypertens Suppl* **16 (1)** S17-24.

Nonaka I (1998) Animal models of muscular dystrophies. *Lab Anim Sci* **48 (1)** 8-17.

Nuss HB & Marban E (1994) Electrophysiological properties of neonatal mouse cardiac myocytes in primary culture. *J Physiol* **479** 265-277.

Okinaka S, Sugita H, Momoi H, Toyokura Y, Kumagai H, Ebashi S & Fujie Y (1959) Serum creatine phosphokinase and aldolase activity in neuromuscular disorders. *Trans Am Neurol Assoc* **84** 62-64.

Pacioretty LM, Cooper BJ & Gilmour RF (1992) Cellular electrophysiology of murine and canine cardiac muscle in Duchenne muscular dystrophy. *Biophys J* **61** A306-A307

Pacioretty LM, Cooper BJ & Gilmour RF (1994) Reduction of the transient outward potassium current in canine X-linked muscular dystrophy. *Circulation* **90 (3)** 1350-1356.

Palmieri GMA, Nutting DF, Bhattacharya SK, Bertorini TE & Williams JC (1981) Parathyroid ablation in dystrophic hamsters. *J Clin Invest* **68** 646-654.

Partridge T (1991) Animal models of muscular dystrophy – what can they teach us? *Neuropathology and Applied Neurobiology* **17** 353-363.

Partridge TA, Morgan JE, Coulton GR, Hoffman EP & Kunkel LM (1989) Conversion of *mdx* myofibres from dystrophin-negative to –positive by injection of normal myoblasts. *Nature* **337** 176-179.

Pastoret C & Sebille A (1995) *mdx* mice show progressive weakness and muscle deterioration with age. *J Neurol Sci* **129** 97-105.

Paulson GD, Pope AL & Baumann CA (1966) Lactic dehydrogenase isoenzymes in tissues and serum of normal and dystrophic lambs. *Proc Soc Exp Biol Med* **122 (2)** 321-324.

Pereon Y, Dettbarn C, Navarro J, Noireaud J & Palade PT (1997) Dihydropyridine receptor gene expression in skeletal muscle from *mdx* and control mice. *Biochim Biophys Acta* **1362** 201-207.

Peri V, Ajdukovic B, Holland P & Tuana B (1994) Dystrophin predominantly localizes to the transverse tubule/Z-line regions of single ventricular myocytes and exhibits distinct associations with the membrane. *Mol Cell Biochem* **130** 57-65.

Periasamy M & Huke S (2001). SERCA pump level is a critical determinant of Ca^{2+} homeostasis and cardiac contractility. *J Mol Cell Cardiol* **33** 1053-1063.

Perloff JK, Henze E & Schelbert HR (1984) Alterations in regional myocardial metabolism, perfusion, and wall motion in Duchenne muscular dystrophy studied by radionuclide imaging. *Circulation* **69 (1)** 33-42.

Pery-Man N, Chemla D, Coirault C, Suard I, Riou B & Lecarpentier Y (1993) A comparison of cyclopiazonic acid and ryanodine effects on cardiac muscle relaxation. *Am J Physiol* **265** H1364-1372.

Peterson BZ & Catterall WA (1995) Calcium binding in the pore of L-type calcium channels modulates high affinity dihydropyridine binding. *J Biol Chem* **270** 18201-18204.

Petrof BJ, Lochmuller H, Massie B, Yang L, Macmillan C, Zhao JE, Nalbantoglu J & Karpati G (1996) Impairment of force generation after adenovirus-mediated gene transfer to muscle is alleviated by adenoviral gene inactivation and host CD8+ T cell deficiency. *Hum Gene Ther* **7 (15)** 1813-1826.

Ponce-Hornos JE, Bonazzola P & Taquini AC (1987) The role of extracellular sodium on heart muscle energetics. *Pflugers Arch* **409** 163-168.

Ponce-Hornos JE, Parker JM & Langer GA (1990) Heat production in isolated heart mycoytes: differences among species. *Am J Physiol* **258** H880-H886.

Ponce-Hornos JE, Marquez MT & Bonazzola P (1992) Influence of extracellular potassium on energetics of resting heart muscle. *Am J Physiol* **262** H1081-H1087.

Porter JD, Khanna S, Kaminski HJ, Rao JS, Merriam AP, Richmonds CR, Leahy P, Li J, Guo W & Andrade FH (2002) A chronic inflammatory response dominates the skeletal muscle molecular signature in dystrophin-deficient *mdx* mice. *Hum Mol Gen* **11 (3)** 263-272.

Poukka R (1966) Tissue lipids in calves suffering from muscular dystrophy. *Br J Nutr* **20 (2)** 245-256.

Prabhu SD (1998) Ryanodine and the left ventricular force-interval and relaxation-interval relations in closed-chest dogs: insights on calcium handling. *Cardiovascular Research* **40** 483-491.

Pressmar J, Brinkmeier H, Seewald MJ, Naumann T & Rudel R (1994) Intracellular Ca^{2+} concentrations are not elevated in resting cultured muscle from Duchenne (DMD) patients and in *mdx* mouse muscle fibres. *Pflugers Arch* **426** 499-505.

Radda GK (1999) Of mice and men: from early NMR studies of the heart to physiological genomics. *Biochem Biophys Res Commun* **266 (3)** 723-728.

Rafael JA, Tinsley JM, Potter AC, Deconinck AE & Davies KE (1998) Skeletal muscle-specific expression of a utrophin transgene rescues utrophin-dystrophin deficient mice. *Nat Genet* **19 (1)** 79-82.

Reilly AM, Williams DA & Dusting GJ (1996) Dexamethasone inhibits endotoxin-induced changes in calcium and contractility in rat isolated papillary muscle. *Cell Calcium* **26** 1-8.

Reimer KA, Lowe JE & Jennings RB (1977) Effect of the calcium antagonist verapamil on necrosis following temporary coronary artery occlusion in dogs. *Circulation* **55 (4)** 581-587.

Richard S, Charnet P, Ouadid H, Tiaho F & Nargeot J (1988) Effects of the Ca-antagonist nicardipine on K^+ currents and Na^+-Ca^{2+} exchange in frog atrial fibres. *J Mol Cell Cardiol* **20 (12)** 1133-1140.

Rifai Z, Welle S, Moxley RT, Lorenson M & Griggs RC (1995) Effect of prednisone on protein metabolism in Duchenne dystrophy. *Am J Physiol* **268 (1 Pt 1)** E67-74.

Rigdon RH (1964) Spontaneous occurring muscular dystrophy in the white Peking duck. *Tex Rep Biol Med* **22 Suppl 1** 930-939.

Ritter M, Su Zz, Spitzer KW, Ishida H & Barry WH (2000) Caffeine-induced Ca^{2+} sparks in mouse ventricle myocytes. *Am J Phys* **278** H666-H669.

Robert V, Massimino ML, Tosello V, Marsault R, Cantini M, Sorrentino V & Pozzan T (2001) Alteration in calcium handling at the subcellular level in *mdx* myotubes. *J Biol Chem* **276 (7)** 4647-4651.

Rohman MS, Emoto N, Takeshima Y, Yokoyama M & Matsuo M (2003) Decreased mAKAP, ryanodine receptor, and SERCA2a gene expression in *mdx* hearts. *Biochem Biophys Res Commun* **310 (1)** 228-235.

Rouger K, Le Cunff M, Steenman M, Potier MC, Gibelin N, Dechesne CA & Leger JJ (2002) Global/temporal gene expression in diaphragm and hindlimb muscles of dystrophin-deficient (*mdx*) mice. *Am J Phys* **253** C773-C784.

Ruegg UT & Gillis J-M (1999) Calcium homeostasis in dystrophic muscle. *Trends Pharmacol Sci* **20** 351-352.

Rybakova IN & Ervasti JM (1997) Dystrophin-glycoprotein complex is monomeric and stabilizes actin filaments *in vitro* through a lateral association. *J Biol Chem* **272 (45)** 28771-28778.

Sadeghi A, Doyle AD & Johnson BD (2002) Regulation of the cardiac L-type Ca^{2+} channel by the actin-binding proteins α-actinin and dystrophin. *Am J Phys* **282** C1502-C1511.

Saito M, Kawai H, Akaike M, Adachi K, Nishida Y & Saito S (1996) Cardiac dysfunction with Becker muscular dystrophy. *Am Heart J* **132** 642-647.

Sakamoto A, Ono K, Abe M, Jasmin G, Eki T, Murakami Y, Masaki T, Toyo-oka T & Hanaoka F (1997) Both hypertrophic and dilated cardiomyopathies are caused by mutation of the same gene, delta-sarcoglycan, in hamster: an animal model of

disrupted dystrophin-associated glycoprotein complex. *PNAS USA* **94 (25)** 13873-13878.

Sakamoto M, Yuasa K, Yoshimura M, Yokota T, Ikemoto T, Suzuki M, Dickson G, Miyagoe-Suzuki Y & Takeda S (2002) Micro-dystrophin cDNA ameliorates dystrophic phenotypes when introduces to *mdx* mice as a transgene. *BBRC* **293** 1265-1272.

Sapp JL, Bobet J & Howlett SE (1996) Contractile properties of myocardium are altered in dystrophin-deficient *mdx* mice. *J Neurol Sci* **142** 17-24.

Sasaki Y, Sasaki Y, Kanno K & Hidaka H (1987) Disorganization by calcium antagonists of actin microfilament in aortic smooth muscle cells. *Am J Physiol* **253 (1 Pt 1)** C71-78.

Sato Y, Kiriazis H, Yatani A, Schmidt AG, Hahn H, Ferguson DG, Sako H, Mitarai S, Honda R, Mesnard-Rouiller L, Frank KF, Beyermann B, Wu G, Fujimori K, Dorn GW & Kranias EG (2001) Rescue of contractile parameters and myocyte hypertrophy in calsequestrin overexpressing myocardium by phospholamban ablation. *J Biol Chem* **276 (12)** 9392-9329.

Scholz GH, Vieweg S, Uhlig M, Thormann M, Klossek P, Goldmann S & Hofmann HJ (1997) Inhibition of thyroid hormone uptake by calcium antagonists of the dihydropyridine class. *J Med Chem* **40 (10)** 1530-1538.

Schramm M, Klieber HG & Daut J (1994) The energy expenditure of actomyosin-ATPase, Ca^{2+}-ATPase and Na^{+},K^{+}-ATPase in guinea-pig cardiac ventricular muscle. *J Physiol (Lond)* **481** 647-662.

Schramm M, Thomas G, Towart R & Franckowiak G (1983) Novel dihydropyridines with positive inotropic action through activation of Ca^{2+} channels. *Nature* **303 (5917)** 535-537.

Schwartz A (1992) Molecular and cellular aspects of calcium channel antagonism. *Am J Cardiol* **70 (16)** 6F-8F.

Schwinger RH, Bohm M, Schmidt U, Karczewski P, Bavendiek U, Flesch M, Krause EG & Erdmann E (1995) Unchanged protein levels of SERCA II and phospholamban but reduced Ca^{2+} uptake and Ca^{2+}-ATPase activity of cardiac sarcoplasmic reticulum from dilated cardiomyopathy patients compared with patients with nonfailing hearts. *Circulation* **92 (11)** 3220-3228.

Semsarian C, Ahmad I, Giewat M, Georgakapoulos D, Schmitt JP, McConnell BK, Reiken S, Mende U, Marks AR, Kass DA, Seidman CE & Seidman JG (2002) The L-Type calcium channel inhibitor diltiazem prevents cardiomyopathy in a mouse model *J Clin Invest* **109-8** 1031-1020.

Sen LY, O'Neill M, Marsh JD & Smith TW (1990) Inotropic and calcium kinetic effects of calcium channel agonist and antagonist in isolated cardiac myocytes from cardiomyopathic hamsters. *Circ Res* **67** (3) 599-608.

Serio R, Bonvissuto F & Mule F (2001) Altered electrical activity in colonic smooth muscle cells from dystrophic (*mdx*) mice. *Neurogastroenterology and Motility* **13 (2)** 169-175.

Sewry CA, Man NT, Lynch T & Morris GE (2001) Absence of utrophin in intercalated discs of human cardiac muscle. *Histochem J* **33 (1)** 9-12.

Skrabek RQ & Anderson JE (2001) Metabolic shifts and myocyte hypertrophy in deflazacort treatment of *mdx* mouse cardiomyopathy. *Muscle Nerve* **24** 192-202.

Slater CR (1987) Muscular dystophy. The missing link in DMD? *Nature* **330** 693-694.

Smith J & Schofield PN (1997) Stable integration of an *mdx* skeletal muscle cell line into dystrophic (*mdx*) skeletal muscle: evidence for stem cell status. *Cell Growth Differ* **8 (8)** 927-934.

Spencer MJ, Croall DE & Tidball JG (1995) Calpains are activated in necrotic fibers from *mdx* dystrophic mice. *J Biol Chem* **18** 10909-10914.

Sperelakis N, Katsube Y, Yokoshiki H, Sada H & Sumii K (1996). Regulation of slow Ca^{2+} channels of myocardial cells. *Mol Cell Biochem* **163/164** 85-98.

Stedman HH, Sweeney HL, Shrager JB, Maguire HC, Panettieri RA, Petrof B, Narusawa M, Leferovich JM, Sladky JT & Kelly AM (1991) The *mdx* mouse diaphragm reproduces the degenerative changes of Duchenne muscular dystrophy. *Nature* **352 (6335)** 536-539.

Stevens ED & Faulkner JA (2000) The capacity of *mdx* diaphragm muscle to do oscillatory work. *J Physiol* **522 (3)** 457-466.

Sugita H, Arahata K & Ishiguro T (1988) Negative immunostaining of Duchenne muscular dystrophy (DMD) and *mdx* muscle surface membrane with antibody against synthetic peptide fragment predicted from DMD cDNA. *Proceedings of the Japan Academy* **64** 37-39.

Takasago T, Imagawa T & Shigekawa M (1989) Phosphorylation of the cardiac ryanodine receptor by cAMP-dependent protein kinase. *J Biochem (Tokyo)* **106** 872-877.

Takahashi T, Allen PD, Lacro RV, Marks AR, Dennis AR, Schoen FJ, Grossman W, Marsh JD & Izumo S (1992) Expression of dihydropyridine receptor (Ca^{2+} channel) and calsequestrin genes in the myocardium of patients with end-stage heart failure. *J Clin Invest* **90 (3)** 927-935.

Tanaka H & Ozawa E (1990) Expression of dystrophin mRNA and the protein in the developing rat heart. *Biochem Biophys Res Commun* **172 (2)** 824-829.

Tang S, Yatani A, Bahinski A, Mori Y & Schwartz A (1993) Molecular localization

of regions in the L-type calcium channel critical for dihydropyridine action. *Neuron* **11 (6)** 1013-1021.

Tay JSH, Low PS, Lee WL, Lai PS & Gan GC (1989) Dystrophin function: calcium-related rather than mechanical. *Lancet* **335** 983.

Torres LFB & Duchen LW (1987) Myopathy in the mouse: morphological studies of nerves, muscles and end-plates. *Brain* **110** 269-299.

Triggle DJ (1999) The pharmacology of ion channels: with particular reference to voltage-gated Ca^{2+} channels. *Eur J Pharmacol* **375 (1-3)** 311-325.

Turner PR (1991) Increased calcium influx in dystrophic muscle. *J Cell Biol* **115** 1701-1712.

Turner PR, Fong P, Denetclaw WF & Steinhardt (1991) Increased calcium influx in dystrophic muscle. *J Cell Biol* **115 (6)** 1701-1712.

Turner PR, Schultz R, Ganguly B & Steinhardt RA (1993) Proteolysis results in altered leak channel kinetics and elevated free calcium in *mdx* muscle. *J Membrane Biol* **133** 245-251.

Tutdibi O, Brinkhmeier H, Rüdel R & Föhr KJ (1999) Increased calcium entry into dystrophin-deficient muscle fibres of *mdx* and *adr-mdx* mice is reduced by ion channel blockers. *J Physiol* **515 (3)** 859-868.

Tweedie D, Harding SE & MacLeod KT (2000) Sarcoplasmic reticulum Ca content, sarcolemmal Ca influx and the genesis of arrhythmias in isolated guinea-pig cardiomyocytes. *J Mol Cell Cardiol* **32 (2)** 261-272.

Urtasun M, Poza JJ, Gallano P, Lasa A, Saenz A, Cobo AM, Leturcq F, Lopez de Munain A & Garcia-Bragado F (1998) Muscular dystrophy due to a mutation in the gene of alpha-sarcoglycan subunit of dystrophin associated protein complex. *Med Clin* **110 (14)** 538-542.

Vaghy PL, Johnson JD, Matlib MA, Wang T & Schwartz A (1982) Selective inhibition of Na-induced Ca release from heart mitochondria by diltiazem and certain other Ca antagonist drugs. *J Biol Chem* **257** 6000-6002.

Valentine BA, Winand NJ, Pradhan D, Moise NS, de Lahunta A, Kornegay JN & Cooper BJ (1992) Canine X-linked muscular dystrophy as an animal model of Duchenne muscular dystrophy: a review. *Am J Med Genet* **42 (3)** 352-356.

Vandebrouck C, Imbert N, Dupont G, Cognard C & Raymond G (1999) The effect of methylprednisolone on intracellular calcium of the normal and dystrophic human skeletal muscle cells. *Neurosci Lett* **269** 110-114.

Vandebrouk C, Martin D, Colson-Van Schoor M, Debaix H & Gailly P (2002) Involvement of TRPC in the abnormal calcium influx observed in dystrophic *(mdx)* mouse skeletal muscle fibres. *J Cell Biol* **158 (6)** 1089-1096.

Vandecasteele G, Verde I, Rucker-Martin C, Donzeau-Gouge P, Fischmeister R (2001) Cyclic GMP regulation of the L-type Ca^{2+} channel current in human atrial myocytes. *J Physiol* **533 (Pt 2)** 329-340.

Verellen C, Markovic V, De Meyer R, Freund M, Laterre C & Worton R (1978) Expression of an x-linked recessive disease in female due to non-random inactivation of the x chromosome. *Am J Hum Gen* **30** 97A.

Vrints C, Mercelis R, Vanagt E, Snoeck J & Martin JJ (1983) Manifestations of Becker-type muscular dystrophy. *Acta Cardiologica* **38** 479-486.

Wagner JA, Weisman HF, Snowman AM, Reynolds IJ, Weisfeldt M & Snyder SH (1989) Alterations in calcium antagonist receptors and sodium-calcium exchange in cardiomyopathic hamster tissues. *Circ Res* **65** 205-214.

Wakai S, Minami R, Kameda K, Okabe M, Nagaoka M, Annaka S, Higashidate Y, Tomita H & Tachi N (1988) Electron microscopic study of the biopsied cardiac muscle in Duchenne muscular dystrophy. *J Neurol Sci* **84 (2-3)** 167-175.

Waldegger S, Niemeyer G, Morike K, Wagner CA, Suessbrich H, Busch AE, Lang F & Eichelbaum M (1999) Effect of verapamil enantiomers and metabolites on cardiac K^+ channels expressed in Xenopus oocytes. *Cell Physiol Biochem* **9** (2) 81-89.

Watanabe H, Ma M, Washizuka T, Komura S, Yoshida T, Hosaka Y, Hatada K, Chinushi M, Yamamoto T, Watanabe K & Aizawa Y (2003) Thyroid hormone regulates mRNA expression and currents of ion channels in rat atrium. *Biochem Biophys Res Commun* **308 (3)** 439-444.

Watkins SC & Cullen MJ (1987) A qualitative and quantitative study of the ultrastructure of regenerating muscle fibres in Duchenne muscular dystrophy and polymyositis. *J Neurol Sci* **82 (1-3)** 181-192.

Wassner SJ, Li JB, Ladda RL, Lorenz RP & Emery AE (1982) Prenatal diagnosis of Duchenne muscular dystrophy: failure of amniotic fluid and maternal serum N tau-methylhistidine analyses to detect affected fetuses. *Am J Obstet Gynecol* **143 (2)** 216-219

Wegener JW & Nawrath H (1995) Extracellular site of action of phenylalkylamines on L-type calcium current in rat ventricular myocytes. *Naunyn-Schmiedebergs Arch Pharmacol* **352** 322-330.

Wendt IR & Stephenson DG (1983) Effects of caffeine on Ca^{2+}-activated force production in skinned cardiac and skeletal muscle fibres of the rat. *Pflugers Arch* **398** 210-216.

Wier WG & Balke CW (1999) Ca^{2+} release mechanisms, Ca^{2+} sparks, and local control of excitation-contraction coupling in normal heart muscle. *Circ Res* **85 (9)** 770-776.

Wilton SD, Lloyd F, Carville K, Fletcher S, Honeyman K, Agrawal S & Kole R (1999) Specific removal of the nonsense mutation from the *mdx* dystrophin mRNA using antisense oligonucleotides. *Neuromuscul Disord* **9 (5)** 330-338.

Witcher DR, Strifler BA & Jones LR (1992) Cardiac-specific phosphorylation site for multifunctional Ca^{2+}/calmodulin-dependent protein kinase is conserved in brain ryanodine receptor. *J Biol Chem* **267** 4963-4967.

Wolff JA, Malone RW & Williams P (1990) Direct gene transfer into mouse muscle *in vivo*. *Science* **247** 1465-1468.

Wrogemann K & Pena SD (1976) Mitochondrial calcium overload: A general mechanism for cell-necrosis in muscle diseases. *Lancet* **1 (7961)** 672-674.

Xiao RP, Cheng H, Lederer WJ, Suzuki T & Lakatta G (1994) Dual regulation of Ca^{2+}/calmodulin-dependent kinase II activity by membrane voltage and by calcium influx. *PNAS USA* **91** 9659-6963.

Xu R & Salpeter MM (1997) Acetylcholine receptors in innervated muscles of dystrophic *mdx* mice degrade as asfter denervation. *J Neurosci* **17(21)** 8194-8200.

Yoshida M, Matsuzaki T, Date M & Wada K (1997) Skeletal muscle fiber degeneration in *mdx* mice induced by electrical stimulation. *Muscle Nerve* **20 (11)** 1422-1432.

Ytterberg SR (1991) Animal models of myopathy. *Curr Opin Rheumatol* **3 (6)** 934-940.

Yue Y, Li Z, Harper SQ, Davisson RL, Chamberlain JS & Duan D (2003) Microdystrophin gene therapy of cardiomyopathy restores dystrophin-glycoprotein complex and improves sarcolemma integrity in the *mdx* mouse heart. *Circulation* **108 (13)** 1626-1632.

Zhao F, Li P, Chen SRW, Louis CF & Fruen BR (2002) Dantrolene inhibition of ryanodine calcium release channels. *J Biol Chem* **276 (17)** 13810-13816.

Zhu X, Wheeler MT, Hadhazy M, Lam M-YJ, & McNally EM (2002) Cardiomyopathy is independent of skeletal muscle disease in muscular dystrophy. *FASEB J **16*** **(9)** 1096-1098.

Zvaritch E, Backx PH, Jirik F, Kimura Y, de Leon S, Schmidt AG, Hoit BD, Lester JW, Kranias EG & MacLennan DH (2000) The transgenic expression of highly inhibitory monomeric forms of phospholamban in mouse heart impairs cardiac contractility. *J Biol Chem* **275,** 14985-14991.

APPENDICES

Appendix A – Oxygen Consumption Assay and Apparatus Development

A series of oxygen consumption experiments were undertaken to determine whether potential futile calcium handling led to metabolic changes in the myocardium of *mdx*. However, these experiments were variable due to the small left atrial tissue size and the sensitivity of the oxygen consumption apparatus.

The Requirement For Oxygen Usage Studies

Dysfunctional calcium handling should be observed metabolically by changes in oxygen consumption. A series of oxygen consumption experiments evaluated energy usage in the *mdx* compared to C57 mice.

During quiescence of the cardiac muscle, energy expenditure is related to extracellular ionic composition (Ponce-Hornos *et al.*, 1987; 1990; 1992). The SERCA, along with the NCX contribute significantly to basal metabolism and are the active processes required for relaxation of the myocardium. SERCA expends energy directly at the rate of 1 ATP/2 calcium, and NCX indirectly and at twice the metabolic cost of 1 ATP/1 calcium (reflecting the 3:1 and 3:2 ionic stoichiometries of the NCX and Na^+-K^+ pump, respectively) (Cooper *et al.*, 2001). SERCA contributes approximately 30% of oxygen consumption (Loiselle, 1987), whereas the Na^+/K^+ pump contributes less than 10% to cardiac resting metabolism (Schramm *et al*, 1994). During contraction, actomyosin ATPase activity of cross-bridges contributes to energy usage (Cooper *et al.*, 2001). Cardiac energy demand increases in response to

increasing intracellular calcium concentrations (Fiolet *et al.*, 1995). Calcium is also an important regulator of mitochondrial function. Impaired oxidative phosphorylation has been observed in dystrophin-deficient muscle cells (Even *et al.*, 1994; Braun *et al.*, 2001), although no mitochondrial abnormalities have been observed in cardiac muscle from 4-6 month old female *mdx* (Kuznetsov *et al.*, 1998). At this age skinned *mdx* cardiac fibres have almost identical respiratory parameters as control in several different substrates (Kuznetsov *et al.*, 1998). Kanai *et al.*, (2001) proposed that elevated calcium activated mitochondrial NOS production, increasing local mitochondrial NO production, which inhibits mitochondrial ATP synthesis to inhibit contractility. Two studies of mitochondrial activity in DMD patients observed mitochondrial calcium overload due to the activity of proteolytic enzymes, and a decrease in ATP synthesis (Lucas-Heron 1996). Robert *et al.*, (2001) observed that the mitochondria in skeletal muscle of *mdx* are responsible for both the apoptosis and impaired calcium homeostasis.

Energy usage in dystrophin-deficient skeletal muscle is altered. It is unknown whether energy usage of the myocardium is unchanged, and whether changes in calcium handling contribute to altered metabolism of the myocardium.

Oxygen Consumption Methodology

A small stainless steel hook was placed in one end of the left atria, and a length of thread that was subsequently attached to the ergometer, (Model 300B, Aurora Scientific Inc., Canada) was attached to the other. The atrium was progressively stretched to the optimum preload and allowed 30 min to equilibrate in a 1.5mL chamber in 35±0.5°C TPSS saturated with carbogen. Oxygen consumption was continually monitored by an electrode in the base of the chamber while the TPSS was

constantly mixed by a magnetic stirrer (Dual Digital Model 20, Rank Brothers LTD). Initial experiments revealed that oxygen consumption was stabilised after 30 min.

The left atrium was field stimulated (1Hz, 10V, 5ms duration; Grass SD9 isolated stimulator) for four sets of 10 min periods, with cessation of stimulation for three 30 min periods for quiescent measurements. Subsequently 40mM KCl TPSS (as for TPSS except in mM: NaCl 102.3, KCl 40) was added for one 30 min period (Fig A.1). Oxygen consumption and contractility were measured concurrently for the duration of the experiment. Prior to each exchange of TPSS the solution was aerated with carbogen until saturation. All data was recorded using Chart 4.0 on a Powerlab/4SP (AD Instruments, Australia) and captured on an Apple iMac. The oxygen electrode was calibrated by measuring 100% dissolved oxygen, 20% dissolved oxygen (compressed air) and 0% dissolved oxygen by the addition of sodium dithionite. A linear plot was constructed and values for oxygen consumption calculated back from the plot (personal communication from the manufacturer indicated linearity of the oxygen electrode). Atria were blotted and weighed. Oxygen consumption was normalised as per tissue weight.

Figure A.1 Oxygen consumption protocol. 1,2,3,4 are 10 min stimulation equilibration periods, ABC are 30min periods of quiescence. Subsequent to quiescence 40mM KCl was added for a 30 min period.

Depolarisation and L-type Calcium Channel Blockade

At the conclusion of the stimulation period, the myocardium was depolarised by the addition of 40mM KCl for a 30 min period. Subsequently, nifedipine was added in 40mM KCl TPSS to remove the effect of L-type calcium influx on the oxygen

consumption of the tissue. Depolarisation and addition of the dihydropyridine drug produced unusually high results, so diltiazem was used as an alternative L-type calcium channel blocker. However, diltiazem produced similarly high values. Finally, experiments were undertaken without tissue present to determine whether the KCl and/or the L-type calcium channel antagonists were affecting the oxygen electrode.

Oxygen consumption data

Preliminary Experiments

Since oxygen consumption in cardiac tissue had not been previously undertaken in our laboratory, preliminary experiments focussed on evaluating the methodology. The oxygen electrode consumes oxygen, so experiments were conducted without tissue (Fig A.2) to measure the amount of oxygen consumed for the duration of the experimental protocol. Preliminary experiments also evaluated the oxygen consumption from immediately subsequent to dissection to determine when oxygen consumption stabilised (Fig A.2). Since oxygen consumption changed markedly for the first 10 – 20min, only the final 10min of the 40 min stimulated equilibration period was used for data comparison. A 30min period was determined to be optimal for the quiescent experiments, since oxygen consumption by the myocardium during quiescence is much lower. Finally, the effects of KCl, nifedipine and diltiazem on the oxygen electrode were evaluated (Fig. A.3). Oxygen consumption was increased markedly without tissue present, in the presence of the L-type Ca^{2+} channel antagonists. The drugs were made up in the final required concentration in TPSS to remove the effect of the solvent on the electrode. The oxygen consumption continued to be high. Because the drugs interfered with the oxygen electrode, they could not be used for any further experiments.

Comparison of Oxygen Consumption in *mdx* and C57

Whole mouse mass was not significantly different between *mdx* (25.3±0.5g, n=14) and C57 (26.4±0.8g, n=8). Left atrial mass was not significantly different between *mdx* (22.8±1.2mg, n=14) and C57 (21.9±1.5mg, n=8). Force of contraction during the stimulation period was significantly smaller ($P<0.05$) in *mdx* (0.89±0.12) compared to C57 (1.28±0.17; Fig A.4). The oxygen usage data was unreliable, with quiescent periods sometimes using more oxygen than stimulation periods. Based on this finding the data was not used further. The variability in the oxygen usage data was presumably due to the small size of the murine atria using too little oxygen for the sensitivity of the apparatus. Hence, this data did not have sufficient rigour and was not included in the main thesis dissertation.

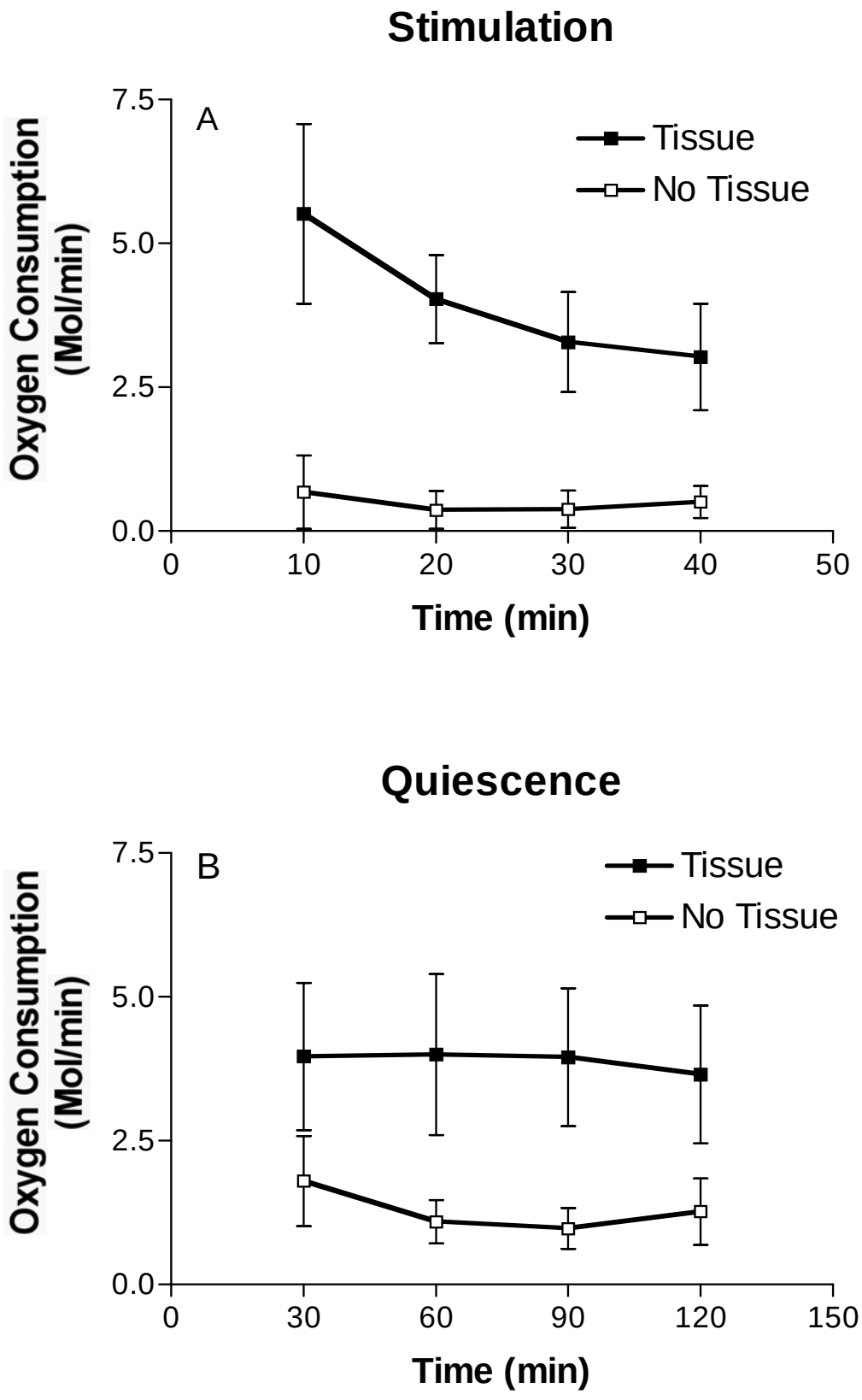

Figure A.2 Determination of oxygen consumption in the absence of tissue. A The oxygen consumption electrode uses oxygen from the solution, so to determine the amount of oxygen used during each experiment, control experiments were conducted without tissue. The data for the 10 minute stimulation periods and the 30 minute quiescent periods are presented here. Due to the nature of the curve, final oxygen consumption for the stimulation period was taken only from the final 10min (n=5 for tissue, n=3 for no tissue).

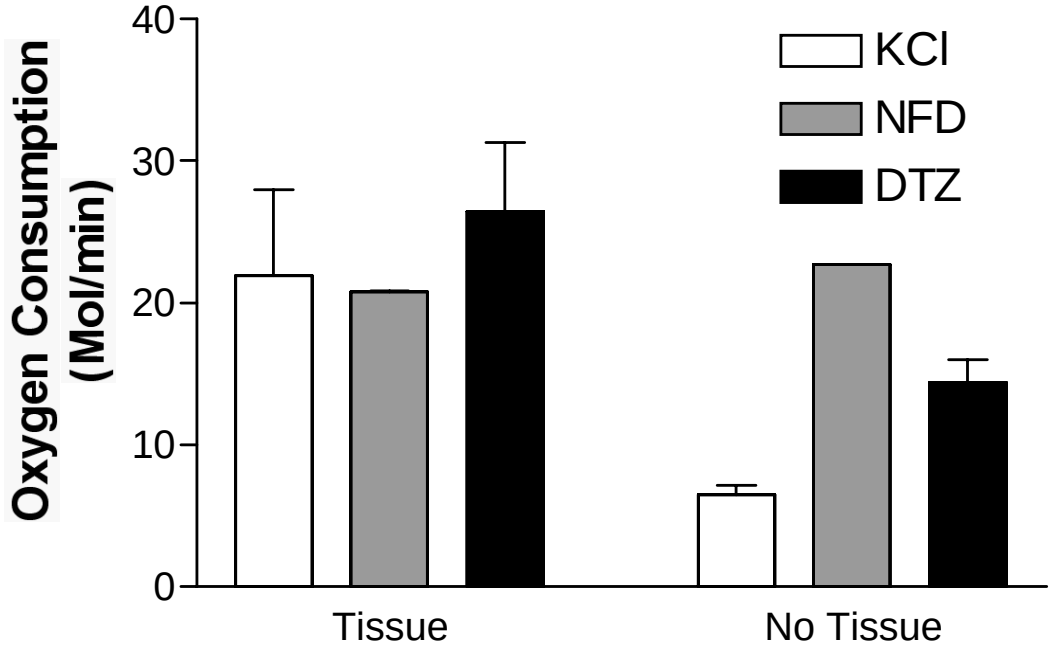

Figure A.3 Comparison of the effects of KCl, nifedipine and diltiazem on oxygen consumption with and without tissue. Preliminary studies examined the effect of KCl (n=3 with and without tissue), nifedipine (NFD; n=4 with tissue, n=1 without tissue) and diltiazem (DTZ; n=4 with tissue, n=2 without tissue) on oxygen consumption in left atrial tissue, and in the absence of any tissue. Because nifedipine and diltiazem greatly increased oxygen consumption in the absence of any tissue, the drugs were not used in further studies.

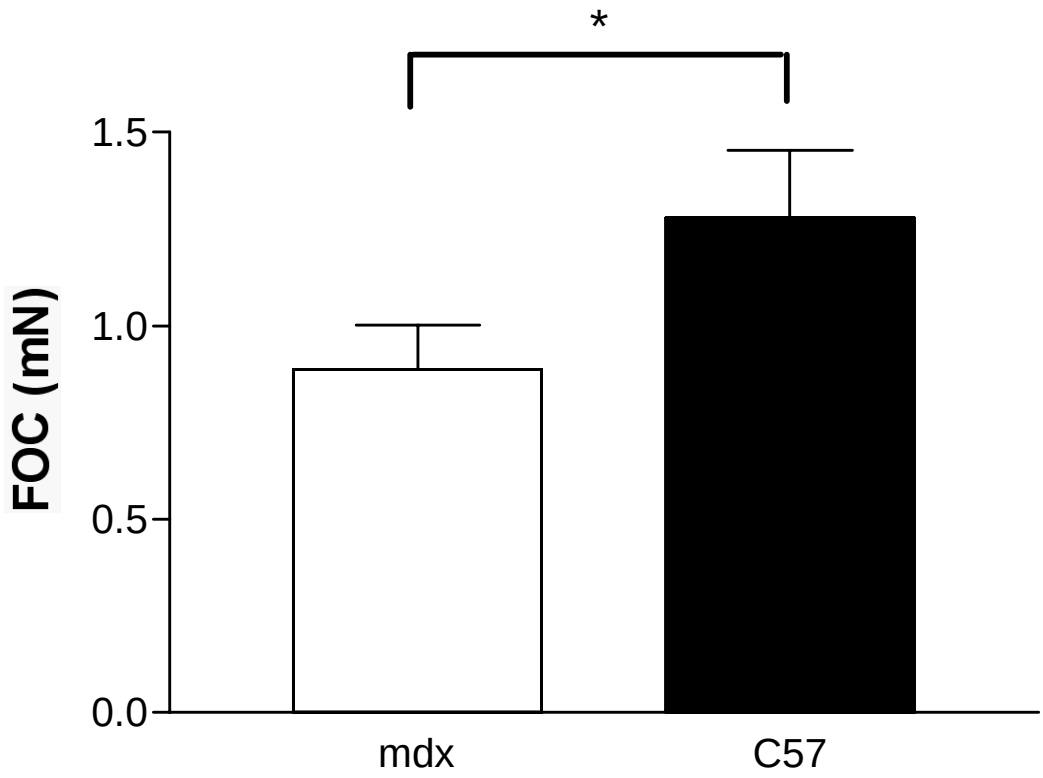

Figure A.4 Contractility of *mdx* (n=9) and C57 (n=8) mice for all of the oxygen consumption experiments.

Appendix B - Patch Clamp Assay and Apparatus Development in our Laboratory

The patch clamp apparatus and protocol had not been used previously in our laboratory, therefore considerable time was spent on development of apparatus, a myocyte isolation protocol and patch methodology.

Initially assay development focussed on isolating functional murine cardiomyocytes. The mouse was euthanased by excess inhalation of carbon dioxide, and the heart rapidly excised and placed into cold, carbogenated TPSS. The aorta was placed on a canula (modified from a 26 gauge needle), with the use of a micro vessel clip (0.75 x 4mm; SSR Cat No. 17-4000) to hold the aorta in place until a length of thread was tied around the aorta and canula. The canula was scarred approximately 2mm from the tip so that the aorta did not slip. The canula was then attached directly to the perfusion apparatus without further handling of the aorta or heart.

A Gilson peristaltic pump was used to deliver carbogenated (95% O_2, 5% CO_2) TPSS (mM: NaCl 136.9, KCl 5.4, $MgCl_2.H_2O$ 1.0, $NaH_2PO_4.2H_2O$ 0.4, $NaHCO_3$ 22.6, $CaCl_2.2H_2O$ 1.8, glucose 5.5, ascorbic acid 0.3, Na_2EDTA 0.05) through a water-jacketed column at 3mL/min prior to mounting of the heart on the apparatus. The temperature of the perfusate was maintained at 37±0.5°C. Once attached to the apparatus, TPSS was perfused for 2 min to ensure appropriate perfusion and the heart was contracting normally. If the perfusion was satisfactory, the excess blood in the coronary vessels of the heart was removed causing the heart to change to a more pinkish colour, and the heart would beat consistently. The TPSS was then changed to a calcium free solution (in mM: NaCl 120, KCl 4.7, KH_2PO_4 1.2, $MgSO_4.7H_2O$ 1.2, Glucose 15, $NaHCO_3$ 25, EDTA 0.5) for 10 min. Finally, collagenase (Life

Technologies Collagenase Type I, lypholized, 220 units/mg) was perfused through the heart for 10 min. The ventricles were then cut free from the atria and minced with scissors. A number of cells would be examined under the microscope at this point, and a small portion of the cells stored. The remaining cardiac tissue was placed in fresh collagenase and put in a 37±0.5°C shaking water bath (2Hz) for 10 min, before a fraction of cells was removed and collagenase added. This was repeated once more for a third fraction of cells. Each of the fractions were diluted in calcium-free solution (with 0.4mM $CaCl_2$ added) containing BSA (1mg/mL) for 10 min. After the cells settled to the bottom of the tube, the supernatant was removed and replaced with a calcium-free solution (with 0.8mM $CaCl_2$ added) containing BSA (1mg/mL). This was repeated another time with calcium-free solution (with 1.2mM $CaCl_2$ added) containing BSA (1mg/mL).

Initial cell yields from the isolation were poor, but provided cells with normal morphology. However, the myocytes were not calcium tolerant, and contracted when the patch pipette contacted them. To improve cell yield and stability for patches several alterations to the isolation protocol were trialled.

The first alteration to the protocol was to lengthen the time that the myocardium was exposed to collagenase. Initially the time was extended to 15 min perfusion, however cell morphology became abnormal when exposed to collagenase for this extended period of time. Therefore the time the cardiomyocytes were exposed to collagenase in the perfusion was reduced to 5 min. The cell yields were improved, however the cells were not stable in the bath solution, nor when contacted by the patch pipette. This led to the use of several different extracellular (bath) and intracellular (pipette) solutions.

Glucose in the calcium free solutions was reduced from 15 to 5mM, and sodium bicarbonate was reduced from 50 to 25mM, in case the calcium free solution may be hyperosmotic. Intracellular solutions that were trialled include: I_{Ca} Solution 1 in mM: $CaCl_2$ 1.0, CsCl 120, EGTA 10, $MgCl_2$ 6, Na_2ATP 5; Solution 2 in mM: CsCl 140, EGTA 10, $MgCl_2.6H_2O$ 4, Hepes 10, ATP-Na_2 4. The bath solution (in mM KCl 4.7, NaCl 120, KH_2PO_4 1.2, $MgSO_4.7H_2O$ 1.2, Glucose 15, $NaHCO_3$ 25, EDTA 0.5, $CaCl_2$ 1.75) was calculated to be 303.4 mOsm, and the intracellular solution 1 (as above) calculated to be 289 mOsm. At this point a glass pipette was used to titrate the cells from the cardiac tissue. While the cell yield was improved, cells continued to contract on application of the patch pipette.

A cleaning solution (0.1M HCl, 0.1M EDTA, pH 7.0 with KOH) was used for the isolation apparatus, and all containers that had solutions for the perfusion, or used for cells. All solutions were made with MilliQ water to reduce the possibility of contaminants affecting the perfusion. A 0.45 μM Millex HA filter was used in line to filter all solutions.

Several different protocols were also used to produce pipettes, usually with a resistance of 1-20MΩ. Pippettes with a resistance higher than 10MΩ were discarded and only pipettes with a resistance of 1-2MΩ were used on the cardiomyocytes. A fire polisher was designed and made in our laboratory to polish the tips of the pipettes.

A report by Sadeghi *et al.,* (2002) was published at this point, a paper that successfully recorded L-type currents from *mdx* neonatal cardiomyocytes. Their solutions were trialled: extracellular (in mM TEA-Cl 145, $BaCl_2$ 10, $MgCl_2$ 1, HEPES, 10; pH 7.4) and intracellular (in mM N-methyl-D-glucamine 130, EGTA 10, HEPES 60, MgATP 2, MgCl 1; MSA to adjust pH 7.3). Another intracellular solution

was also trialled (in mM Na_2ATP 3, EGTA 10, CsCl 120, HEPES 10, $MgCl_2$ 2; pH 7.3).

Rat cells were also used, to observe whether yield and contracture problems continued. The yield was much greater with rat heart (possibly due to more tissue and the absence of calcium overload), and cells were more stable, but a gigaseal was not obtained.

Protease (0.12mg/mL) was used in the isolation in the collagenase solution. Also a portion of the cells was centrifuged in 1.2mM Ca^{2+} and the cells removed from the BSA albumin to ensure that the BSA was not affecting the gigaseal.

A gigaseal was still not obtained, so the amount and time in collagenase was reduced. Colleagues who routinely patch murine cardiomyocytes were contacted for assistance and correspondence continued for several weeks.

A simple intracellular solution containing EGTA, CsCl, $MgCl_2$ and HEPES was used. The rate of the perfusion was tested, and trialled at two different rates. The pH of all solutions was observed throughout the perfusion and oxygen and carbogen were both tried and compared for pH changes to the solutions.

Temperature was also measured as a potential source of the problem. The earth electrode was also re-chlorided.

Appendix C - Patch Clamp Assay and Apparatus Development at the University of Adelaide

External expertise in patch clamping cardiomyocytes was sought since the protocol was unsuccessful in our laboratory. At the University of Adelaide, rat cardiomyocytes were routinely patch clamped.

Initially perfusion was ineffective, so a soft plastic canula was made, similar to canula's used in their laboratory for rat, except of a smaller diameter. The first extracellular solution used consisted of in mM: TEA-Cl 145, $MgCl_2$ 1, $BaCl_2$ 10, HEPES 10, adjusted to pH 7.4 with CsOH; and the first intracellular solution in mM: $CsCl_2$ 130, EDTA 10, HEPES 60, $MgCl_2$ 3, K_2ATP 2, adjusted to pH 7.3 with CsOH. The collagenase used for the isolation was Type 1 from Gibco-BRL (220 units/mg), and was successful in isolating rat cardiomyocytes previously. The mouse was given an injection of heparin five minutes prior to euthanasia. Sodium currents were obtained from these murine cardiomyocytes, but not calcium currents. The extracellular solution caused crystals and the cells contracted spontaneously and then burst. Several different solutions were sought from the literature to produce L-type currents in heart cells (Hamplova-Peichlova *et al.*, 2002; Vandecasteele *et al.*, 2001; De Paoli *et al.*, 2002; DuBell *et al.*, 2002; Chen *et al.*, 2001). Following this a simple extracellular solution was made consisting of in mM Tris 140, $BaCl_2$ 10. Cells still contracted spontaneously and imploded on contact with the pipette.

A heavily buffered intracellular solution with low free calcium was attempted, as follows in mM: CsCl 130, EGTA 20, HEPES 60, K_2ATP 2, $MgCl_2$ 3, pH 7.4 with CsOH. A rat heart was used since mice numbers were becoming low. Calcium currents were obtained from this rat that was injected with heparin prior to euthanasia.

The heart was placed on the plastic canula and a 1.5 mM calcium Tyrodes solution bubbled with O_2 was run through the heart at 3mL/min for 5min. The Ca^{2+}-free tyrodes was circulated through the heart for 20min, and then collagenase (Type 1 Gibco-BRL 220 units/mg) was circulated for 20min and the heart removed, abrased with scissors tearing the ventricular tissue and placed into a BSA storage solution. The cells were then put through a series of Ca^{2+}-containing solutions to raise the Ca^{2+} tolerance.

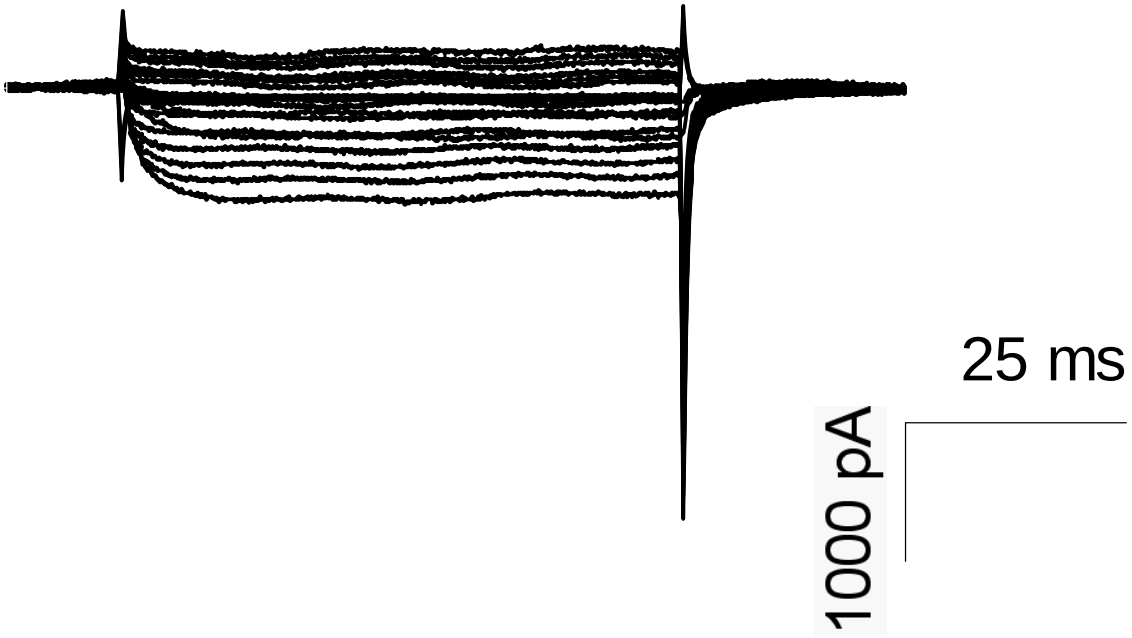

Figure C.1 Superimposed current records from *mdx* cardiomyocytes. Each current was elicited by voltage-clamp steps from a holding potential from –40mV to potentials between –40 and +120mV (in 5mV increments).

The calcium currents produced by the rat cardiomyocytes were completely abolished on the addition of diltiazem, proving that these currents were from the L-type calcium channels.

The next *mdx* mouse produced a good yield of healthy looking cells. The heart was digested for 10min, and extracellular Calcium brought up to 0.5mM over 20min. Calcium currents were produced by these cardiomyocytes, though the seals were leaky, and the cells often died immediately after a calcium current was produced. After the completion of these studies an n of 2 for *mdx* and 0 for C57 were obtained.

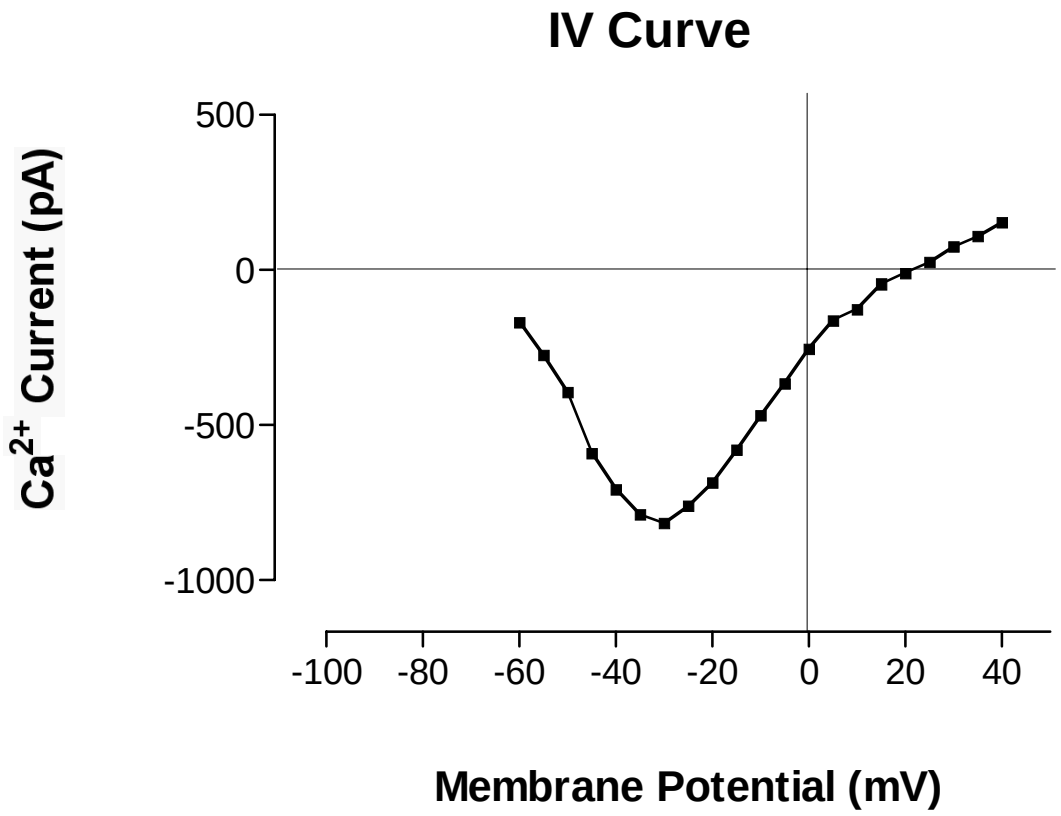

Figure C.2 A calcium current IV curve from a 12 week old *mdx*.